

Attachment 1: US 74 Resiliency Study



**North Carolina Flood Mitigation:
PROTECTing US 74 at the Lumber River**



U.S. 74 RESILIENCY STUDY

January 2023

Prepared by

ATKINS

Member of the SNC-Lavalin Group

Contents

Acronyms vii

1 Executive Summary 1-1

1.1 Introduction1-1

1.2 Study Approach1-1

1.3 Study Goal and Objective Statements.....1-2

1.4 Study Questions.....1-2

1.5 Vulnerability Findings1-3

 1.5.1 Question 1 Findings: Future Disruption 1-3

 1.5.2 Question 2 Findings: Critical Facilities 1-5

 1.5.3 Question 3 Findings: Disadvantaged Populations..... 1-5

1.6 Adaptation and Mitigation1-5

2 Introduction..... 2-1

3 Study Objectives and Questions 3-1

3.1 Study Goal and Objectives3-1

3.2 Study Questions.....3-1

 3.2.1 Question 1: Future Disruption 3-1

 3.2.2 Question 2: Critical Facility Accessibility..... 3-2

 3.2.3 Question 3: Disadvantaged Population Accessibility..... 3-2

4 Approach and Modeling Assumptions 4-1

4.1 Using Dynamic Simulation to Measure Resilience4-1

4.2 Simulation Drivers: Projected Future Conditions.....4-2

 4.2.1 Rainfall 4-2

 4.2.2 Temperature..... 4-12

 4.2.3 Sea Level 4-13

4.3 Building and Structure Modeling4-19

 4.3.1 MegaBuildings 4-19

 4.3.2 Controlled Access Road Segments..... 4-20

 4.3.3 Building Flooding Not Simulated 4-20

4.4 Travel Modeling.....4-21

 4.4.1 Simulating Trip Disruption 4-21

 4.4.2 Creating the Road Network 4-21

 4.4.3 Calibrating the Travel Model 4-23

4.5 Agent Modeling4-23

 4.5.1 Calibration with Data from the U.S. Census American Community Survey..... 4-24

| | | |
|-------------|---|-------------|
| 4.5.2 | Calibration to Reported AADT | 4-24 |
| 4.6 | Flood Modeling..... | 4-24 |
| 4.6.1 | Riverine Flood | 4-25 |
| 4.6.2 | Pluvial Flood..... | 4-26 |
| 4.6.3 | Coastal Flood | 4-27 |
| 4.6.4 | Tidal Flood | 4-27 |
| 4.6.5 | Summary of Flood Model Types Used in Simulation | 4-27 |
| 4.6.6 | Disruptions from Flood Events | 4-28 |
| 4.7 | Asset Lifecycle Cost Modeling..... | 4-30 |
| 4.7.1 | Asset Types | 4-30 |
| 4.7.2 | Condition Decay..... | 4-30 |
| 4.7.3 | Condition Category System..... | 4-31 |
| 4.7.4 | Maintenance Events | 4-32 |
| 4.7.5 | Cost Modeling..... | 4-34 |
| 4.7.6 | Calibration of the Cost Model with Actual Costs from NCDOT SAP system | 4-35 |
| 4.8 | Sea Level Rise Modeling..... | 4-37 |
| 4.8.1 | Simulating Nuisance Flooding..... | 4-37 |
| 4.8.2 | Simulating Sea Level Rise Impact on Storm Surge | 4-38 |
| 4.9 | Heat Impact Modeling | 4-38 |
| 4.9.1 | Probabilistic Heat Event Simulation..... | 4-39 |
| 4.9.2 | Disruptions from Heat Events..... | 4-40 |
| 4.9.3 | Disruptions from Heat Events..... | 4-41 |
| 4.10 | Freight Impact Modeling | 4-41 |
| 4.10.1 | AADT Truck Metric..... | 4-41 |
| 4.10.2 | Adaptation Approach..... | 4-42 |
| 4.11 | Rail Impact Modeling | 4-42 |
| 4.11.1 | Rail Crossing Flood Frequency Metric..... | 4-42 |
| 4.11.2 | Adaptation Approach..... | 4-42 |
| 4.12 | Disruption to Disadvantaged Populations..... | 4-43 |
| 4.12.1 | Approach..... | 4-43 |
| 4.12.2 | Inaccessibility Index | 4-43 |
| 4.13 | Impacts to Critical Facilities | 4-45 |
| 4.13.1 | Approach..... | 4-46 |
| 4.13.2 | Inaccessibility Index | 4-46 |
| 4.13.3 | Opportunities for Improvement | 4-49 |
| 4.14 | Addressing Future Inflation | 4-49 |
| 4.14.1 | Approach..... | 4-49 |
| 4.14.2 | Comments on Inflation Approach..... | 4-50 |

5 Vulnerabilities..... 5-1

5.1 Study Question 1 Findings: Future Disruption5-1

5.1.1 Finding 1.1: Climate change impacts are projected to increase disruption to daily trips 108% by 2060, with riverine and pluvial flood causing the highest percentage of disrupted trips followed by heat and then sea level rise. 5-1

5.1.2 Finding 1.2: Flood vulnerability occurs across the corridor with the highest disruption locations in the transportation network supporting U.S. 74..... 5-4

5.1.3 Finding 1.3: Large storms are projected to increase in severity. 5-9

5.1.4 Finding 1.4: Heat is projected to be an increasingly disruptive problem. 5-11

5.1.5 Finding 1.5: I-95 is prone to flood disruption. 5-14

5.1.6 Finding 1.6: Rail crossings are relatively resilient, with only three potential overtopping locations. 5-17

5.1.7 Finding 1.7: A 10-year period at the early part of the timeline with a series of storms with return periods like Matthew and Florence will cause average annual \$3.85M in damage (2020 dollars). In the latest 10-year period in the timeline, a series with the same return periods will cause \$5.3M in average annual damage (2020 dollars). The increase is due to extreme storms becoming larger in the future. 5-19

5.1.8 Finding 1.8: Coastal roads are projected to be increasingly impacted by tidal overtopping and seawater inundated freeboard..... 5-21

5.2 Study Question 2 Findings: Critical Facilities5-24

5.2.1 Finding 2.1: Critical facility risk varies depending on overtopping risk and remoteness/redundancy in the facility service area. 5-24

5.2.2 Finding 2.2: Climate change impacts will likely exacerbate inaccessibility for critical facilities..... 5-25

5.3 Study Question 3 Findings: Disadvantaged Populations5-26

5.3.1 Finding 3.1: Inaccessibility to sustenance facilities currently impacts disadvantaged populations..... 5-26

5.3.2 Finding 3.2: Climate change is likely to exacerbate inaccessibility for disadvantaged populations..... 5-34

6 Adaptation and Mitigation 6-1

6.1 Rationale6-1

6.2 Resilience-Focus Scenario6-2

6.2.1 Improved Protection Level from 50-Year Storm to 500-Year Storm 6-2

6.2.2 Balance Between Improvements and Increased Risk and Level of Service 6-5

6.2.3 Varied Asset Improvement Timing to Increase Resilience..... 6-7

6.2.4 Highest ROI Targets 6-8

7 Recommendations and Next Steps 7-1

7.1 Increased Information and Awareness.....7-1

7.2 Policy and Planning.....7-1

7.3 Incorporate habitat and natural system concerns into future studies. General Infrastructure Improvement.....7-1

7.4 Physical Countermeasures to Climate Change.....7-2

8 Further Reading 8-1

Appendix A. Data

Appendix B. Heat Modeling

Figures

Figure 4.1: How City Simulator Works4-1

Figure 4.2: The U.S. 74 Digital Twin, with Selected Statistics4-2

Figure 4.3: Future Rainfall Projection Algorithm4-3

Figure 4.4: U.S. 74 Historical Max Rainfall (Inches)4-5

Figure 4.5: Projection of Future Rainfall at Lumberton, NC4-7

Figure 4.6: 95th Percentile Rain Projection at Lumberton NC with Severity Estimates4-9

Figure 4.7: Early and Late Rainfall Projections at Lumberton NC4-11

Figure 4.8: Days Per Year Above 90° at Sunny Point, NC.....4-13

Figure 4.9: Trends in Sea Level at NOAA 8658120 Station, Wilmington, NC.....4-15

Figure 4.10: Projected Mean Sea Level at Wilmington, NC4-16

Figure 4.11: Projected Max Daily Sea Level at Wilmington, NC.....4-17

Figure 4.12: Days above MHHW at Wilmington, NC When Using NOAA Intermediate SLR Forecast.....4-18

Figure 4.13: MegaBuildings.....4-20

Figure 4.14: Flood Response Curve Example4-25

Figure 4.15: Results from 331 HEC-RAS 1D Riverine Hydraulic Models4-26

Figure 4.16: Percentage of Water Crossing Assets Overtopped by Flood by Model Type and Storm Size4-28

Figure 4.17: Simulating the Impact of a Flood on Transportation Assets.....4-29

Figure 4.18: Example of Asset Condition Simulated with a Logarithmic Decay Model in the Simulation4-31

Figure 4.19: Maintenance Event Simulation Procedure4-33

Figure 4.20: Water Crossing Replacement Events4-34

Figure 4.21: Regression of Past Bids to Estimated Replacement Cost of Culverts and Bridges vs. Hydraulic Volume.....4-35

Figure 4.22: Historical Spending on Bridges, Culverts, and Drainpipes in the US 74 Corridor4-36

Figure 4.23: Flushing Impacts4-39

Figure 4.24: Probability of Flushing as a Function of Cumulative Heating Degree Days4-40

Figure 4.25: Sustenance Inaccessibility Index.....4-44

Figure 4.26: Critical Facilities Evaluated4-46

Figure 4.27: Example Service Area for a Critical Facility4-48

Figure 5.1: Average Annual Disrupted Trips at the Beginning of the Simulation and at the End.....5-2

Figure 5.2: Disruption Metrics5-3

Figure 5.3: Locations with Trip Disruption Greater than 1,000 Average Annual in the U.S. 74
Corridor.....5-4

Figure 5.4: Top Ten Disrupted Locations by Division.....5-5

Figure 5.5: Average Annual Storm/Flood Disrupted Trips on U.S. 74 Proper vs. Off-U.S. 74.....5-8

Figure 5.6: 100-Year 24-Hour Storm Event at Lumberton, NC5-9

Figure 5.7: Lumberton, NC Historical Rainfall.....5-10

Figure 5.8. Historical Number of Day Above 90°F5-11

Figure 5.9: Max Temperature Projection at Sunny Point, NC.....5-12

Figure 5.10: Number of Days per Year Above 90°F at Sunny Point, NC5-13

Figure 5.11: Locations with Potential for Overtopping.....5-14

Figure 5.12: Current Work on I-955-16

Figure 5.13: Average Annual Days Disrupted at Rail Crossings5-18

Figure 5.14: Spending on Transportation Asset System5-19

Figure 5.15: Asset Conditions Across All Assets.....5-20

Figure 5.16: Road Segments at Risk of Overtopping for 2025 and 20605-22

Figure 5.17: Road Segments with Seawater within Two Feet of Overtopping for 2025 and 20605-23

Figure 5.18: Critical Facilities by Remoteness/Redundancy and Overtopping Risk.....5-25

Figure 5.19: Top Ten Least Accessible Disadvantaged Population Streets.....5-27

Figure 5.20: Division 3 –Disadvantaged Population Streets and Supporting Water Crossing Assets.....5-27

Figure 5.21: Division 6 – Top 10 least accessible Disadvantaged Population Streets5-28

Figure 5.22: Division 6 –Disadvantaged Population Streets and Supporting Water Crossing Assets.....5-29

Figure 5.23: Division 8 – Top 10 least accessible Disadvantaged Population Streets5-30

Figure 5.24: Division 8 – Disadvantaged Population Streets and Supporting Water Crossing
Assets5-31

Figure 5.25: Division 10 – Top 10 Least Accessible Disadvantaged Population Streets, Part A5-32

Figure 5.26: Division 10 – Top 10 Least Accessible Disadvantaged Population Streets, Part B.....5-32

Figure 5.27: Division 10 –Disadvantaged Population Streets and Supporting Water Crossing
Assets5-33

Figure 6.1: Base Run and Resilience-Focus6-2

Figure 6.2: Present Day to Mid-Century Trip Disruption Comparison.....6-3

Figure 6.3: Comparison of Baseline and Resilience-Focused Scenarios6-4

Figure 6.4: Detail of U.S. 74/U.S. 76 (Andrew Jackson Hwy) Crossing Alligator Creek Near
Wilmington, NC.....6-6

Figure 6.5: Sensitivity to Scheduling of Improvement Projects6-8
 Figure 6.6: Disrupted Trips as a Function of Budget Allowed for Resilience-Focused Improvement6-9

Tables

Table 4.1: Modeling Parameters for Flood Impacts on Transportation Assets4-30
 Table 4.2: Parameters for Rail Crossing Operations Interruption and Hardening.....4-43
 Table 5.1: Top Ten Disruptive Locations by Division5-5
 Table 5.2: Early and Late Period Flood-risk Rail Crossings.....5-17
 Table 5.3: Division 3 - Disadvantaged Population Streets and Supporting Water Crossing Assets.....5-28
 Table 5.4: Division 6 - Disadvantaged Population Streets and Supporting Water Crossing Assets.....5-29
 Table 5.5: Division 8 - Disadvantaged Population Streets and Supporting Water Crossing Assets.....5-31
 Table 5.6: Division 10 - Disadvantaged Population Streets and Supporting Water Crossing Assets.....5-33
 Table 6.1: Protection Level and Percent of Replacement Cost.....6-1

Acronyms

| | |
|--------|---|
| AADD | Average Annual Disrupted Days |
| AADT | Average Annual Daily Trips |
| ACS | American Community Survey |
| ADCIRC | Advanced Circulation |
| B | Billion |
| BCSD | Bias-Corrected Spatially Dis-Aggregated |
| BOT | Board of Transportation (NCDOT) |
| CMIP | Coupled Model Intercomparison Project |
| CPI | Consumer Price Index |
| DEM | Digital Elevation Model |
| EPA | Environmental Protection Agency |
| FEMA | Federal Emergency Management Agency |
| FFE | First Floor Elevation |
| GCM | General Circulation Model |
| GCR | General Condition Rating |
| GIS | Geographic Information System |
| GHG | Greenhouse Gas |
| HAZUS | Hazards United States |
| INFRA | Infrastructure for Rebuilding America |
| LiDAR | Light Detection and Ranging |
| LOCA | Local Analog |
| LRS | Linear Route System |
| M | Million |
| MHHW | Mean Higher High Water |
| MPO | Metropolitan Planning Organization |
| NBIS | National Bridge Inventory System |
| NCDOT | North Carolina Department of Transportation |
| NCEM | North Carolina Emergency Management |
| NCFPM | North Carolina Floodplain Mapping Program |
| NOAA | National Oceanic and Atmospheric Administration |
| NPV | Net Present Value |
| OSM | Open Street Map |
| PAT | Project Action Team |
| PRI | Priority Replacement Index |
| QC | Quality Control |
| RCP | Representative Concentration Path |

| | |
|--------|--|
| RMSE | Root Mean Squared Error |
| ROG | Rain-on-Grid |
| ROI | Return on Investment |
| SAP | System Analysis Program |
| SLR | Sea Level Rise |
| SR | Sufficiency Rating |
| STIP | Statewide Transportation Improvement Program |
| TAC | Technical Advisory Committee |
| TAZ | Traffic Analysis Zone |
| TPD | Transportation Planning Division |
| UNIPCC | United Nations Intergovernmental Panel on Climate Change |
| WHAFIS | Wave Height Analysis for Flood Insurance Studies |

1 Executive Summary

1.1 Introduction

Session Law 251-2019 (Senate Bill 356) and the 2020 U.S. 74 Infrastructure for Rebuilding America (INFRA) Grant required the North Carolina Department of Transportation (NCDOT) to perform a vulnerability assessment on U.S. 74. Like many transportation arteries, the 190-mile stretch of U.S. 74 from Wilmington to Charlotte, North Carolina is projected to encounter intensifying storms, increasing temperatures, and rising sea levels. Given its role as a conveyance of people and goods connecting I-95 and major urban centers, NCDOT conducted this resilience study using the Atkins City Simulator tool. The study simulated the 1.1 Million (M)-person, 3,700 square-mile corridor over a 40-year planning period (i.e., 2020–2060), simulating corridor growth and urbanization as well as future climate change influenced events including storms, sea level rise, and extreme heat.

This document presents the findings of the study, first in summary form in this executive summary and then in more detail in the following chapters. The modeling approach is presented in Chapter Four. Chapter Five discusses the vulnerabilities while Chapter Six talks about adaptation and mitigation. Chapter Seven presents a list of recommendations based on the study findings. Finally, the Chapter 8 and the report appendices provide details on further reading and methodologies used.

1.2 Study Approach

The study was managed by a project action team (PAT) comprised of members from NCDOT Hydraulics Unit, Environmental Policy Unit, and Transportation Planning Division. The PAT hosted a series of technical advisory committee (TAC) workshops, where the TAC included stakeholders from NCDOT, rural planning organizations, metropolitan planning organizations, as well as state and federal agencies. Advice from the TAC was sought on defining the study scope and questions to be answered, describing the study findings, and preferred adaptation and mitigation actions.

Through advice from the TAC, the PAT defined a series of three study questions that focused on how climate change will impact the U.S. 74 corridor in the future. To answer the questions, the team developed a U.S. 74 corridor simulator to simulate concurrent corridor growth and operations along with impacts from climate change-influenced disasters from 2020 to 2060. The simulation analysis domain was a 10-mile buffer on either side of the 190-mile stretch of U.S. 74 from Charlotte to Wilmington, NC. The simulation included 6,509 miles of road with a focus on water-crossing transportation assets such as pipes, bridges, and culverts above 54 inches in diameter. Also included were rail crossings and buildings.

The simulation was driven by projections of rainfall, temperature, and sea level, which were derived from general circulation model (GCM) projections of these variables following the United Nations Intergovernmental Panel on Climate Change's Representative Concentration Path (RCP) 8.5 greenhouse gas control scenario. This so-called "business as usual" scenario posits that global governments maintain current greenhouse gas (GHG) control policies and generally predicts increasingly severe storms and

steadily increasing extreme temperatures and sea level in the corridor. Recognizing uncertainty in future weather prediction, a probabilistic approach was used to generate thousands of projections of daily rainfall from 2020-2060; the 95th percentile most severe projection was used to drive the simulation to ensure proposed solutions would provide resilience in near worst-case conditions.

Through the simulation, key performance metrics such as storm damage, disrupted trips, and lost productivity were quantified and used to answer the study questions. The simulation baseline scenario did not include any adaptation and mitigation measures, and therefore exposes vulnerabilities in the corridor to climate change if no resilience-focused action is taken. A second scenario added mitigation and adaptation measures to existing planned and asset condition-triggered maintenance events. For example, elevating bridges to the present-day 500-year flood water surface elevation when they are replaced. This resilience-focused scenario helped to quantify the value that additional spending on resilience would bring.

1.3 Study Goal and Objective Statements

Study goals were defined in the project scope, verified by the PAT, and refined with consultation from the key stakeholders. The PAT consisted of key staff from NCDOT's Technical Services, Environmental Policy Unit and Transportation Planning Division (TPD) unit, as well as Atkins staff.

Following NCDOT's existing goals and objectives on resilience, the goal of the study was to maintain NCDOT's high-quality transportation system during extreme weather events and ensure critical transportation infrastructure withstood harsher future conditions. Three study objectives were identified to achieve the goal.

Objective 1: Identify and explore ways to reduce failure risk: Keep key assets from failing due to extreme weather events.

Objective 2: Preserve continuity: Keep people moving following extreme weather events.

Objective 3: Foster equity: Make improvements to manage extreme weather event risks that are socially equitable and ensure vulnerable populations are served appropriately.

1.4 Study Questions

Through a collaborative workshop exercise, the PAT developed three questions for the study to answer. The questions specified the hazards to be simulated, the infrastructure of interest, the population, and the metrics of interest. The questions were:

1. Which assets (roads, bridges, culverts and pipes) will cause the most (and least) disruption to road and rail traffic if future climate change-influenced events (floods, storms, heat waves and sea level rise [SLR]) took them offline? Which assets or events are most likely to be impacted given their current condition?
2. Which critical facilities (hospitals, emergency care, shops, schools, DOT facilities, fire stations, and police) are most at risk of being cut off from access through the transportation system?

Which assets (roads, bridges, culverts, and pipes) are included in the transportation networks that serve these facilities?

3. How will disadvantaged populations be affected by climate change-influenced disruptions to the transportation system in the future?

1.5 Vulnerability Findings

The study revealed several vulnerability findings as well as adaptation and mitigation actions. The findings responded directly to the study questions and were organized as three sets accordingly.

1.5.1 Question 1 Findings: Future Disruption

1.5.1.1 Finding 1.1: Climate change impacts are projected to increase disruption to daily trips 108% by 2060, with riverine and pluvial flood causing the highest percentage of disrupted trips followed by heat and then sea level rise.

Across the corridor, the simulation projected trip disruption will increase 108% by 2060. This is largely due to two factors. First, the steady increase in transportation system usage caused by increasing populations and business activities implies that each successive disaster will impact the future significantly. For example, I-95 near Lumberton is projected to increase from 65,000 trips per day on average to 108,000 trips by 2060. The second factor is increasing severity and frequency of future storms, which will result in deeper floods and more storm damage to the transportation system.

1.5.1.2 Finding 1.2: Flood vulnerability occurs across the corridor with the highest disruption locations in the transportation network supporting U.S. 74.

Several locations on U.S. 74 were vulnerable to future floods, though the highest vulnerability was in the road network connecting to U.S. 74. Key locations vulnerable to flood were in Wilmington and on I-95 near Lumberton.

1.5.1.3 Finding 1.3: Large storms are projected to increase in severity.

Large storms increased dramatically over the past several decades and are projected to continue increasing into the future. A statistical analysis estimating the 100-year 24-hour rain depth from 1913 through 2100 showed approximate stationarity (not changing with time) up to the last two decades. The extreme storms in the last two decades increased the estimate of the 100-year 24-hour rain depth by 24%. Global climate models project a continued increase in this important statistic throughout the 21st century.

1.5.1.4 Finding 1.4: Heat is projected to be an increasingly disruptive problem.

Maximum temperatures rose steadily across the corridor and pushed the number of days above 90°F to more than three times higher in 2060 than in 2020. This rise in temperatures is projected to increase disruption to road and rail traffic through phenomena like flushing, where the bitumen in asphalt becomes unstable in high heat events and the aggregate is pulled out by vehicle tires. The resulting increase in bitumen density causes lower static friction, increasing the frequency of needed asphalt

replacement and potentially creating dangerously slippery conditions that may require controlled traffic slowdowns to ensure safety.

1.5.1.5 Finding 1.5: I-95 is prone to flood disruption.

I-95 supports approximately 65,000 average annual daily trips (AADT) in the section close to the I-95/U.S. 74 interchange. The simulation showed that multiple locations in this area were at risk for future flooding causing large disruptions to I-95 travelers and freight. Of note was that the risk became severe for storms larger than the 100-year event. The currently planned work that will elevate the road deck in this area to above Hurricane Florence flood levels is expected to mitigate this risk.

1.5.1.6 Finding 1.6: Rail crossings are relatively resilient, with only three potential overtopping locations.

Generally, rail crossings in the U.S. 74 corridor were fairly flood resilient. The inventory of flood models projected that only three out of the 528 crossings in the corridor will potentially be impacted by flooding, and this flooding will occur with very large storms. No crossing was projected to be flooded by the presently published 100-year flood event. Flooding was projected to occur at the present day 500-year storm level for three rail crossings near Laurinburg.

1.5.1.7 Finding 1.7: A 10-year period at the early part of the timeline with a series of storms with return periods like Matthew and Florence will cause average annual \$3.85M in damage (2020 dollars). In the latest 10-year period in the timeline, a series with the same return periods will cause \$5.3M in average annual damage (2020 dollars). The increase is due to extreme storms becoming larger in the future.

Maintenance of the system of bridges, culverts, and pipes is projected to cost an average \$5.3M per year across the corridor in the coming 40 years, which includes an annual average of \$4.0M in planned maintenance and \$1.3M per year on repair to flood-caused damaged. The spending rate is projected to increase by 20% from 2020 to 2060, largely attributed to increasing flood damage from climate change-influenced storms. The study found that if NCDOT initiated proactive, resilience-focused solutions in advance of storms, this would reduce unpredictable future costs substantially. See the adaptation and mitigation section for more details.

1.5.1.8 Finding 1.8: Coastal roads are projected to be increasingly impacted by tidal overtopping and seawater inundated freeboard.

Coastal roads in the Wilmington area were found to be relatively resilient to tidal flooding. Two segments of road were found to experience nuisance flooding in 2022. This was projected to increase to seven road segments by 2060. A more serious concern was seawater invading the freeboard zone - within two feet of the road deck. With sea water inundation likely to accelerate deterioration of road assets, the projected widespread and regular occurrence of this type of event by 2060 is a reason for concern.

1.5.2 Question 2 Findings: Critical Facilities

1.5.2.1 *Finding 2.1: Critical facility risk varies depending on overtopping risk and remoteness/redundancy in the facility service area.*

Critical facilities ranged from highly accessible through redundant routes to having single access paths that were prone to increasing flood levels with climate change. Increasing redundancy of routes to the most inaccessible facilities and focusing on making them less flood prone will help in ensuring level of service.

1.5.2.2 *Finding 2.2: Climate change impacts will likely exacerbate inaccessibility for critical facilities.*

Already challenged by limited accessibility, some critical facilities are expected to face increasingly limited access with future climate change.

1.5.3 Question 3 Findings: Disadvantaged Populations

1.5.3.1 *Finding 3.1: Inaccessibility to sustenance facilities currently impacts disadvantaged populations*

Disadvantaged populations, particularly in rural areas, are already facing low accessibility to sustenance facilities like gas stations, emergency care, shops, and emergency shelters. Low availability of redundant routes combined with flood risk along the routes that exist reduces options for these populations during hurricanes and large storm events.

1.5.3.2 *Finding 3.2: Climate change is likely to exacerbate inaccessibility for disadvantaged populations*

Inaccessibility will be a concern for disadvantaged populations across the corridor. Expected SLR compounded with storm surge, riverine, and pluvial flooding at the coast will lead to significant increases in flood risk in Division 3. Isolated disadvantaged populations in rural areas of Divisions 6, 8, and 10 will all see increasing flood risk from pluvial and riverine sources.

1.6 Adaptation and Mitigation

An initial adaptation and mitigation scenario was created that implemented the following actions:

- When they are due for maintenance in the future, elevate road decks over bridges and culverts to the 2020 500-year, 24-hour flood level,
- Hardening rail crossings to reduce down-time when they flood.

The study found that even with increasing future demands on the transportation system, the following actions will reduce future disruption by 12%.

Further, currently planned actions like elevating the I-95 deck over the Lumber River by approximately four feet above the water surface experienced during Hurricane Florence will ensure the transportation network continues to serve a growing population.

The study found that some locations may require an even higher level of protection than the 500-year flood level. Specifically, locations at the coast like the U.S. 74/Andrew Jackson Highway near Wilmington were found to be exposed to severe damage even from a current 100-year storm surge event. Larger

storms of the future could cause even higher levels of damage and longer periods of unusable infrastructure and disrupted trips. With the demand for level of service of these important highways projected to increase substantially in the future, extraordinary adaptation approaches are needed such higher deck elevations and hardening for thoroughfares.

To explore ways to reduce disruption even further, a sensitivity analyses was conducted to assess how adjusting the timing of when resilience-focused improvements were made can increase resilience. The analysis assumed that when water crossing assets (bridges, culverts, drainpipes) were improved, they were improved to withstand their 2020 500-year 24-hour flood level. The analysis varied the timing of when improvements occur as follows:

- 1) An impractically expensive improvement of the full network in the corridor in the first year of simulation, at a cost of \$3.6 billion.
- 2) An annual pro-active piece-wise improvement strategy where a 50% increase in the current maintenance budget is used to improve several assets per year, and
- 3) A post-major storm only strategy, where assets are only improved if damaged.

The result showed that with unlimited funding, an approximate 73% reduction in disruption was possible over the next 40 years, but this essentially required the replacement cost of the corridor's transportation assets, plus 50% for resilience-focused design, or about \$3.6 Billion (B) in one year.

The best tradeoff between spending and benefit was the annual improvement approach, which allowed NCDOT to be proactive, retrofitting existing assets one by one. While it is impossible to predict when a damaging future storm will happen, this approach showed that by being pro-active assets will often be prepared for major storms before they occur. The approach showed that an approximately 40% reduction in future disruption is achievable with this strategy.

2 Introduction

The U.S. 74 transportation corridor forms a vital pathway from coastal North Carolina inland to Charlotte. Home to major cities and towns such as Wilmington, Charlotte, Lumberton, Monroe, Laurinburg, and Rockingham, the corridor is destined for continual economic and population growth. Challenging this growth are changing future weather conditions which may bring larger floods and longer and more intense heat waves over the next several decades.

To understand the potential vulnerabilities that will be exposed by continued growth along with future weather challenges, a holistic assessment of the transportation corridor and its various interacting systems is required.

This study used a scenario-based approach to simulate the corridor from 2020-2060. Using Atkins City Simulator tool, a high-detail digital twin of the corridor was created that contained 6,500 miles of road and approximately 3,200 bridge, culvert, and drainpipe assets. The simulation was agent-based, meaning that the 1.1M residents of the corridor were simulated moving throughout the transportation system, using it daily for commuting, commerce, and recreation. Further usage of the transportation system was also included in the simulation for activities such as freight transport through road and rail and pass-through trips through major conveyances like I-95.

An initial baseline scenario simulated the corridor with currently master planned capital improvements projects as well as asset condition-triggered maintenance events, with no additional action aimed at increasing resilience. A second scenario focused on resilience, elevating and hardening assets to the flooding levels resulting from the current 500-year 24-hour rainstorm. Results of the two scenarios were used to quantify the additional resilience provided and additional cost required to incorporate resilience into corridor operation in the future.

The study was run by a PAT comprised of members from NCDOT divisions in the corridor and specialist divisions focused on hydraulic and planning. The PAT hosted a series of TAC workshops, where the TAC included stakeholders from NCDOT, corridor municipalities, counties, and municipal planning organizations, as well as state and federal-level agencies. Advice from the TAC was sought on defining the study scope and questions to be answered, describing the study findings, and preferred adaptation and mitigation actions.

This report lays out the study questions and objectives in Chapter Three, methods and assumptions in Chapter Four, vulnerability assessment results in Chapter Five, adaptation and mitigation results in Chapter Six, recommendations and conclusions garnered through the study process in Chapter Seven, and further reading listed in Chapter Eight. The other report appendices present links to and notes on the data used and supplemental information and more detailed descriptions of several of the modeling approaches used.

3 Study Objectives and Questions

An initial step in the study was to set clear study goals and objectives with consultation from the key stakeholders. Study goals were defined in the project scope and verified by the PAT. This team consisted of key staff from NCDOT's Technical Services and TPD unit, as well as Atkins staff. Based on the study objectives, the PAT identified concise questions that were answered through the course of the study.

3.1 Study Goal and Objectives

Several existing plans were considered when developing the goals and objectives of this study. They included:

- NC MOVES 2050's objectives to:
 - Provide transportation access through building roads and bridges to withstand and endure major weather events,
 - Maintain a high-quality system through developing and mainstreaming risk/resiliency practices.
- The NCDOT Transportation Asset Management Plan's call to *"Perform predictive analysis to identify vulnerable areas within critical corridors."*

The goal of the study was to find actions to maintain NCDOT's high-quality transportation system during extreme weather events and ensure critical transportation infrastructure will withstand future conditions. Study objectives were:

Objective 1: Identify and explore ways to reduce failure risk: Keep key assets from failing due to extreme weather events.

Objective 2: Preserve continuity: Keep people moving following extreme weather events.

Objective 3: Foster equity: Make improvements to manage extreme weather event risks that are socially equitable and ensure that vulnerable populations will be served appropriately.

3.2 Study Questions

Based on the overall goal and three objectives identified, three study questions were identified by the PAT and agreed by the TAC.

3.2.1 Question 1: Future Disruption

Which assets (roads, bridges, culverts and pipes) will cause the most (and least) disruption to road and rail traffic if future climate change-influenced events (floods, storms, heat waves, and SLR) took them offline? Which assets or events are most likely to be impacted given their current condition?

3.2.2 Question 2: Critical Facility Accessibility

Which critical facilities (hospitals, emergency care, shops, schools, DOT facilities, fire stations, and police) are most at risk of being cut off from access through the transportation system? Which assets (roads, bridges, culverts, and pipes) are included in the transportation networks that serve these facilities?

3.2.3 Question 3: Disadvantaged Population Accessibility

How will disadvantaged populations be affected by climate change-influenced disruptions to the transportation system in the future?

4 Approach and Modeling Assumptions

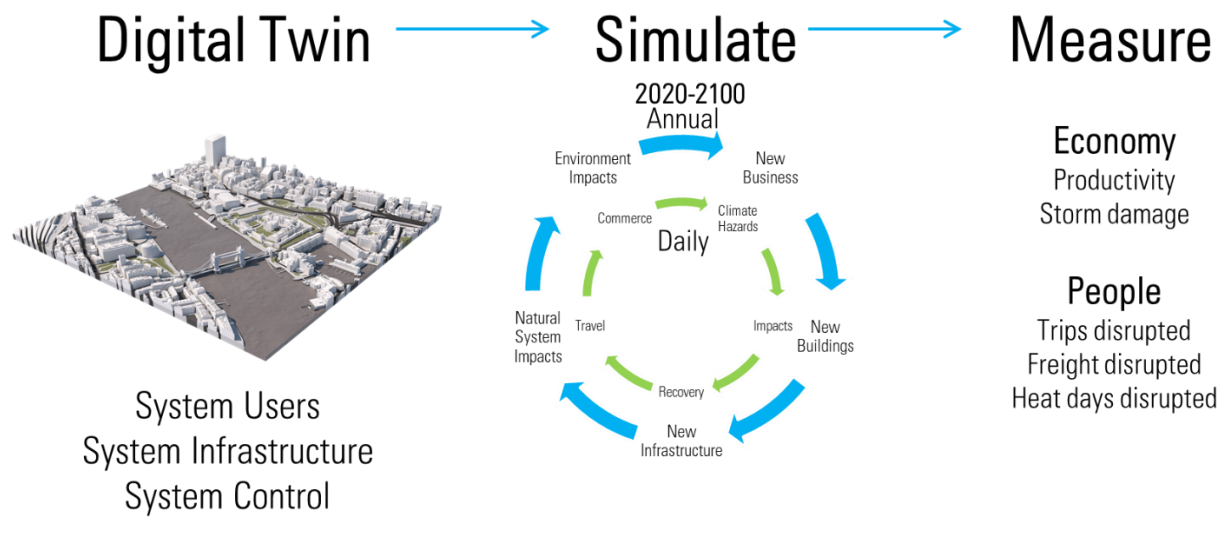
The findings and recommendations in the study required dynamic simulation of a digital twin of the corridor from 2020-2060. The approach, techniques, and assumptions involved are described in this chapter.

4.1 Using Dynamic Simulation to Measure Resilience

This study used Atkins' City Simulator resilience modeling tool (see Figure 4.1). City Simulator is a Geographic Information System (GIS)-based tool that creates a digital twin of a city, county, state, or region and evolves it over the planning period (i.e., 40 years) to quantify future climate change impacts and find ways to mitigate and adapt.

A 3,800-square mile U.S. 74 corridor digital twin was developed, consisting of the U.S. 74 highway and all transportation infrastructure, buildings and natural systems within a 10-mile buffer on either side of the highway (see Figure 4.2). The digital twin simulated growing, operating, and being hit with climate change-influenced disasters from 2020-2060.

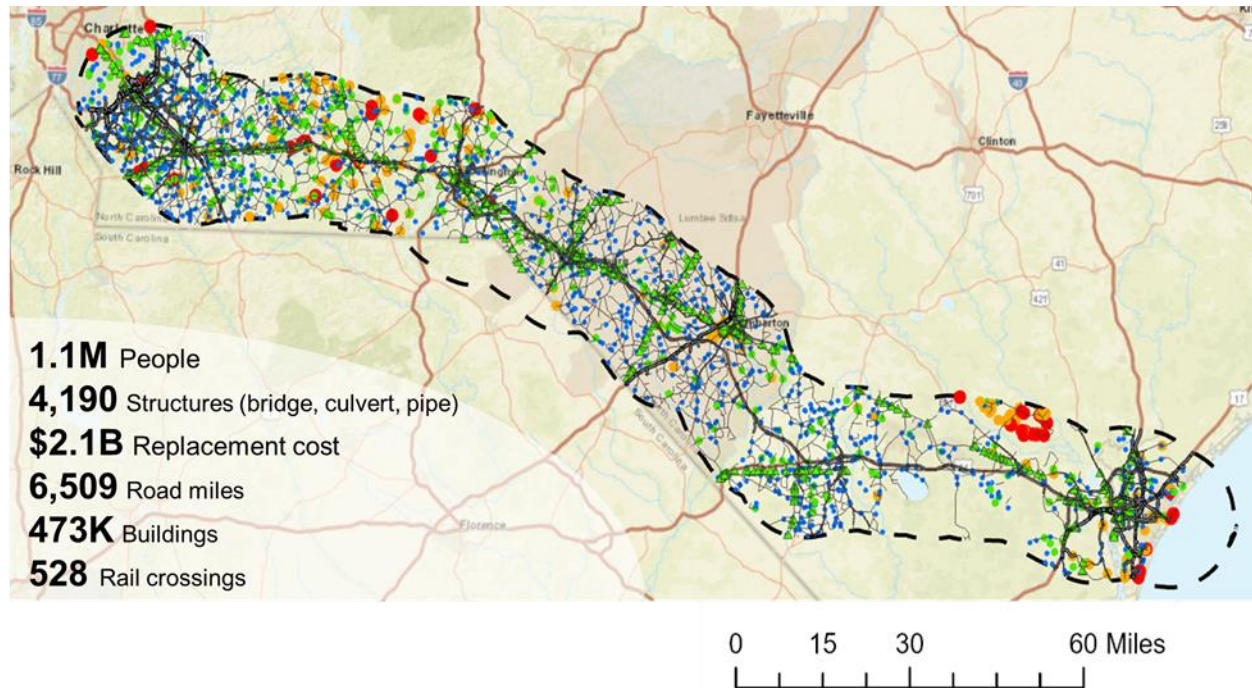
Figure 4.1: How City Simulator Works



How City Simulator Works. A digital twin was created that included system users, infrastructure, and control. This digital twin was then evolved in a daily simulation from 2020 to 2060. The simulation included growth in infrastructure, population, and economy. Additionally, it included climate change-influenced disasters, like hurricanes and heat waves. Key performance metrics were evaluated throughout the simulation. A baseline simulation was conducted first without any adaptation and mitigation measures. Then, an adaptation/mitigation scenario was conducted that added actions like elevating bridges above the flood levels caused by the current 500-year, 24-hour rain event. The resulting key performance metrics were compared to quantify the increased resilience of the adaptation/mitigation measures.

City Simulator is an agent-based model, which means it creates a population of people in the corridor that is matched statistically to the real population. The U.S. 74 simulator included avatars for the 1.1M people that live within the buffer, plus agents moving into and out of the area along other highways. To simulate daily travel, residential and commercial buildings were added to the simulation to act as workplaces and homes for the avatars. Each day of the run, the avatars were simulated commuting from home to work and school. This allows for street-level estimating of future disruption from flooding and other disasters.

Figure 4.2: The U.S. 74 Digital Twin, with Selected Statistics



The U.S. 74 digital twin was compiled from multiple datasets of global climate model projections, historical weather and tide time series, flood models, digital elevation models, demographics data from the US Census, and GIS datasets of buildings, parcels, transportation, and rail systems.

4.2 Simulation Drivers: Projected Future Conditions

The simulation was driven by projections of daily rainfall, temperature, and sea level. The approaches used to incorporate these three drivers are detailed below.

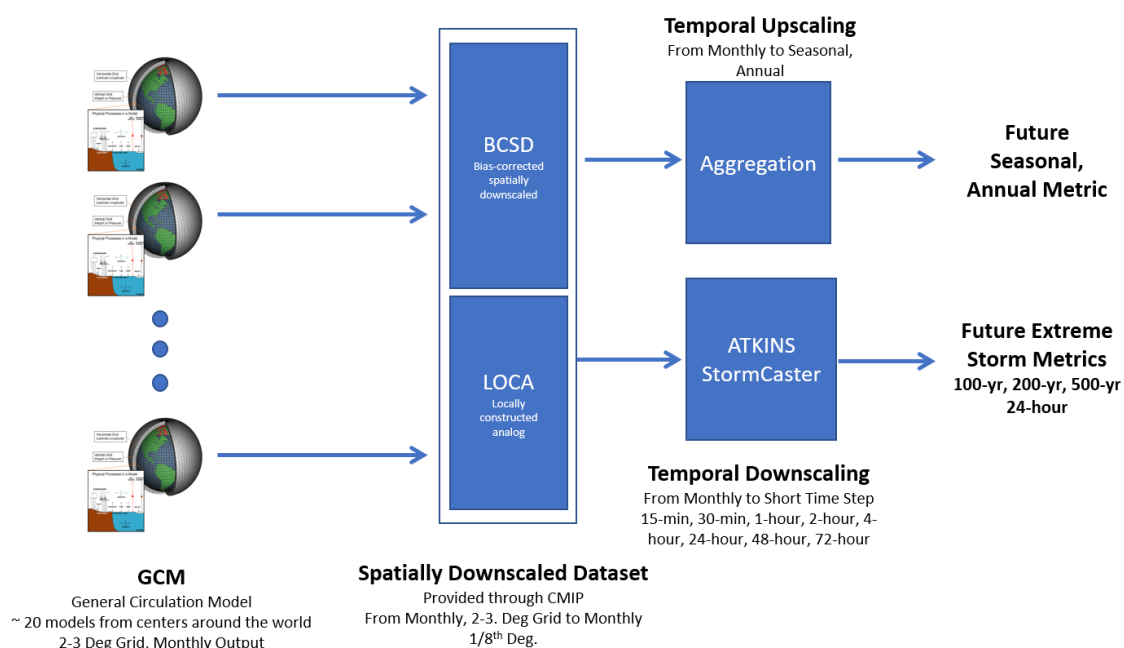
4.2.1 Rainfall

As Figure 4.3 shows, rainfall projections started with an ensemble of monthly projections from the coupled model intercomparison project's (CMIP5) bias-corrected spatially dis-aggregated (BCSD) dataset. The BCSD process takes monthly (2020—2100) projections from twenty GCMs and converts them to a common grid at 1/16th degree latitude/longitude spacing, a process called spatial downscaling. ([More information on the BCSD dataset.](#))

The assessment used the United Nations Intergovernmental Panel on Climate Change (UNIPCC)-defined representative concentration pathway (RCP)8.5 and RCP4.5 scenario results from each GCM. RCP scenarios define plausible global future conditions in terms of GHG emissions. The number designation - 4.5, 8.5 – is measured in watts per square meter and refers to the amount of energy retained in the atmosphere because of GHG emissions. ([More details on RCPs.](#))

The RCP8.5 scenario is considered the "business-as-usual" scenario, where there is no attempt to control GHG emissions and global temperatures and extremes in weather continue to rise until the end of the century. The RCP4.5 scenario represents a concerted effort on the part of global governments to control GHG emissions which results in a stabilization of global temperatures and weather by the end of the century.

Figure 4.3: Future Rainfall Projection Algorithm



Future rainfall and temperature amounts were derived from CMIP5-based projections, which, in turn, were derived from GCM results. For rainfall, the spatially downscaled, monthly time-step BCSD dataset was used as input to the Atkins StormCaster algorithm, which temporally downscaled the data to daily time-step. For temperature, the temporally and spatially downscaled LOCA dataset provided data in daily time-step.

4.2.1.1 Ensuring Extremes for Stress-Testing

With its short time-step requirement, City Simulator required daily rainfall projections. While daily projections were available from the CMIP5-based Local Analog (LOCA) dataset, a review of the extreme events in the projections in the U.S. 74 corridor showed that 24-hour total rainfall projections were often not as large as recent events such as Hurricanes Florence and Matthew. Given an upward trend in historical 24-hour extreme event rainfall depths, it is unlikely that future events will become less extreme. As such, the Atkins Stormcaster downscaling algorithm was used to temporally downscale the BCSD projections from monthly to daily time-step.

The StormCaster algorithm disaggregates projected monthly rainfall totals with a focus on:

- 1) extrapolating recent trends in historical variance in rainfall events from the prior 30 years, and
- 2) inflating/deflating daily extreme events (both high and low rain events – i.e., drought) such that monthly climatologies derived from projected future daily events match with projected monthly climatologies from the BCSD dataset.

This process ensures that extreme rain events in the projected future are at least as extreme as those seen in recent years and are often more extreme.

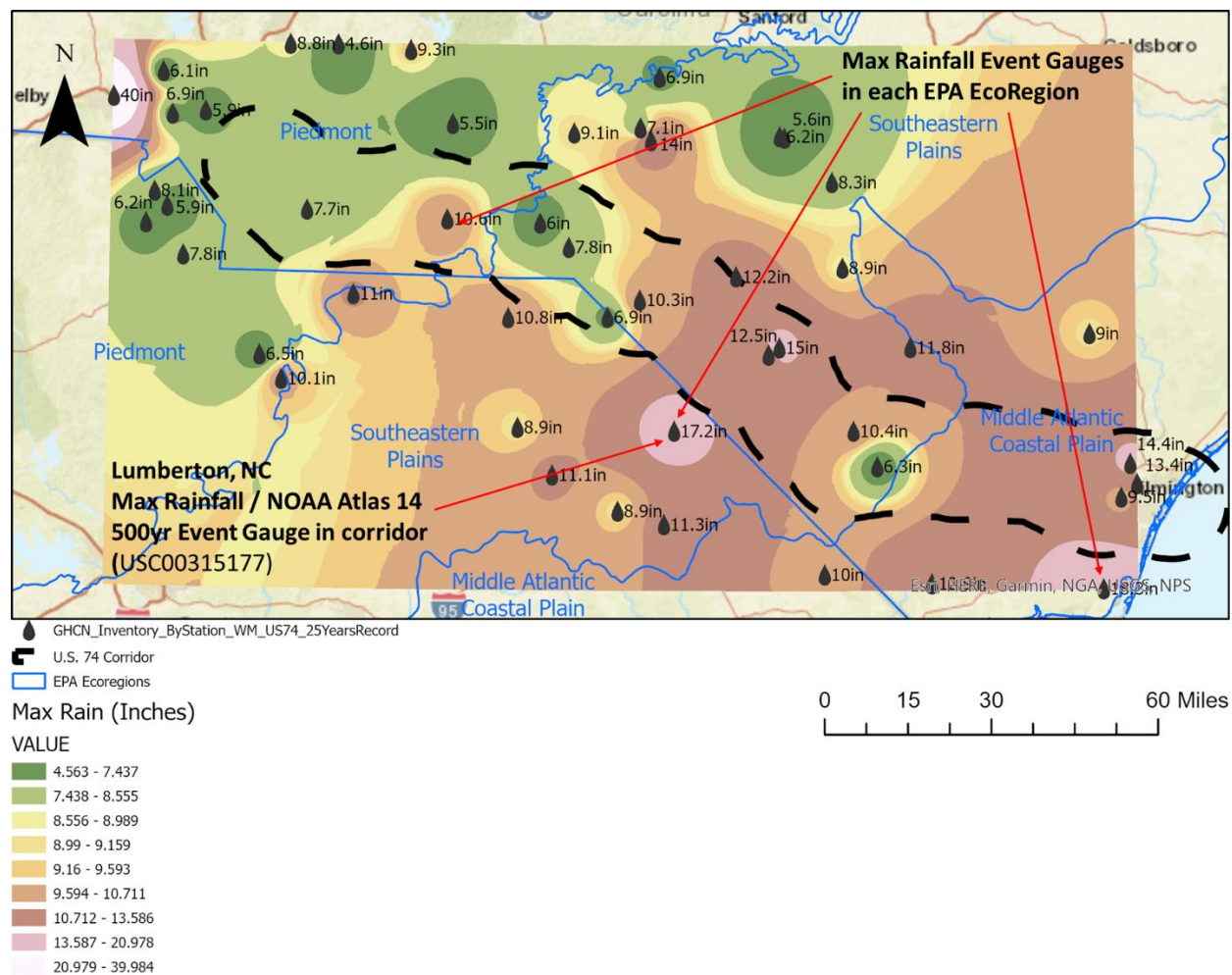
The rationale for this approach is that it is preferable to take a conservative approach, where plausibly higher extreme future realizations are better to stress-test the digital twin. Using the higher extremes will provide a higher level of confidence in future robustness and resilience if the results of the study are used to inform resilience planning.

4.2.1.2 Accounting for Regional Variability in Rainfall Totals

The maximum historical rainfall event in inches over 24 hours is shown in Figure . The northwest to southeast gradient from smaller maximums to larger reflects the change from higher elevation to lower and the attendant microclimates. To account for this regionality in the rainfall statistics, the gauge within the corridor with the maximum historical rain depth was found. This was the Lumberton, NC gauge, where its 15.01-inch rain event was 127% higher than the National Oceanic and Atmospheric Administration (NOAA) Atlas 14 500-year rain depth estimate for this location. A daily rain projection was then created for this gauge, which acts as the single rain projection for the corridor in the simulation.

Regional adjustment factors were developed for each Environmental Protection Agency (EPA) Level III eco-region (Piedmont, Southeastern Plains, Middle Atlanta Coastal Plains), where the factor was defined as the maximum 24-hour rain depth in the region divided by the maximum 24-hour rain depth at the Lumberton gauge. The regional factors were then applied to the rain projection at each water-crossing asset (bridges, culverts, drainpipes, road low points) to produce a regionally adjusted rain projection specific to the asset.

Figure 4.4: U.S. 74 Historical Max Rainfall (Inches)



Maximum 24-hour rain event (at all gauges) in the corridor region. The maximum return-period event was at the Lumberton, NC, gauge, which was 127% higher than its 500-year, 24-hour estimate provided by NOAA Atlas 14.

Using this approach, when a rain event hits the corridor, it is assumed to impact the full corridor with an equal statistical impact. That is, if a 100-year 24-hour rain event is projected, infrastructure in each eco-region will be hit with a rain depth at the 100-year 24-hour rain depth specific to the eco-region.

4.2.1.3 Generating the Corridor-wide Rainfall Projection

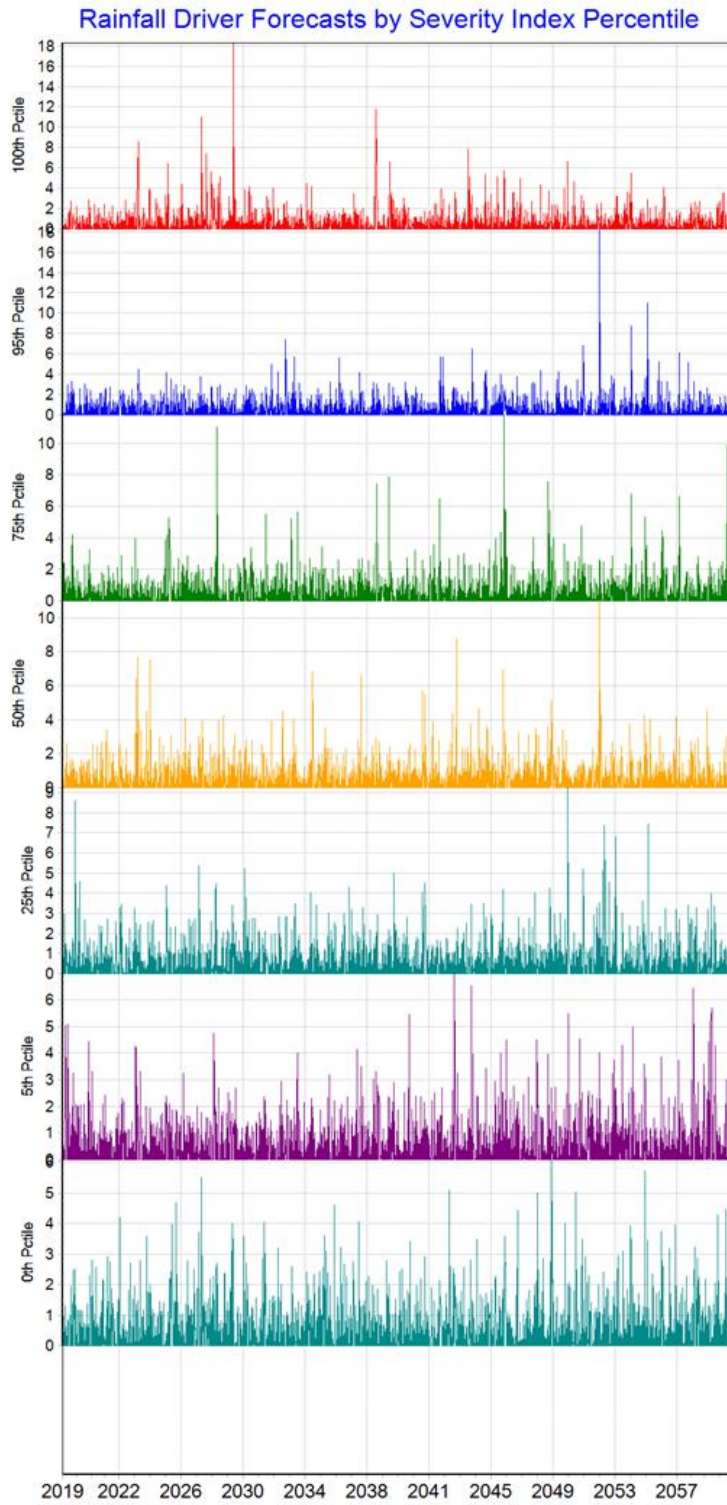
An ensemble of rainfall projections was created based on the maximum rainfall event gauge in the region (Lumberton, NC, USC00315177) (see Figure 4.5). This ensemble included 1,000 realizations of future rainfall created through downscaling 20 GCM projections based on RCP8.5 with historical rainfall data at Lumberton, NC. The realizations were ranked by their severity over the 40-year simulation timeline, where severity was defined as the cubed sum of daily rainfall depths over the timeline.

Figure 5 shows a series of projections corresponding to 0th, 5th, 25th, 50th, 75th, 95th, and 100th percentile severity. Note, the 100th percentile projection contains two very significant 24-hour rain events approximately 15 inches in depth (on the order of magnitude of a Hurricane Matthew- or Florence-size

storm). In addition, there were several very large rain events from eight to nine inches. The current 100-year event at Lumberton is 9.01 inches, according to NOAA Atlas 14. In the lower-percentile projections, the number of large events reduced steadily. The 0th-percentile projection, for example, had no events over approximately five inches, which was approximately equivalent to the 10-year storm at Lumberton.

It is important to note that each of these projections was based on a plausible future for the corridor. As the objective of this assessment was stress-testing the corridor for future extremes, more extreme projections were used in the analysis. The 95th-percentile projection was adopted as the primary forecast for simulation.

Figure 4.5: Projection of Future Rainfall at Lumberton, NC



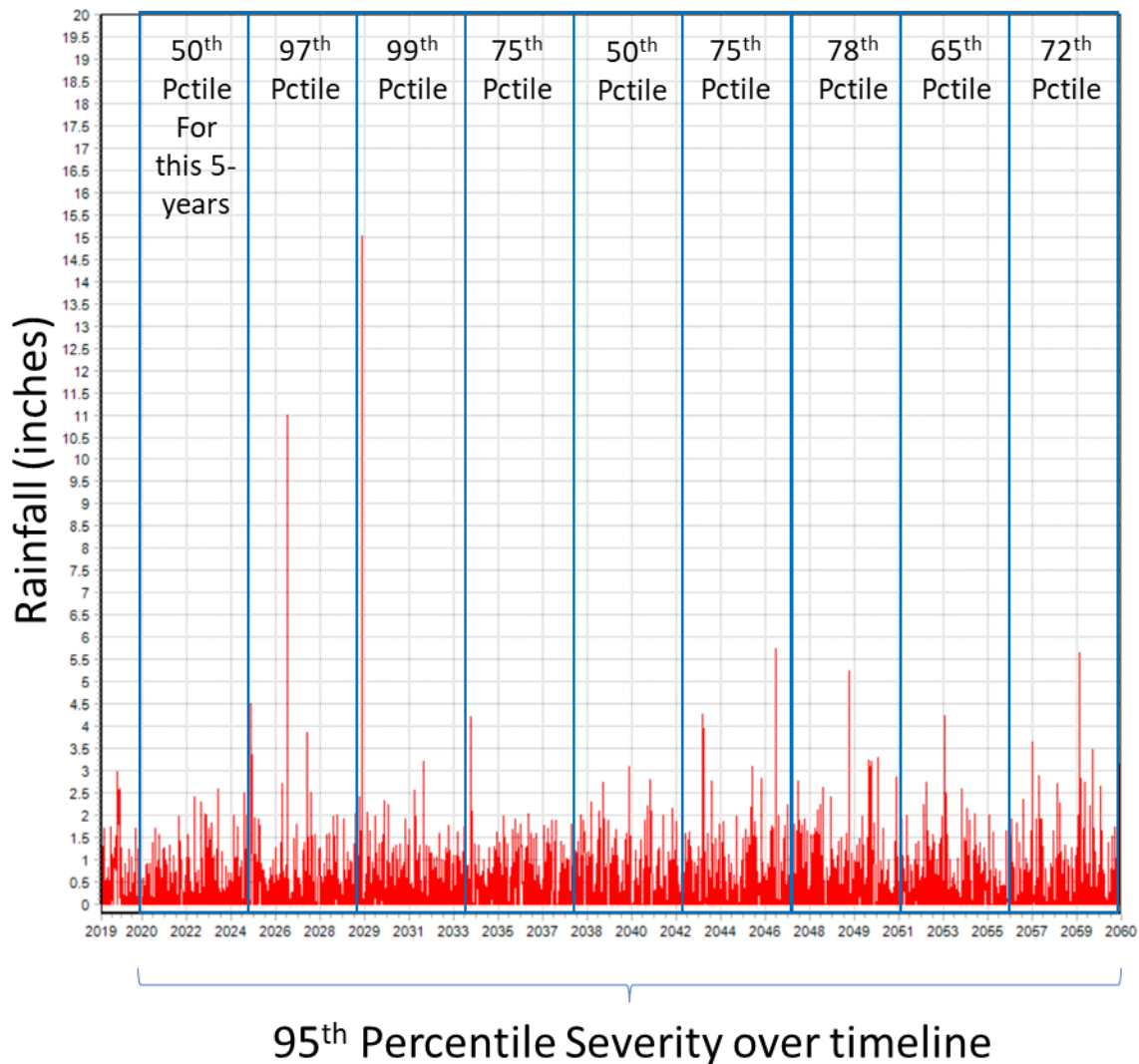
The projections were generated using a combined temporal statistical downscaling and Monte Carlo algorithm that blended historical daily rainfall with monthly general circulation model projections of rainfall for the area.

4.2.1.4 *Enabling Comparison of Present-Day and Mid-Century to Quantify Climate Change Impact*

One of the key questions of the study is how the impacts of climate change are changing over time. The majority of GCMs predict that extreme storms will become more extreme as the century progresses. This implies that the choice of weather projections used to drive the simulation should embed these changes in storm statistics over time.

The assessment of severity described above does not consider when in the timeline the severe events are occurring. This means that if a specific projection is selected to drive the simulation – say the 95th percentile projection – storms within the projection can potentially be early in the timeline, late in the timeline, or any combination in between. As long as the specific storms are large enough, an infinite set of rainfall projections is possible. Moreover, as Figure 4.6 shows, if the timeline is split into bins, while the full forecast may have the 95th percentile severity metric, the bins will have varying severity when the severity of only the storm events within the bin are compared to other storm events projected in different realizations.

Figure 4.6: 95th Percentile Rain Projection at Lumberton NC with Severity Estimates



The 95th percentile daily rainfall projection for Lumberton, NC. Note the projection is ranked 95th percentile severity overall but varies in severity ranking when considered in 5-year bins. To ensure a meaningful comparison of early and late period rain statistics, an early and late period projection was created where the first five years and last five years were ranked 95th percentile severity in addition to the full timeline being ranked 95th percentile severity. Note: Pctile is short for Percentile.

This presented a challenge for answering the climate change impact study question. If the projection selected to drive the simulation is front-loaded (severe storms early in the timeline), it will show that climate change impacts are minimal if we simply compare the impacts in the period at the end of the simulation to the impacts in the period at the beginning. Comparing statistically similar impact levels at the start and end of the timeline is therefore required.

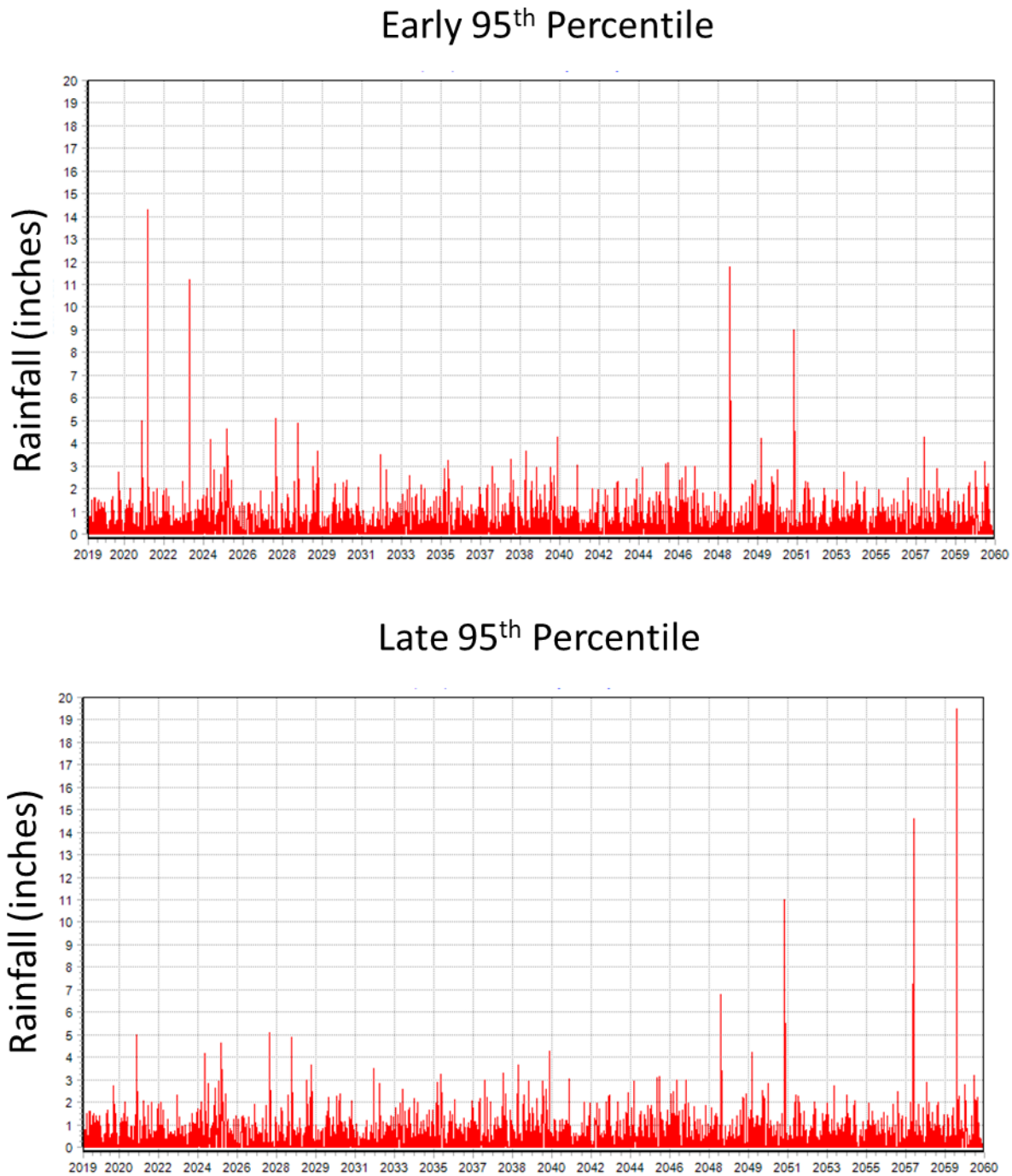
To solve this problem, the simulation was run with two rainfall projections, an early and late projection. The severity analysis was run both for the full timeline and for the 2021-2025 and 2056-60 bins. The

early scenario was both 95th percentile severe over the full timeline and for the 2021-2025 bin. The late scenario was both 95th percentile severe over the full timeline and the 2056-60 bin.

Estimates of climate change impact across the various metrics in the simulation (disrupted trips, storm damage, lost productivity, etc.) were then evaluated for the early bin using the early rain projection and for the late bin using the late rain projection.

The early and late rain projections – based at Lumberton, NC – are shown in Figure 4.7.

Figure 4.7: Early and Late Rainfall Projections at Lumberton NC



Early and late 95th percentile daily rainfall projections for Lumberton, NC were generated using Atkins Stormcaster algorithm. These realizations were ranked 95th percentile most severe compared to a library of 1,000 realizations created with the same algorithm. Further, the early scenario is ranked 95th percentile severity in the years 2019-2024 compared to other realizations in the same time frame. The late scenario is ranked 95th percentile severity in the years 2056-60 compared to other realizations in the same time frame.

4.2.1.5 *Worst Case Scenario*

A key modeling parameter is the rainfall severity percentile used in the final simulations. Within this study, the 95th percentile was used throughout. Like the logic of assessment using a design storm, the rationale is to use this near-worst case future realization to ensure vulnerabilities are exposed and solutions stress-tested under the more adverse conditions the corridor is likely to experience.

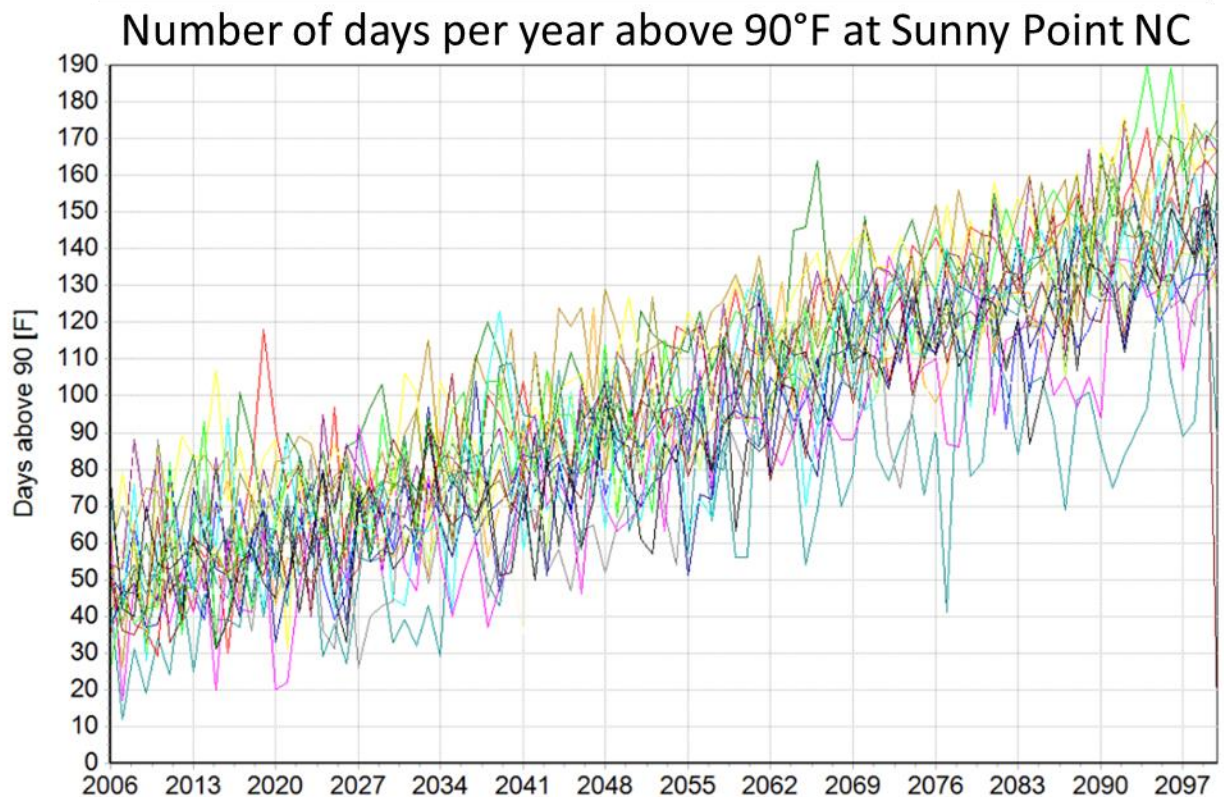
4.2.1.6 *Discussion on Early vs. Late Severity Rainfall Projections*

The choice of early or late severity rainfall projections raised considerations about which was a stronger stress-test for the transportation corridor. Intuitively, a front-loaded rain projection – with the most severe storms in the 2020s – will generally present a higher impact scenario, because NCDOT will not have had time to implement resilience measures before the storms occur. A back-loaded rainfall projection, given the impacts of climate change, will have more severe storms by magnitude than a front-loaded one, but by the time the storms occur, NCDOT will have had time to build a more resilient transportation system. These situations were observed in the simulation, particularly in the resilience-focused scenario described in the Adaptation and Mitigation section later in this document. Consult the results chapters for further discussion on this topic.

4.2.2 Temperature

Daily temperature projections used in the simulation were extracted from the LOCA dataset, as shown in Figure 4.8 which is a spatially and temporally downscaled product derived from the CMIP5 GCM projections. The LOCA dataset is downscaled to 1/16th degree and daily time-step. Daily maximum temperatures from the UNIPCC RCP8.5 scenario version of the LOCA dataset were used in the study to estimate heat exposure impacts to corridor residents and travelers, as well as impacts on the railroads in the form of potential track buckling.

Figure 4.8: Days Per Year Above 90° at Sunny Point, NC



An ensemble of 22 GCM-based projections of maximum temperature were used from the LOCA dataset. Here, the 22 members of the ensemble at a single grid cell near Lumberton, NC, was evaluated by the number of days exceeding 90° F each year. The upward, projected trend showed strong agreement among the models that future temperature increased dramatically over the coming century.

4.2.3 Sea Level

By 2060, mean sea level was projected to rise in Wilmington, NC between 1.28 feet and 2.26 feet relative to current mean higher high water (MHHW) (NOAA SLR Viewer). By 2100, this range varies from 2.17 feet to 6.66 feet. Rising sea levels will give rise to both chronic and acute disruption events, namely tidal or nuisance flooding and storm surges exacerbated by higher mean sea levels. To capture this disruption in detail, a high-detail sea level projection was needed that included tidal fluctuation.

4.2.3.1 Creating a Daily Projection of Sea Level with Tidal Fluctuation

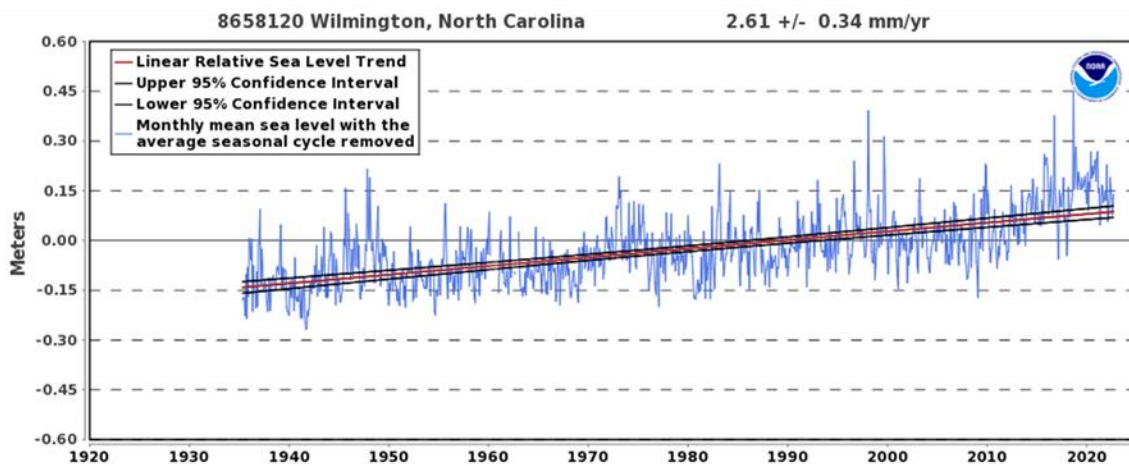
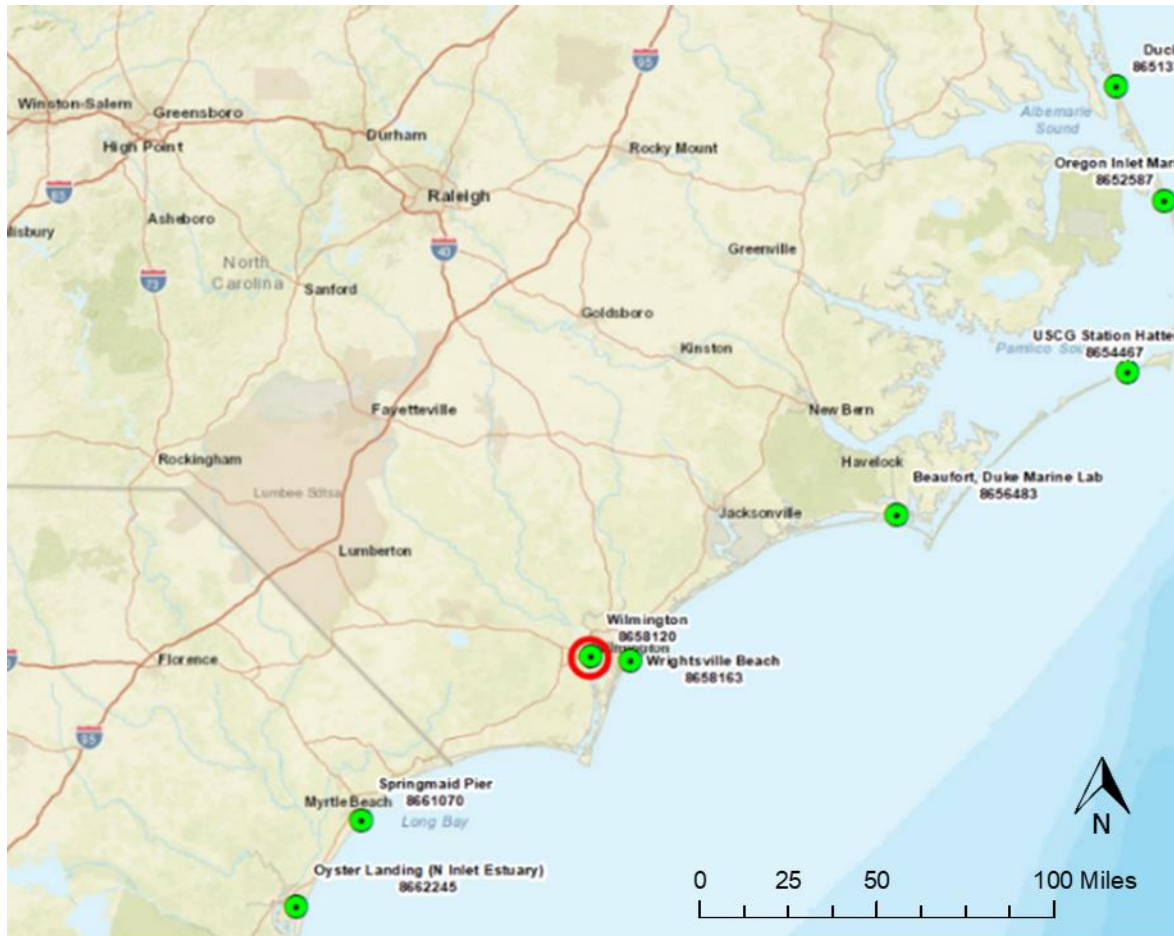
Daily projections of three phenomena were developed and superposed to produce the tide projection. The three phenomena included:

- **Mean Sea Level** – To reflect projected sea level rise, the NOAA intermediate projection of mean sea level at Wilmington, NC was used (Figure 4.9). The intermediate projection was selected from the array of projections (low, intermediate, high, extreme) by comparing the measured sea level increase in Wilmington, from 2000 to 2020, with the four projections for the same period.

The lowest root mean squared error (RMSE) projection was intermediate. See Figure for a comparison. Under this projection, the mean sea level in the simulation is projected rise by 1.54 feet over the course of the simulation.

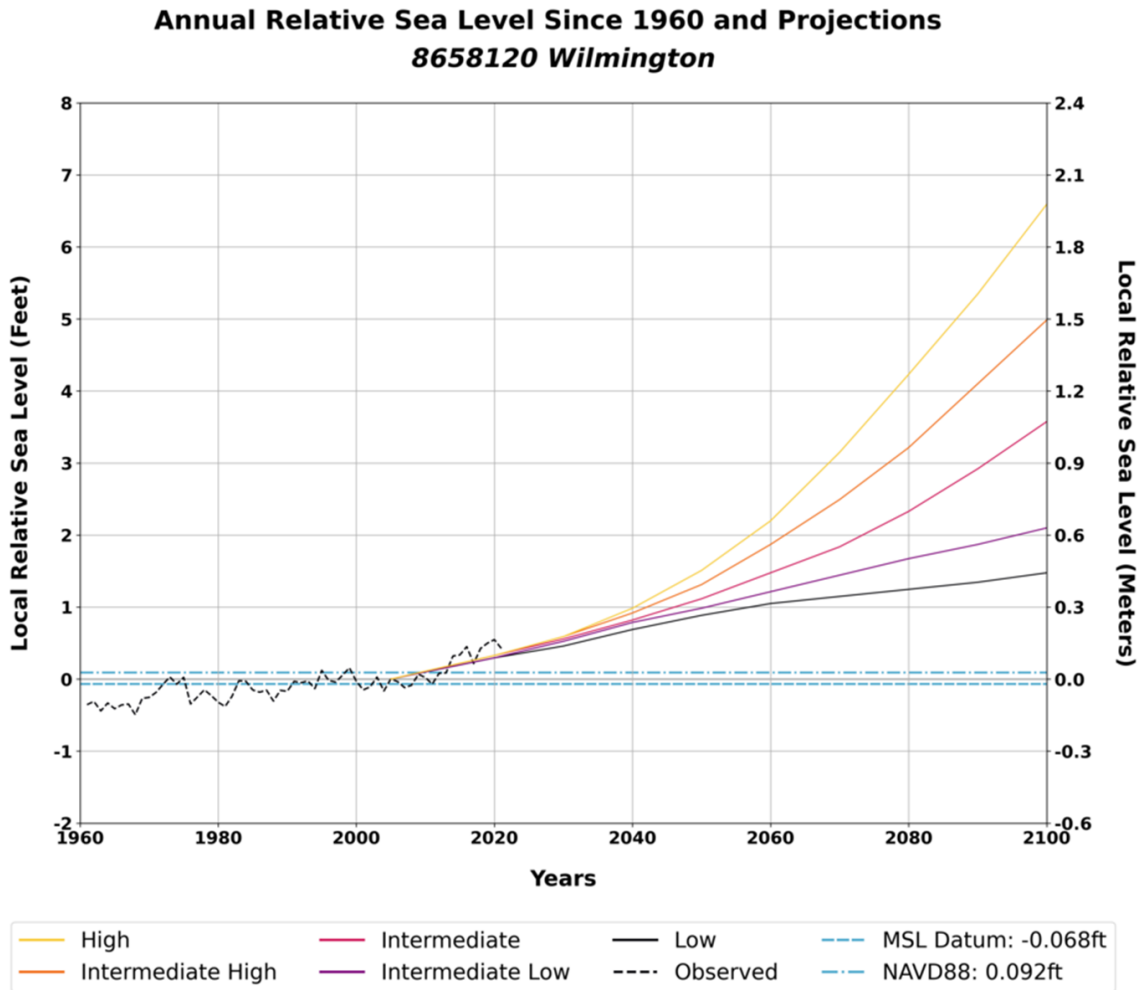
- **Tidal Predictions from Gravity Effects** – To reflect the effects of gravity on tides from bodies such as the sun and moon, 2020—2060 tidal predictions were downloaded from NOAA’s water levels server for Wilmington, NC. These predictions provided estimates of daily high and low tides.
- **Tidal Prediction Residuals Based on Historical Residuals** – To reflect the impacts of phenomena like windstorms, rainstorms, and river flows on tide levels, a historical set of residuals was developed by subtracting actual tide levels at Wilmington, NC from the tidal predictions mentioned above. These residuals were used to calibrate a Markov probabilistic model that predicts the residual for a given day, based on the value of the residual from the previous day. The process used to generate the projection was embedded in City Simulator. The approach is, for this specific part of the analysis is considered proprietary. But Markov probabilistic models are used for stochastic weather, tide, and a host of other types of time series for decades. For an overview on the process, [please refer to this reference](#).

Figure 4.9: Trends in Sea Level at NOAA 8658120 Station, Wilmington, NC



Notes: Upper panel – location map of the 8658120 tide station. Lower Panel – trends in sea level as provided by NOAA water levels site. Note provided by NOAA water levels site: “The relative sea level trend is 2.61 millimeters/year with a 95% confidence interval of +/- 0.34 mm/[year] based on monthly mean sea level data from 1935 to 2021 which is equivalent to a change of 0.86 feet in 100 years.”

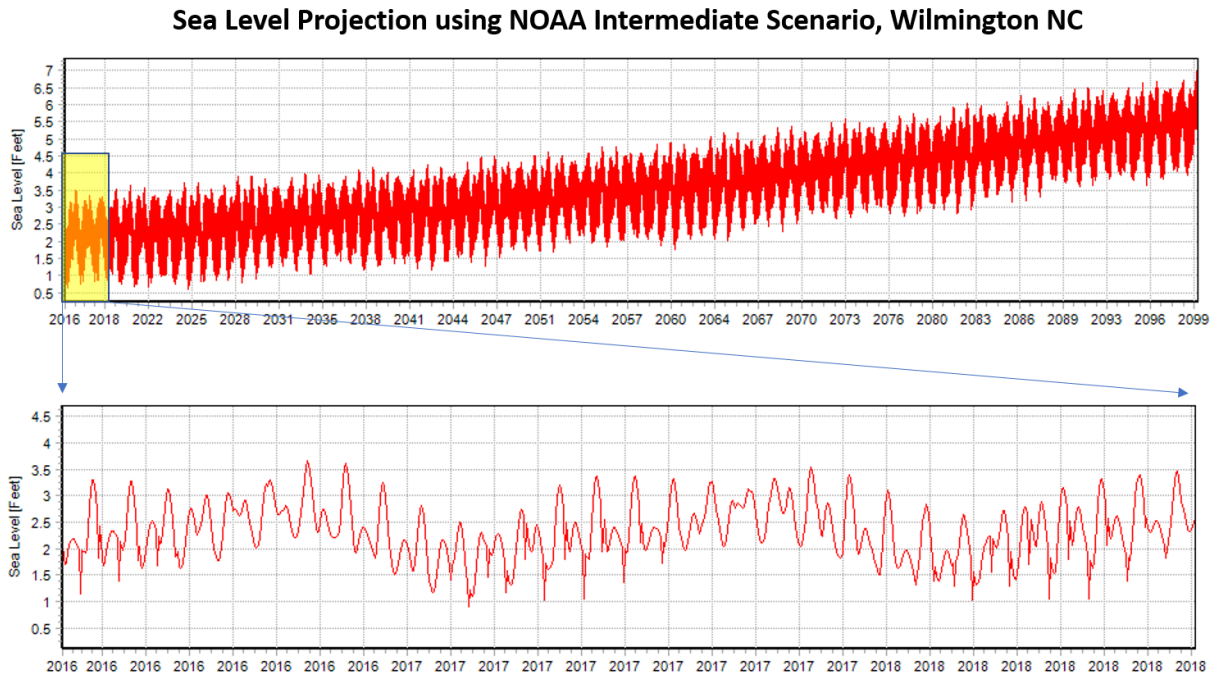
Figure 4.10: Projected Mean Sea Level at Wilmington, NC



Notes: Projections of sea level from NOAA, plus historical observed tide. In this study, the intermediate projected mean sea level scenario was used as it matched with an observed increase from 2000-2020. From the NOAA tide level site: “The projection of future sea levels that are shown below were released in 2022 by a U.S. interagency task force in preparation for the Fifth National Climate Assessment. The projections for five sea level change scenarios are expected to assist decision makers in responding to local relative sea level rise. The 2022 Sea Level Rise Technical Report provides further detailed information on the projections.”

The resulting projected tide series is presented in Figure 4.11. The upper chart presents the full time series generated from 2018 – 2100. The portion used in the simulation was from 2020-2060. Note the upward slope in the projection, which reflects the NOAA intermediate mean sea level projection. The lower panel in Figure 4.11 shows a zoom-in to the first several years of the chart, highlighting the tidal fluctuations which are key to understanding day-to-day disruptions from tidal flooding in the eastern portion of the corridor.

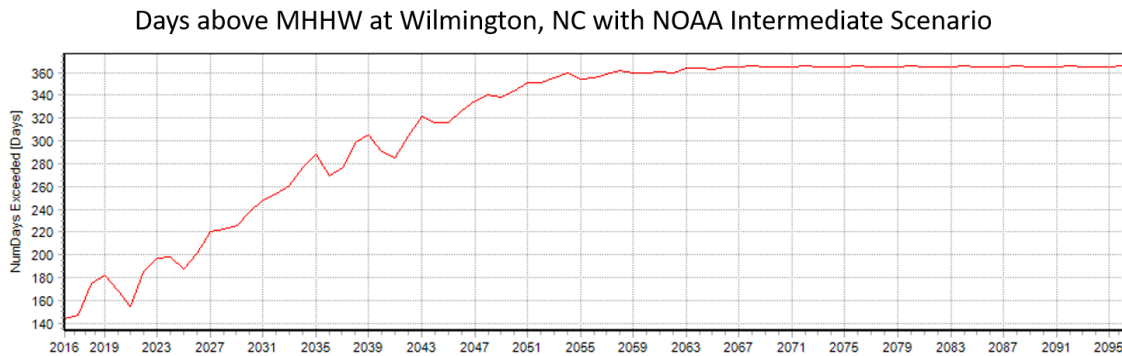
Figure 4.11: Projected Max Daily Sea Level at Wilmington, NC



The projection blended gravitational effect predictions of the tide at the gauge probabilistic-model-based projection of actual tide-predicted tide residuals and the NOAA intermediate mean sea level scenario projection described in the image above.

An assessment of the tide projection was conducted to evaluate the number of days above MHHW at the Wilmington station, as shown in Figure 4.12. The chart shows that from 2016 to mid-century (approximately 2050), there is a steady rise in the number of days above MHHW. After this point, tide levels are projected to reach MHHW every day of the year. This has important implications for disruption from sea level rise, as both nuisance flooding and elevated storm surge on higher seas will steadily become increasing disruptors.

Figure 4.12: Days above MHHW at Wilmington, NC When Using NOAA Intermediate SLR Forecast



The projected sea level time series (see Figure 4.11) was used to derive days above MHHW metric from 2016 to end of century at the location of the Wilmington, NC gauge. The chart shows that by mid-century, tidal inundation will be an everyday occurrence.

4.2.3.2 Recommendations for Tide Simulation in Future Studies

The tidal projection developed could be improved in several ways to reveal even more detail on potential future tide-related flooding:

- Incorporate uncertainty in the mean sea level projection** – the mean sea level projection has significant uncertainty, which grows into the future. The approach of selecting the scenario from the array of NOAA scenarios that best match the 2000-2020 actual tide levels provides confidence that the simulation matches conditions being observed in Wilmington. But the remaining scenarios from NOAA should be used to estimate the uncertainty in the projection – or some other suitable method for uncertainty estimation. This uncertainty should be propagated through the simulation to provide error-bars for tidal disruption estimates, which will improve decision support.
- Improve tidal residual estimates** – the projection of tide residuals uses a Markov probabilistic model that is dependent on historical residuals. Implicit in this approach is an assumption of stationarity. That is, that the residuals will have the same distribution and dynamics they had in the past. As climate change proceeds, daily tidal behavior may shift statistically in response. As such, an investigation into methods to project the shift of the statistics of the Markov-based projections with time should be undertaken.

Alternatively, a different approach could be taken for tidal projections that is more physically based, such as incorporating a 2D or 3D hydrodynamic model into the tide projection framework. While this would have a significantly higher level of effort, existing hydrodynamic models of the coastal region around Wilmington do exist and may be useful in taking this approach.

4.3 Building and Structure Modeling

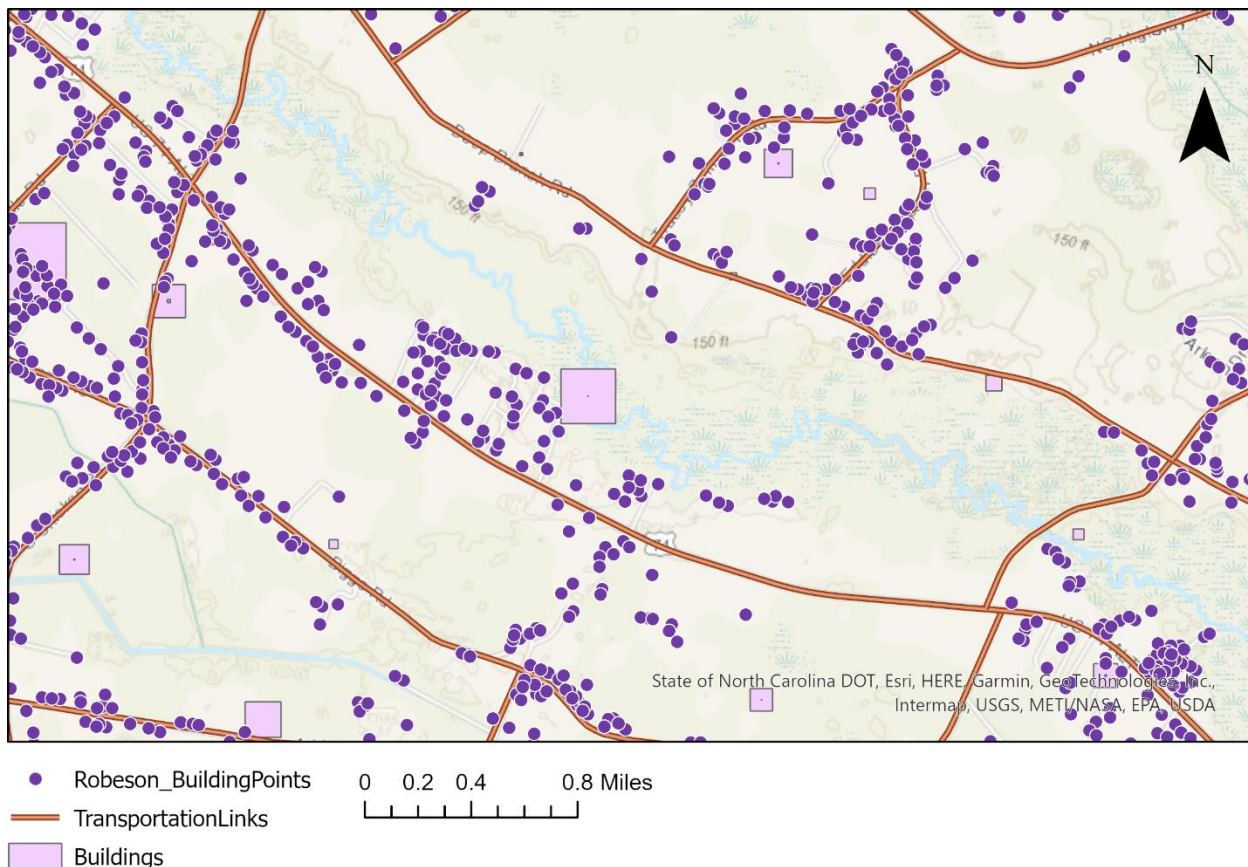
There were approximately 473,000 buildings in the U.S. 74 study area. These buildings were partitioned into residential and commercial categories. The population of 1.1M in the corridor were represented as agents that live in the residential buildings and work in the commercial buildings. The process for synthesizing the agent population is described in the demographics section below.

The buildings were sourced from a joint building footprint/parcel GIS layer couplet. The building footprints were derived from a building footprint layer developed by Microsoft, and the parcels were derived from the statewide parcel layer prepared by North Carolina Emergency Management (NCEM). This joint GIS layer, developed by Atkins before the start of the U.S. 74 study, is stored as county-level geodatabases in Atkins' servers. The geodatabases for the counties that covered the corridor were used.

4.3.1 MegaBuildings

Because the study questions focused more on the transportation system and less on the system of buildings, the buildings were converted to so-called "MegaBuildings" as shown in Figure 4.13. In this process, single buildings along each road segment were merged into an effective multi-family residential building and multi-tenant commercial building located at the geographic centroid of the road segment. This process also had the effect of speeding up simulation run times.

Figure 4.13: MegaBuildings



MegaBuildings (pink squares) were created at the centroid of each road segment. These structures were modeled as multi-family residential and multi-business buildings. The number of units/businesses in each MegaBuilding was evaluated as the number of real structures (purple circles) present on the road segment of interest. This figure shows an example set of road segments in Robeson County. Megabuildings were created for all road segments in the corridor.

4.3.2 Controlled Access Road Segments

Because controlled access road segments (i.e., interstates, U.S. highways) do not typically support residential or commercial structures directly, these road segments were not assigned MegaBuildings in the simulation.

4.3.3 Building Flooding Not Simulated

The process of generating MegaBuildings necessarily eliminated building-by-building simulation of flood from the simulation. In other simulations conducted with City Simulator, each building's first-floor elevation (FFE) is compared to the riverine, pluvial and, where appropriate, storm surge and tidal flood levels when storm events occur. When the projected flood exceeds the FFE, building flooding is assumed to occur and storm damage is estimated by way of Hazards United States (HAZUS) depth/damage curves. With the megabuilding approach, building storm damage estimation was removed from the simulation.

4.4 Travel Modeling

The simulation integrated a travel model that simulated corridor residents and outsiders using the road system in daily activities, such as commuting, recreation, carrying freight and other activities. With the daily time-step used, travel was simulated as the usage of a set of road segments per day by each corridor resident. The specific road segments used were determined in the population synthesis step. See the section on agent modeling (following this section) for more details on this process.

4.4.1 Simulating Trip Disruption

One of the key functions of the travel model was to pinpoint where disruption from climate change-influenced events occurred during the simulation. Road segments were impacted by both flooding events and heat events. When these events occurred, a disaster event was created and associated with the road segment. The disaster event had a recovery period that went from a single day for minor flood overtopping events and heat events to many months for major flooding events. The specific recovery duration rules for each disaster type are specified below in the sections on flood and heat modeling.

For each day of the recovery period, all trips that normally occurred on the associated road segment were recorded as disrupted. Therefore, disrupted trips become an important metric for understanding how climate change impacts transportation — both at hotspots in the road network and rolled up to the county, division, and full corridor level.

4.4.2 Creating the Road Network

The road network was a key GIS model component in the travel simulation. The network was held in the transportation links and transportation nodes layers of the City Simulator database. Each agent in the simulation was associated with two buildings: a workplace and a residence. The buildings were associated with the closest transportation node. As part of setting up the simulation, the complete set of shortest paths from each transportation node to each other transportation node was evaluated, a computationally intensive process that followed the well-known Dijkstra algorithm.

The modeling goal was to represent the transportation network in sufficient detail so the likely door-to-door path each traveler takes from origin to destination was represented explicitly for the majority of travelers. Furthermore, sufficient detail in the road network was needed to capture locations of flooding and the disrupted traffic accurately. The competing goal was to reduce the number of road segments in the network and to reduce the number of computations needed to define the commute paths. For this reason, the transportation network typically included interstates, ramps, state and arterial route classes. Local roads were typically excluded, and the buildings they served were schematically connected to the higher volume road segments which connected the places to their local roads.

Additionally, the higher volume network was pruned to reduce the number of road segments. The pruning process included the following steps. Each step is described in general terms, and then a note is provided describing the specific actions for the U.S. 74 study related to the step. Using a combination of these steps, plus careful quality control, a detailed but simplified network of road segments was created, minimizing the computational burden during simulation but also capturing the majority of locations of highly disruptive flooding.

Removing Danglers — This included finding road segments that were shorter than a threshold and were only connected to the network at one end. These segments were removed from the final network.

- **U.S. 74:** Danglers shorter than one mile were removed. This was done after removing ring roads, a process that often resulted in and created danglers.

Removing Ring Roads — These were roads with an end point that was the same as their start point. Typically, these road segments represented the circuit route in a small neighborhood. They were also removed. Another road type classified as ring roads were roads with a start point and end point that connected to the same route. These were identified and removed as well.

- **U.S. 74:** Ring roads were removed, which simplified the network. This process was run iteratively, combined with removing danglers to prune much of the high-density route networks, and represented non-local routes in subdivisions.

Unsplitting - Unsplitting means uniting two roads that have a start point and endpoint in common and no other road connecting at the same point. Used as a post-process after removing danglers, unsplitting typically achieves a large drop in the number of road segments.

- **U.S. 74:** During the course of developing the network, a Quality Control (QC) process found multiple route segments that had opposing flow directions in the original data provided from the NCDOT linear route system (LRS). Using Esri's unsplit tool resulted in unsplit routes where the vertices of a portion of the segment flowed in one direction, while the vertices of the remaining route segment flowed in the other. This caused problems with transportation simulation because road segments are required to be single direction. To remedy this problem, a new unsplit tool was developed within City Simulator that corrected the direction of flow of one of the road segments before combining the two road segments. Unsplit was used repetitively in the network development process, typically after the removal of danglers and ring roads, as their removal by definition results in two road segments that qualified for unsplitting.

Planarizing — This process is one of the advanced editing tools in Esri ArcMap. It splits road segments where other road segments intersected them.

- Planarizing was used in sequence with unsplit, as unsplit occasionally joined two route segments where a joining route existed.

Merging Divided Highways - This Esri geoprocessing tool identified routes that ran parallel to each other within a set tolerance and merged them into a single line. This tool was used carefully in the pruning process, as often flooding had impacted one side of a divided highway and not the other.

- **U.S. 74** – As the focus of the study was on U.S. 74, which is a divided highway, the merge divided highway tool was not used. This preserved the main U.S. 74 infrastructure, as well as I-95 and other interstate infrastructure, which was key to understanding flooding on these roads.

Removing Segments by Route Class – This step involved pruning road segments by identifying those that were not likely needed by route class and deleting them.

- **U.S. 74** - All classes, except for interstate, U.S., and state highways and ramps were removed from the network. Notably, this meant no local roads were considered in the analysis.

The resulting set of tools and processes created during the road network creation will be a valuable resource in future City Simulator studies of other corridors in North Carolina. The process helped to identify the QC goals for future modeling. Additionally, the process developed unique tools that aided greatly in developing networks in other corridors. As the road network is the key geographic scaffolding for the study, ensuring high quality was essential in its creation.

4.4.3 Calibrating the Travel Model

Calibrating the travel model was completed with two datasets, recorded AADT on a subset of road segments and results data from the NCDOT Statewide 2045 Transcad travel demand model, Charlotte Regional Transportation Planning Organization 2050 Transcad travel demand model, and Wilmington Urban Area Metropolitan Planning Organization (MPO) 2045 Transcad travel demand models. All data was collected and provided by NCDOT.

The reported AADT data was used to set AADT in the simulation in the base year. The process of population synthesis created the simulation agents and assigned their commutes paths, resulting in a set of AADT for corridor residents. Where there was a discrepancy between the corridor AADT defined by the simulation and the reported AADT, it was assumed that outsider agents were making up the remaining trips. The agents were created and assigned homes and workplaces in phantom buildings on the border of the corridor analysis domain.

The Transcad models were used to corroborate the increase in trips throughout the simulation, which is driven by corridor population growth. The Transcad models results provided estimated trips on major roads in 2017 and 2045. These data were used to calculate a projected growth rate for each road segment. During the simulation, a growth rate was evaluated for each road segment and, where a Transcad estimate was available, compared to the projected Transcad growth rate. Where the simulated growth rate was lower than the Transcad growth rate, additional outsider agents were added to the phantom buildings during the simulation and given commute paths along the routes with under-projected trips.

4.5 Agent Modeling

The simulation represented users of the transportation system as agents. Agent activities that used the transportation system such as commuting were simulated daily. They typically followed the assumption that agents joined the transportation network at the node closest to their home and traveled to the transportation node closest to their destination (i.e., their workplace) using the shortest path, which was derived by the Dijkstra algorithm as mentioned in the section on travel modeling above.

4.5.1 Calibration with Data from the U.S. Census American Community Survey

Population, jobs, households, and distribution of commute times at the census block group level were downloaded from the American Community Survey (ACS). These data were used to synthesize the population of agents, distributing them to the MegaBuildings so that the population, jobs, and households matched at the census block group level. Further, the agents' residences and workplaces were distributed, such that the estimated commute time distributions of agents in each census block group matched the reported commute time distribution.

The Transcad models provided by NCDOT (see Section 4.4.3) was used to set population growth rates in the simulation. The models provide population estimates at the traffic analysis zone (TAZ) level. A growth rate for each TAZ was defined using the 2017 and 2045 estimates provided. As new residential buildings were added to the corridor during simulation, the number of people in them was estimated using the growth rate of the TAZ in which they were placed. For example, if a TAZ was expected to grow in population 50% from 2017 to 2045 and its initial population was 10,000 people, then in each year of the simulation, the additional population should be equal to $0.5 * 10,000 / 40$ years, or 125 people. In this case, when a new residential building was added in the simulation, the simulator would ensure there were 125 people multiplied by the number of years since the last residential building. This ensured that growth rates matched the Transcad models.

4.5.2 Calibration to Reported AADT

Residents within the corridor comprised some percentage of daily trips in the corridor. Out-of-corridor agents on trips that entered and left the corridor represented a larger percentage. As such, NCDOT's reported AADT in the first year of the simulation were used to further calibrate the model.

To match the trips to the reported AADT, phantom residential and commercial buildings were created, where roads entered/left the corridor. A portion of corridor residents was assigned to workplaces at phantom commercial buildings, while a population of phantom agents was created with residences at the border of the corridor that worked within the corridor. A third set of phantom agents was created that conducted pass-through trips in the corridor, which means that they did not stop in the corridor on their trips. For I-95, in particular, this population was large to match the tens of thousands of trips per day that passed through the corridor daily without stopping.

These populations of phantom agents and in-corridor agents that left the corridor daily were synthesized, such that the AADT at each road segment matched reported AADT, while commute time distributions for each census block group matched reported distributions.

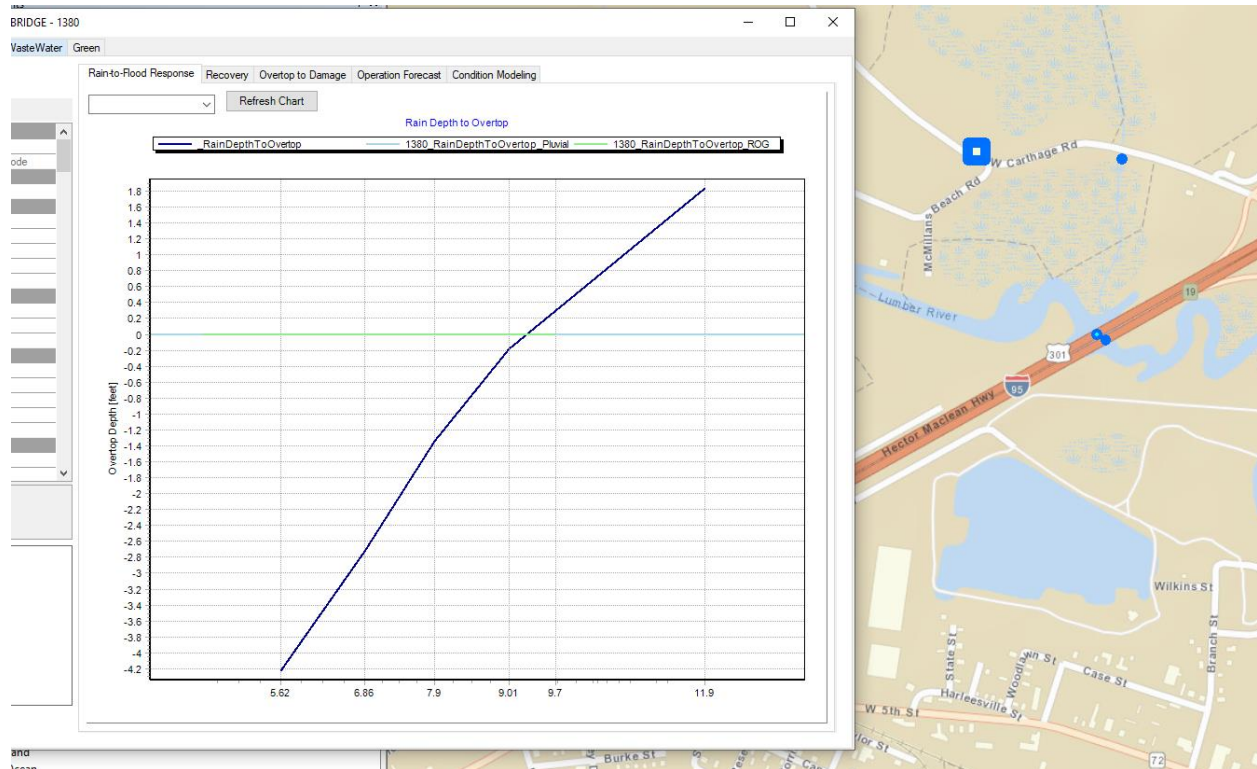
4.6 Flood Modeling

Multiple flood modeling datasets were used in the study, accounting for the different types of flooding experienced in the corridor. The flood types included pluvial, riverine, coastal, and tidal. Each flood tracking point in the simulation — culverts, bridges, pipes, and other known flood points on the road system — was assigned flood response curves from each set of models, where applicable.

The flood response curves relate the depth of rainfall to the depth of flooding at the tracking point, assuming that the return period of the rain event matches the return-period of the resulting flood.

When a rain event is simulated, the simulator uses the response curves to estimate the depth of each type of flooding at the tracking point. See Figure 4.14 for an example of a flood response curve.

Figure 4.14: Flood Response Curve Example

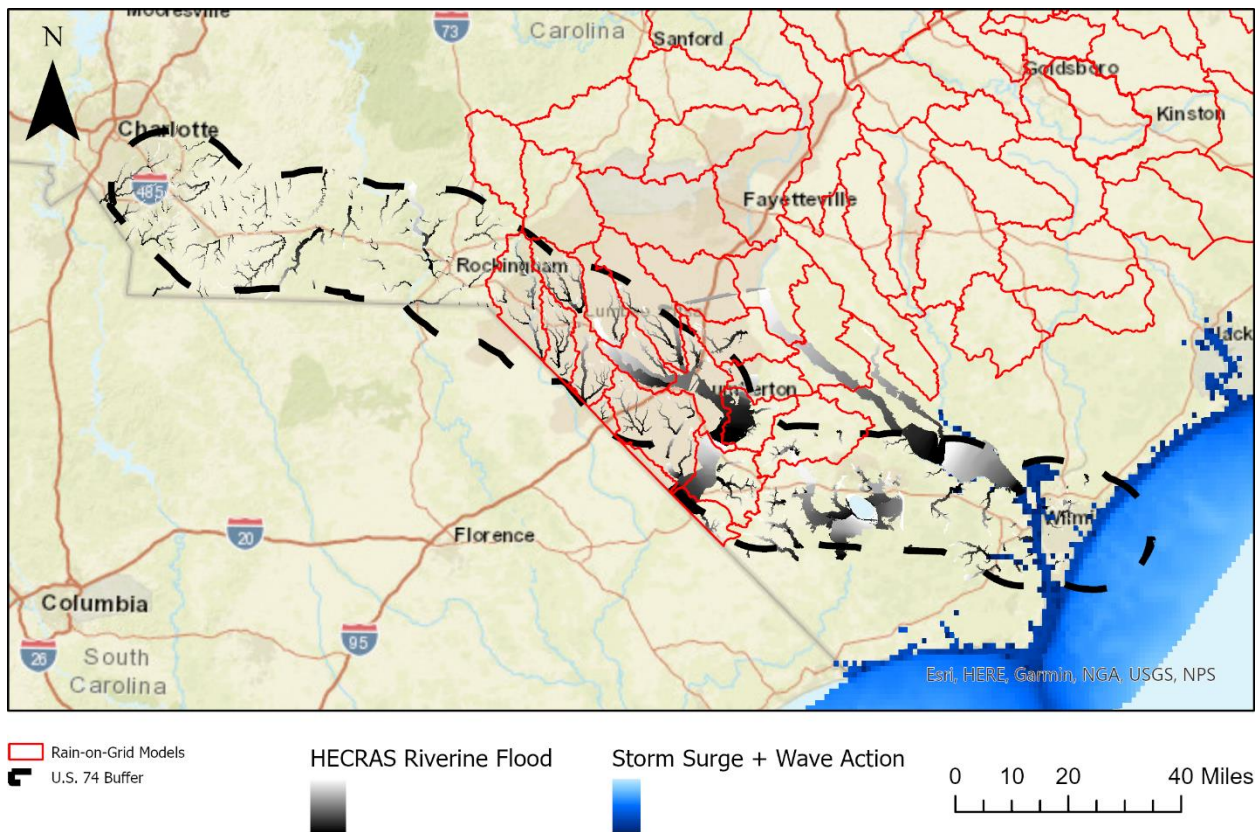


Screenshot of a flood response curve in the City Simulator tool. The rain depth to road overtop curve was a key piece of data tying the GIS-based digital twin of the corridor to the modeled flooding response from pre-existing flood models. The curve provides an estimate of the level of overtopping at a specific location on the road network (blue square on map), given a certain depth of rain from a storm. The curves were derived from a huge database of flood models described later in this section.

4.6.1 Riverine Flood

Riverine flood occurs when river flow becomes deep enough to overtop banks. A dataset of 331 existing HEC-RAS 1D models was used to build flood response curves at the 4,028 bridges, culverts, and other tracking points in the simulation. The models were developed and maintained by the North Carolina Flood Mapping Program (NCFMP) and provided by NCFMP for use in this study. The return-periods used were 10-year, 50-year, 100-year, and 500-year. See Figure 4.15 for a map of the model inventory.

Figure 4.15: Results from 331 HEC-RAS 1D Riverine Hydraulic Models



Riverine, pluvial, and coastal flood models covering the corridor were collected and sampled at the locations of the transportation assets (culverts, bridges, drainpipes, road low points) to create flood response curves that related rain depth to flood depth at each asset. There were 331 HEC-RAS 1D models (gray areas), HEC-RAS 2D Rain-on-Grid models covering approximately 40% of the corridor, and an Advanced Circulation (ADCIRC) model combined with a Wave Height Analysis for Flood Insurance Studies (WHAFFIS) model to estimate storm surge and wave action.

4.6.2 Pluvial Flood

Pluvial flood occurs when heavy rainfall ponds, causing localized flooding. Two datasets of pluvial flood models were used in this study:

Atkins Pluvial — This is a nationwide set of Telemac-2D models with a three to ten meter horizontal resolution produced by Atkins. For this study, the models covered the full corridor and were used to create rain-to-flood response curves at 10, 100, and 1,000-year return-periods for each of the stormwater tracking points.

Rain-on-Grid — These HEC-RAS 2D models were produced by the NCFMP. Each covers a HUC10 watershed, as shown in the map in Figure 4.15. These models are similar in nature to the Atkins Pluvial Telemac-2D models but have higher accuracy in their terrain and rainfall input data. Further, they have a more accurate depiction of hydraulic structures, like bridges, which has a substantial impact on model accuracy. The available models covered approximately 40% of the U.S. 74 corridor.

4.6.3 Coastal Flood

Coastal flood occurs with storm surge when heavy wind events push seawater inland. The total water level reached during these events includes both the surge component, as well as impacts of wave action. ADCIRC and WHAFIS models were used in this study to estimate the depth of flooding of these two components. See Figure 4.15, where the extent of the model is mapped.

4.6.4 Tidal Flood

The sea level projection mentioned above was used to estimate daily flood levels caused by tidal inundation. The section below covers sea level rise modeling and how tidal flooding was quantified in the simulation.

4.6.5 Summary of Flood Model Types Used in Simulation

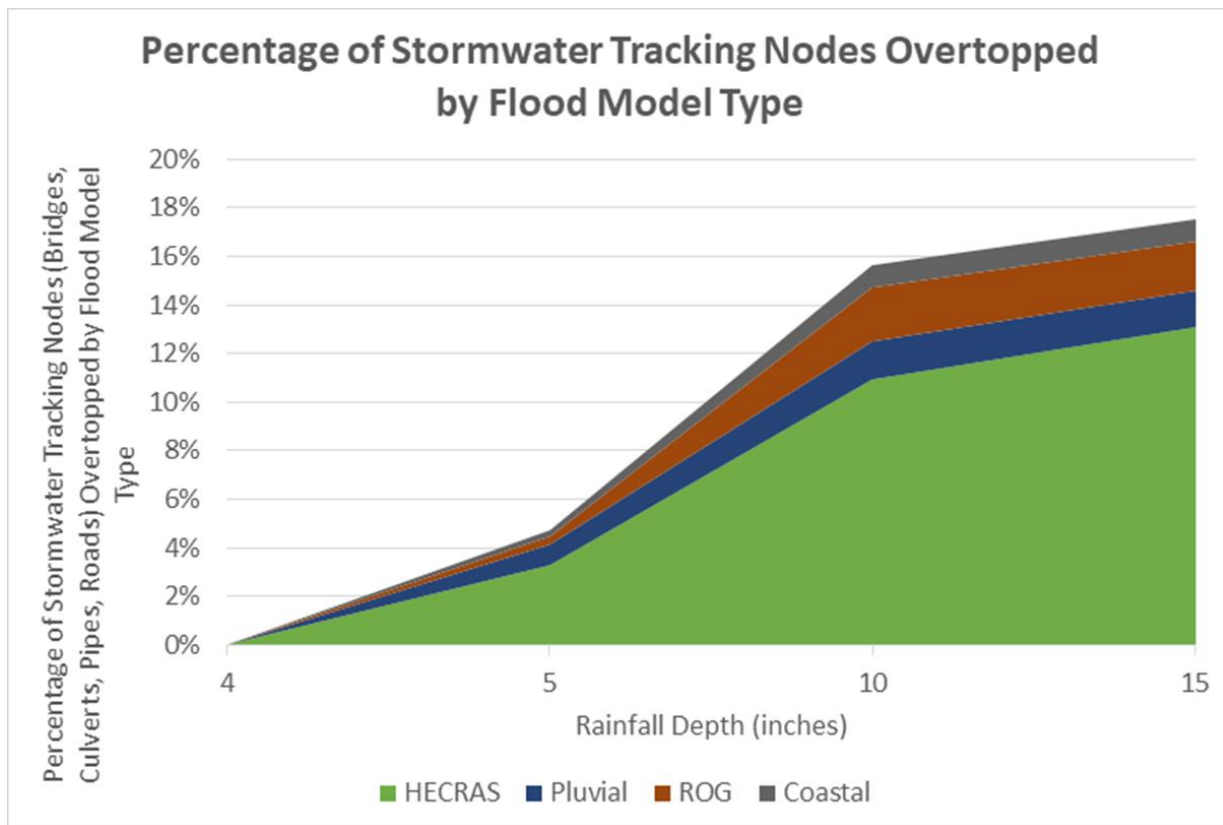
When a flood occurs in the simulation, the multiple flood models provide a varying set of flood depth estimates at each water crossing asset. The simulation was configured to take the deepest flood estimate as the expected flood level. The exception to this rule was the Atkins pluvial flood model set, which was only used when no other flood models were available for the asset of interest. See the section on avoiding overestimation of flood below for more detail.

In reality, in situations where multiple flood types occur in the same location, compound flooding may occur, resulting in a higher water surface elevation than any of the models predict. For this reason, the analysis team recommends investigation of compound flooding more closely in future studies.

Figure 4.16 summarizes the percentage of each flood model type used for storms ranging from four inches of total rain depth to fifteen inches. The chart shows that a total of approximately eighteen percent of the water-crossing assets experienced overtopping for the largest storms. For comparison, these storms were larger than recent large ones, like Hurricanes Matthew and Florence.

HEC-RAS 1D models were the majority model type used for flood depth estimation, comprising about 72% of cases. This was expected because these models depict the collection of water in floodplains over the landscape and therefore likely provided the deepest flood estimates. The remaining models, ROG, Atkins Pluvial and Coastal were used in the remaining flood estimates, with pluvial flooding (ROG and Atkins Pluvial) totaling about 22% of total flood events. This indicates that flooding outside the Federal Emergency Management Agency (FEMA) floodplain makes up a considerable portion of future floods.

Figure 4.16: Percentage of Water Crossing Assets Overtopped by Flood by Model Type and Storm Size



4.6.5.1 Avoiding Overestimation of Flood

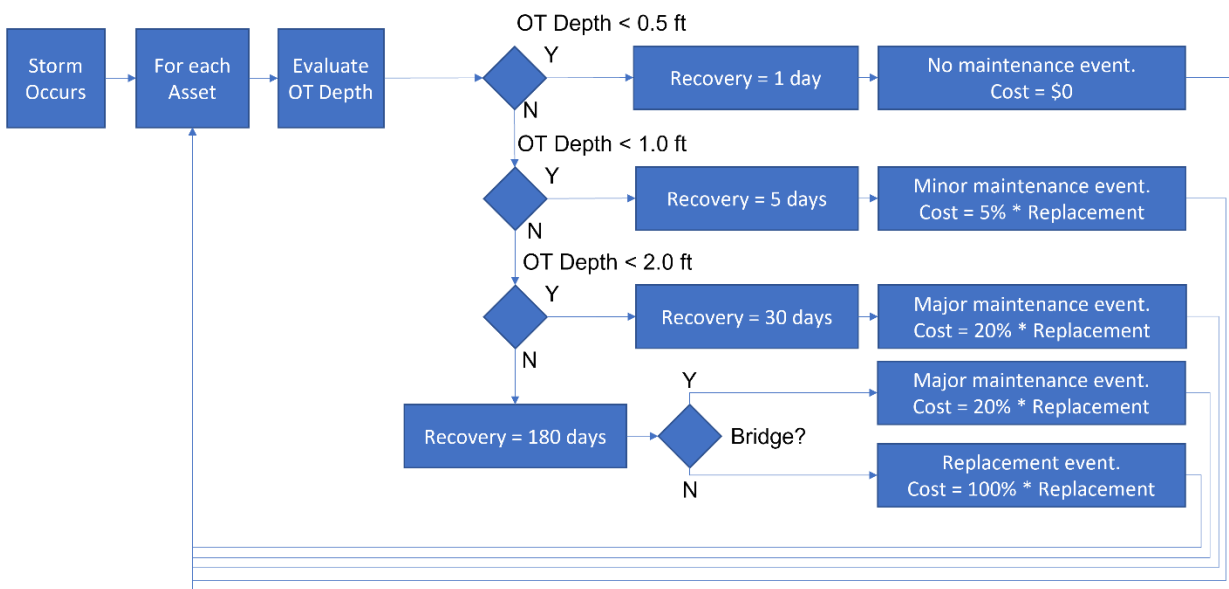
Sensitivity analysis showed that very often the deepest flood estimate came from the Atkins Pluvial models, and that when large events occurred, these models estimated upwards of 60% of water crossing assets were overtopped. Qualitative comparison between a simulation of an event similar to Hurricane Florence and drone footage of actual flooding during the same event revealed that 60% was likely a high overestimate. As a result, the simulation was configured to use only the Atkins Pluvial flood estimate when no other flood type estimate was available. This resulted in the percentages shown in Figure 4.16.

4.6.6 Disruptions from Flood Events

When one of the flood models predicts overtopping at a tracking point, the simulator creates a disaster event associated with the tracking point. The level of overtopping determines the recovery duration – the length of time that the asset of interest is non-operational. The rationale is a small depth of flooding may cause perhaps a day or two of traffic disruption and will likely cause no physical damage, while several feet of flooding will likely cause severe damage and even destruction of a road, resulting in months of recovery before the road segment is restored.

Figure 4.17: Simulating the Impact of a Flood on Transportation Assets

Simulation of Disaster Events in US74 Resiliency Study



The flowchart shows how the simulator assesses each asset when a flood event occurred. If the overtopping (OT) level, as estimated by the flood models described above, exceeds certain thresholds, then the asset is disabled and put into a period of recovery, and a maintenance event is created. The duration of the recovery period and the costs of the maintenance event increased with the depth of overtopping. Table 4.1 specifies the overtopping thresholds, recovery periods and maintenance event costs used in the simulation.

The flowchart in Figure 4.17 lays out the process the simulator uses for determining if an asset is in recovery and length of recovery. The parameters for the flowchart vary depending on the asset type (bridge, culvert, drainpipe). The specific parameters used for each asset type are shown in Table 4.1.

Table 4.1 lists the assets by type and the related overtopping thresholds that trigger each type of event (none, minor, major, replacement). As shown, the recovery period was set to increase with the level of overtopping and varies from one day to 180 days depending on asset type. Also listed are the type of maintenance event required to repair the flood damage and the cost of the work as a percentage of the replacement cost of the asset.

The set of model parameters were set so that the total cost for storm damage in a multi-year simulation that included major storms like Hurricanes Matthew and Florence matched the real spending during a period of the same duration. See the section on cost modeling below (4.7.5) for details on this calibration procedure.

Table 4.1: Modeling Parameters for Flood Impacts on Transportation Assets

Simulation of Disaster Events in US74 Resiliency Study

| Asset Class | Overtop Threshold (ft) (ie. Level <= threshold) | Recovery Period (days) | Maintenance Event Type | Cost as percentage of replacement cost (%) |
|-------------|---|------------------------|------------------------|--|
| Bridge | 0.5 | 1 | None | n/a |
| | 1.5 | 5 | None | n/a |
| | 4.0 | 30 | Minor | 3 |
| | Max | 180 | Major | 15 |
| Culvert | 0.5 | 1 | None | n/a |
| | 1.5 | 5 | Minor | 3 |
| | 4.0 | 30 | Major | 15 |
| | Max | 180 | Replacement | 100 |
| Pipe | 0.5 | 1 | None | n/a |
| | 1.5 | 5 | Minor | 3 |
| | 3.0 | 30 | Major | 15 |
| | Max | 60 | Replacement | 100 |

4.7 Asset Lifecycle Cost Modeling

Asset cost modeling was implemented within the simulation using the following methods.

4.7.1 Asset Types

There were 3,262 bridge, culvert, and pipe assets that were cost-modeled in the study. Additionally, there were 766 flood-prone road points modeled. This gave a total of 4,028 stormwater tracking points. The asset data was provided by the NCDOT from their GIS-based National Bridge Inventory System (NBIS) and non-NBIS databases. For the simulation, assets only above 54 inches in diameter were considered.

Note that while flood modeling was included for all tracking points, cost modeling was only done for water-crossing transporting assets (culverts, bridges, and pipes). Road maintenance and installation costs were not modeled.

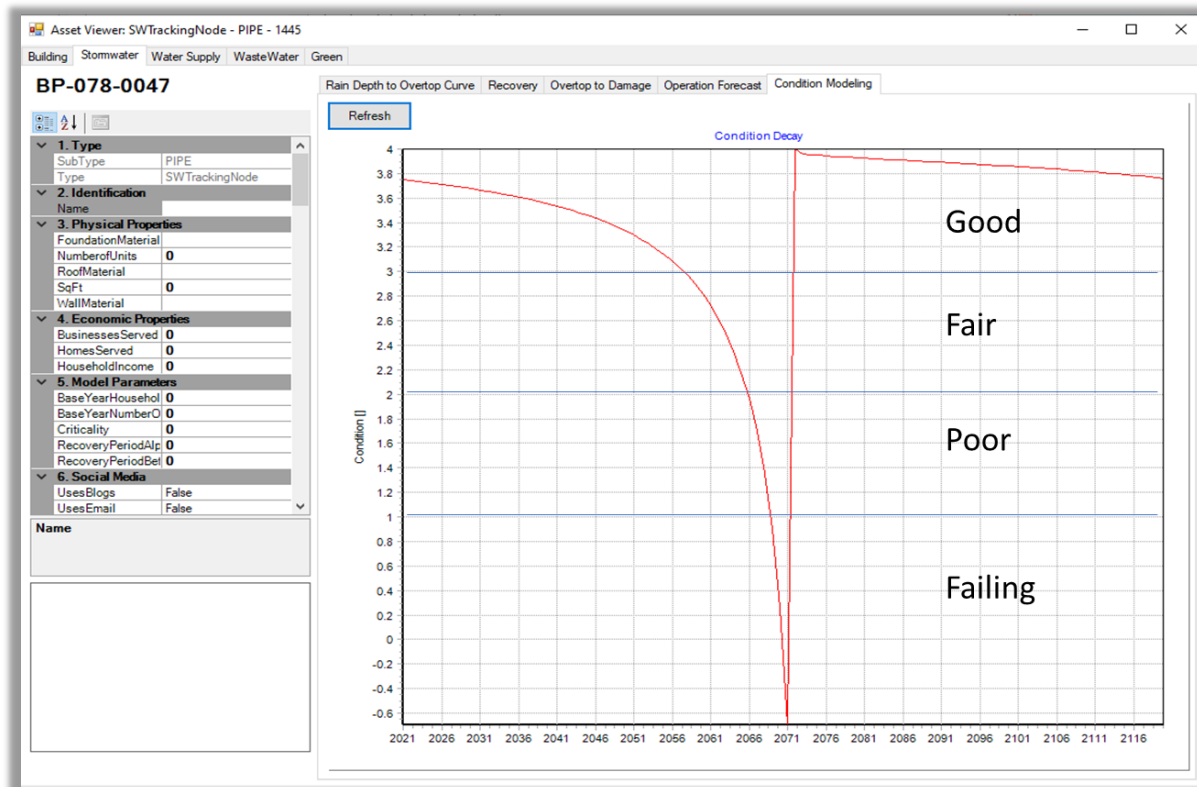
4.7.2 Condition Decay

Bridge, culvert, and pipe assets were simulated within the digital twin as stormwater node assets. Each was fitted with a decay model that projects the condition of the asset in the future according to a logarithmic decay pattern. Condition categories included Good, Fair, Poor, and Failing, which are

assigned numeric categories of 4, 3, 2, and 1, respectively. These categories were specified to match the existing condition category system used for the non-NBIS assets at NCDOT.

The logarithmic decay pattern reduces condition gradually at the beginning of the asset's lifespan and moves to increasingly faster decay toward the end of the lifespan. See Figure 4.18 for an example.

Figure 4.18: Example of Asset Condition Simulated with a Logarithmic Decay Model in the Simulation



Each asset was fitted with a similar model, and the 2020 condition for the asset was used as an initial condition.

4.7.3 Condition Category System

To start the simulation, initial conditions of the assets were set using the current asset ratings at the time of the analysis (Summer 2022).

A challenge in the simulation was to convert the two different asset rating systems for NBIS and non-NBIS assets into a single rating system. While the non-NBIS assets are classified in a simple good/fair/poor/failing system that corresponds to the whole asset, the NBIS system is multi-part, assigning different condition ratings to the superstructure, substructure, and other systems that make up the bridge.

To solve this, the non-NBIS condition category system (good, fair, poor, failing) was adopted as the system the simulator would use and a method for cross-walking between the two systems was developed to categorize NBIS structures into the four-category system. The crosswalk method is shown below.

Each NBIS structure has the following attributes:

- SR = Sufficiency Rating
- PRI = Priority Replacement Index
- GCR = General Condition Rating: Deck Condition, Substructure Condition, Superstructure Condition, Culvert Condition

The 4-category rating for the NBIS structure was set using the following conditions:

- IF SR 60 OR #PoorGCR > 1 OR SUBSTR <= 4 OR Any GCR <= 3 THEN "FAILING"
- ELSE IF #PoorGCR = 1 THEN "POOR"
- ELSE IF Any GCR in (5, 6) THEN "FAIR"
- ELSE "GOOD"

4.7.4 Maintenance Events

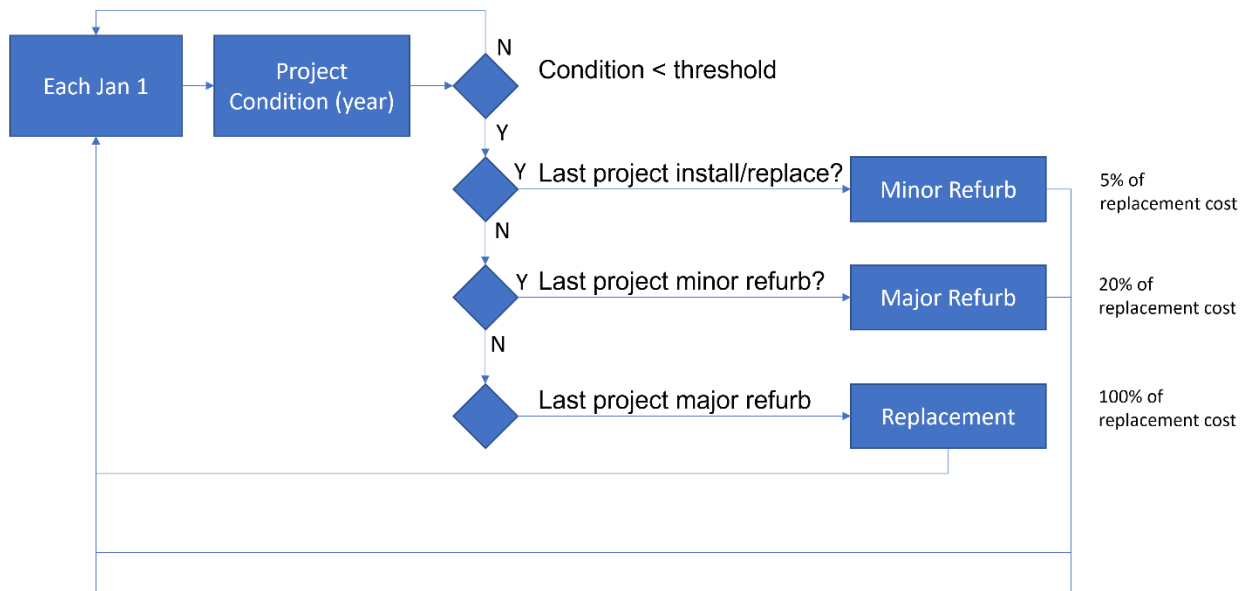
Maintenance events were simulated throughout the 40-year simulation. Figure 4.19 provides a flowchart describing the procedure the simulator uses to insert these events. At the beginning of each year, the asset condition is projected. If the condition crosses into failing, i.e., is less than or equal to 1.0, a maintenance event is created and associated with the asset.

In the simulator, maintenance events can be of several types including minor, major, and replacement events. They are inserted in that order as the asset ages: first minor, then major, then replacement. If no storm-damage occurs on the asset prompting early repair, the simulator adds minor events approximately 30 years since installation/replacement, major events at approximately 60 years since installation/replacement, and replacement events at approximately 75 years since installation/replacement.

The cost for the event is determined by event type, the replacement cost of the asset, and the type of asset (bridge, culvert, drainpipe). Figure 4.20 provides an example of the percentages of replacement cost for a generic asset. The actual percentages used are listed in Table 4.1 above.

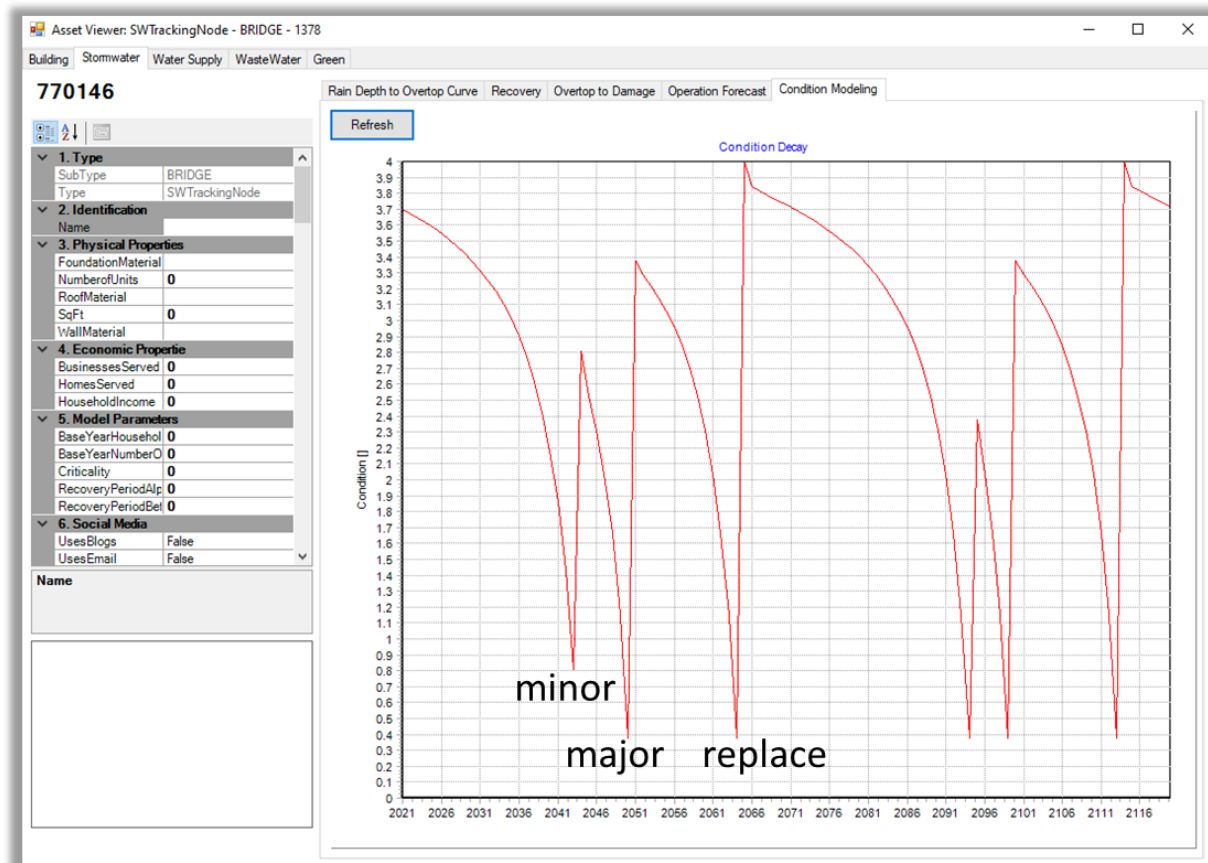
Figure 4.19: Maintenance Event Simulation Procedure

Simulation of Maintenance Events in US74 Resiliency Study



The percentages of replacement costs shown as examples of a generic asset. The percentages used were calibrated so that total spending matched actual spending reported in the NCDOT SAP database (see discussion below on calibration and Table 4.1 for a list of the percentages used in the study).

Figure 4.20: Water Crossing Replacement Events



The simulation inserts minor, major, and replacement events for each water crossing asset (bridge, culvert, pipe) in the corridor. These events occur when projected condition of the asset falls below 1.0 or failing condition.

4.7.5 Cost Modeling

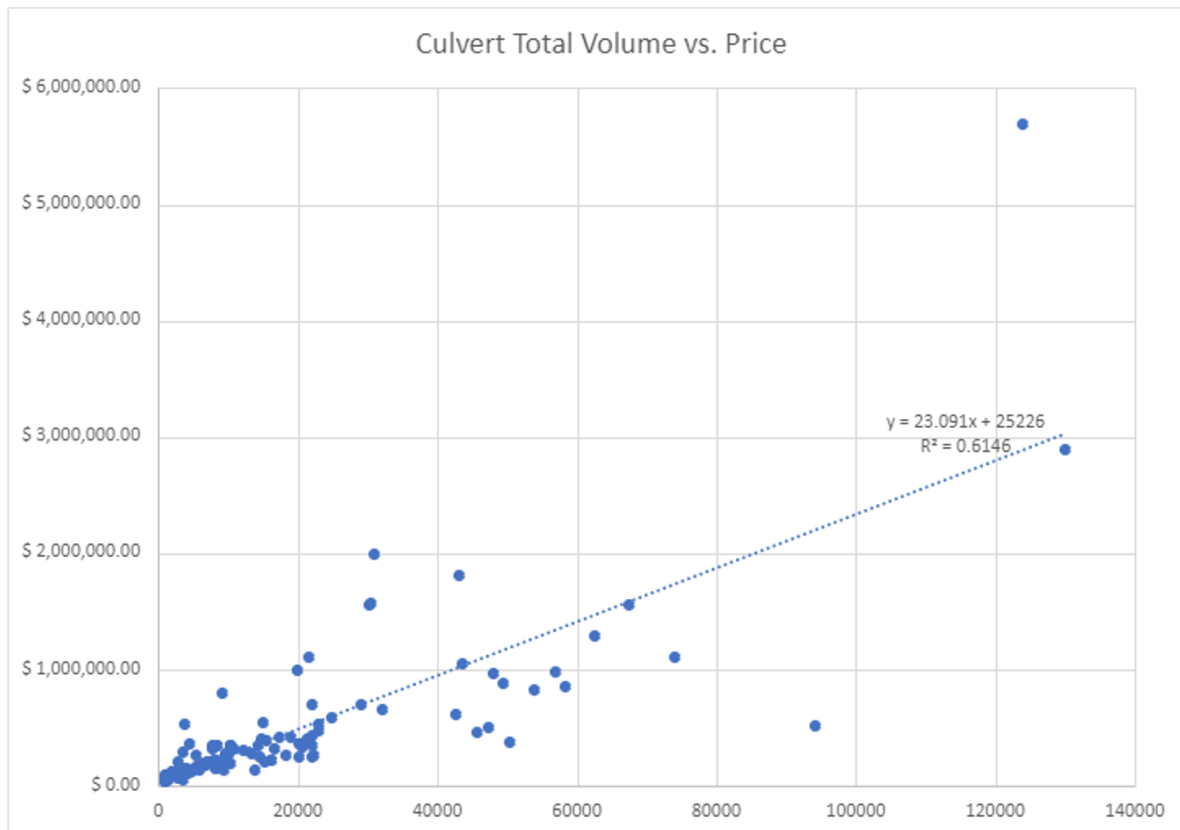
As described in Section 4.7.4, maintenance and replacement events were assigned costs as a percentage of the replacement cost of the asset. Multiple methods were used to estimate replacement costs depending on asset type:

- **NBIS asset replacement costs from Statewide Transportation Improvement Program (STIP)** - NBIS asset replacement costs were developed from a separate bridge study conducted as part of the NCDOT STIP.
- **NBIS asset replacements costs not estimated in STIP** - For those bridges where a STIP replacement cost was not provided, the deck area for the bridge was estimated by multiplying the bridge's length by its width (L x W). A per square foot (p.s.f.) value of \$145 p.s.f. was used to convert the area of a replacement cost.
- **Non-NBIS assets** – A linear regression-based formula was developed for replacement costs of the non-NBIS assets (culverts and drainpipes) from a record of past bids for asset replacement focused on a subset of non-NBIS culverts and drainpipes throughout the state (see Figure 4.21).

The analysis estimated the "total hydraulic volume" of each culvert and pipe as the product of the number of barrels and the hydraulic volume (hydraulic area multiple by the average barrel length). A linear regression of total hydraulic volume to proposed cost revealed a relationship of:

$$\text{Replacement Cost} = \$25,226 + \text{Hydraulic Volume (cu. ft.)} * \$23.091.$$

Figure 4.21: Regression of Past Bids to Estimated Replacement Cost of Culverts and Bridges vs. Hydraulic Volume



$$\text{Culvert Volume} = \text{Length} * \text{Area} * \text{Num Barrels}.$$

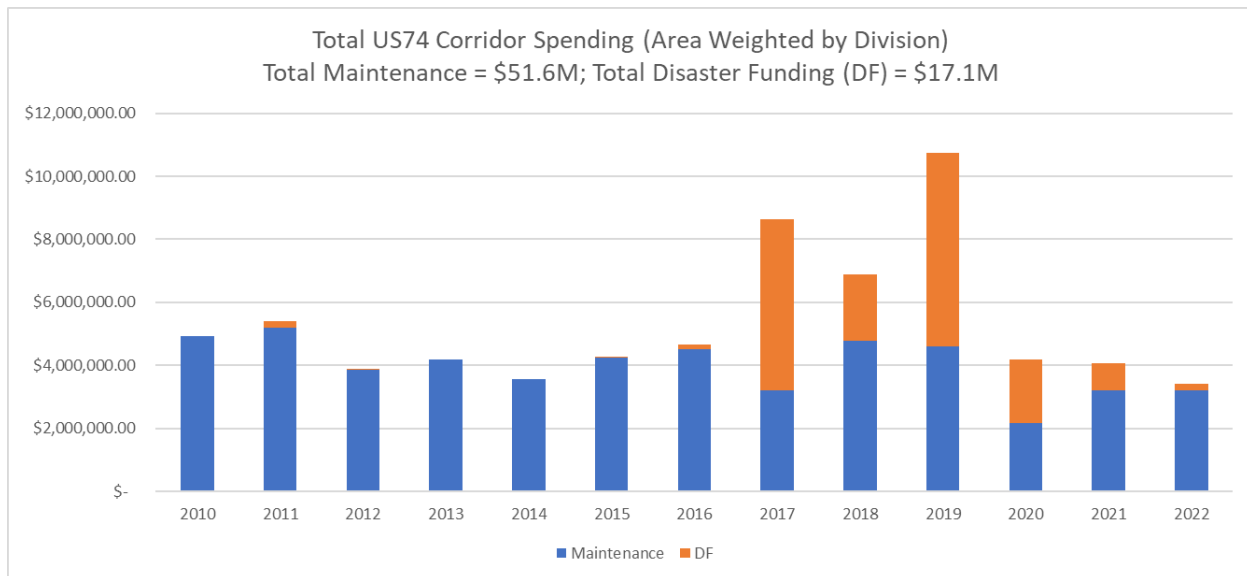
To estimate replacement costs for all non-NBIS assets in the corridor, a state-wide record of past bids on non-NBIS assets was used to estimate a relationship between hydraulic volume of assets and replacement cost.

4.7.6 Calibration of the Cost Model with Actual Costs from NCDOT SAP system

Both the projected maintenance costs and storm-caused costs were calibrated against a query from the NCDOT SAP system, which tracks actual historical spending in both categories of cost. A query was made of all costs on bridges, culverts, and pipes in the U.S. 74 corridor for the years 2010–2022 (13 years). See Figure 4.22.

These costs were summarized into average annual costs for master plan-triggered and condition-triggered maintenance (\$3.97M per year) and repair of assets due to flood damage from storms (\$1.32M per year). In the 2010–2022 period, storm damage costs including costs incurred during Hurricanes Matthew and Florence and were \$17.1M total.

Figure 4.22: Historical Spending on Bridges, Culverts, and Drainpipes in the US 74 Corridor



A query of NCDOT Divisions 3,6,8, and 10 of the NCDOT SAP system was used to estimate historical spending in the corridor. The total division spending was area-weighted to estimate spending only within the corridor by division. The query was partitioned into maintenance spending and disaster funding (DF), which was assumed to match spending on condition-triggered maintenance and storm-triggered repair in the simulation.

The implicit assumption made in this calibration was that the total non-disaster spending on bridge, culvert, and drainpipe assets over 54” in diameter is equal to the simulated minor/major/replacement-based spending in the simulation. Further, spending on storm-caused damage is implicitly assumed to match disaster funding spending rates reported historically.

To ensure this assumption is true within the simulator, the 2010-2022 historical rainfall was used to drive the simulator over a calibration period of the same duration. Model parameters including overtopping thresholds, types of maintenance events triggered by overtopping events and the cost of these events as a percentage of replacement cost were initially guessed and then adjusted until the average annual maintenance spending matched the historical and storm spending average. The calibrated parameters are listed in Table 4.1.

An important note is that a duration of maintenance event was introduced, which split spending on larger projects over several years. This mirrors how spending actually occurs and resulted in a closer match to the historical spending. The pattern used to estimate maintenance event duration specified:

- If trigger by master plan,
 - If planned cost is greater than \$100M, ten years,
 - If planned cost is from \$10M - \$100M, eight years,

- If planned cost is from \$5M - \$10M, six years,
- If planned cost is from \$1M - \$5M, four years,
- If planned cost is less than \$1M, two years,
- If triggered by flood,
 - Four years – assumes a replacement occurs,
- If triggered by maintenance,
 - Two years.

4.8 Sea Level Rise Modeling

As mentioned in the section above on projecting future conditions, the mean sea level is projected to rise in Wilmington, NC between 1.28 feet and 2.26 feet by 2100 (NOAA SLR Viewer). This will cause both chronic disruptions from nuisance flooding during high tides and acute disruptions from storm surges exacerbated by higher mean sea levels.

In the simulation, the rationale for modeling SLR was to produce a daily projection of high tide levels and use this to estimate the impacts of both tidally-driven nuisance flooding and tidally-influenced storm surges when these events occur.

4.8.1 Simulating Nuisance Flooding

In the simulation, each road segment was assessed against the projected high tide level each day to simulate nuisance flooding events. When flooding occurred, a disaster event was recorded for the affected asset.

Note that buildings were not assessed within the simulation, only road segments. Assessing impacts on buildings can be incorporated into future simulations, if desired.

A key measurement that impacted the simulation was deck elevation, the elevation of the road segment above which overtopping and road disruption occurs. To estimate this elevation, each road segment was measured for elevation at a 30 meter interval, or 98.4 feet. The minimum elevation along the road segment was retained as the overtopping elevation of the road segment. Through this approach, the simulation implicitly assumed that if any part of the road segment had overtopped, then all trips were disrupted along the road segment. This is most likely a conservative assumption, as a percentage of real trips are likely to use a portion of a road segment. However, to ensure that any level of disruption was captured in the simulation results, the assumption was retained.

The digital elevation model (DEM) used was the so-called “ribbon” provided by NCDOT, which is a high-detail (ten-foot horizontal resolution) Light Detection and Ranging (LiDAR)-based DEM with data only along the road segments in the NCDOT Linear Referencing System.

Recognizing that high tide levels that do not overtop road segments still have an impact by inundating the road structure with seawater, a “freeboard flooding” metric was also introduced to the simulation. This metric recorded disruptions the same way as the overtopping metric but set the overtopping threshold as the road segment’s overtopping threshold minus two feet. The simulation results present both the nuisance flooding metric and the freeboard flooding metric. Disrupted trips presented in Chapters Five and Six include both metrics.

4.8.2 Simulating Sea Level Rise Impact on Storm Surge

Acute impacts of rising sea levels will happen in the future when storm surge sits atop elevated mean sea levels. As mentioned above, in the section on coastal flood modeling, an ADCIRC model was combined with an EPA WHAFIS model to estimate the depth of flooding in the coastal region of the corridor for 10, 50, 100, 500, and 1,000-year events. NOAA Atlas 14 was then referenced to find the equivalent rainfall for each return period. See Section 4.2.1 for more detail on rain modeling.

The depth rasters produced for each return-period were then sampled at the low points of each road segment. The result was an overtopping curve for each road segment that related rain depth of an incoming storm with overtopping depth above the road deck elevation. When large storm events occurred during the simulation, these curves were used to rapidly estimate overtopping depths at each road, and thereby, estimate disrupted trips.

The ADCIRC+WHAFIS model-based estimates were configured with the assumption of mean sea level in 2020 as a boundary condition. As the sea level rose in the simulation, this assumption causes the inundation estimates for both chronic and acute flooding to become less accurate — i.e., they are underestimated.

A more accurate estimate could be found by re-running the ADCIRC+WHAFIS models with a varying range of mean sea level and then using the appropriate version of the model based on the estimated mean sea level at the time of the future event. As running multiple ADCIRC+WHAFIS models was beyond the scope of this study, a more approximate method was used to estimate inundation during future storms. Namely, in each year, the projected increase in mean sea level was calculated. If a storm surge event occurred in that year, the depth of inundation in the flood response curve was augmented with the estimated SLR projection for the year.

4.9 Heat Impact Modeling

As temperatures increase with climate change, impacts on the road and rail system are expected. In the case of asphalt road segments, a common problem is flushing (see Figure 4.23), which occurs when temperatures are high enough during the day to destabilize the bitumen, allowing aggregate to move within the road. The threshold temperature is approximately 85°F.

When this situation occurs, vehicle tires then grab onto the aggregate. As the situation occurs over and over as the road asset ages, the ratio of bitumen to aggregate increases. High bitumen density is dangerous because it reduces skid resistance. To keep the road safe, roads with this problem often operate at reduced speed limits.

Figure 4.23: Flushing Impacts



<https://www.abc.net.au/news/2018-01-06/how-heat-affects-roads-trains-and-planes/9308342>

High heat can cause other problems with transportation infrastructure as well. Concrete road segments, for example, expand in high heat and can buckle. While this is known and accounted for in current road design with gaps between the concrete sections, the gaps are designed for a certain maximum temperature, which is projected to be exceeded in future years. Appendix A of this report provides links to multiple sites and articles that go into future detail on problems that can occur within increasing heat.

For the purpose of simulating disruption within this study, flushing was assumed to be treatable as a generic disruption event and applicable to all road segments, regardless of if they are asphalt, asphalt and concrete, or concrete only.

4.9.1 Probabilistic Heat Event Simulation

In each quarter, the heating degree days for each road segment was evaluated since the last maintenance event on the road segment. For example, if the last maintenance event occurred 10 years before the current time step in the simulation and the average atmospheric temperature was 90°F, the heating degree days are $10 \text{ years} * 365 \text{ days/year} * 90^\circ\text{F} = 328,500 \text{ }^\circ\text{F-days}$. The simulator includes projected maximum temperature from the LOCA dataset (see section above on climate stressor projections) and the latest maintenance event on each road segment. These were used to evaluate the heating degree days for the road.

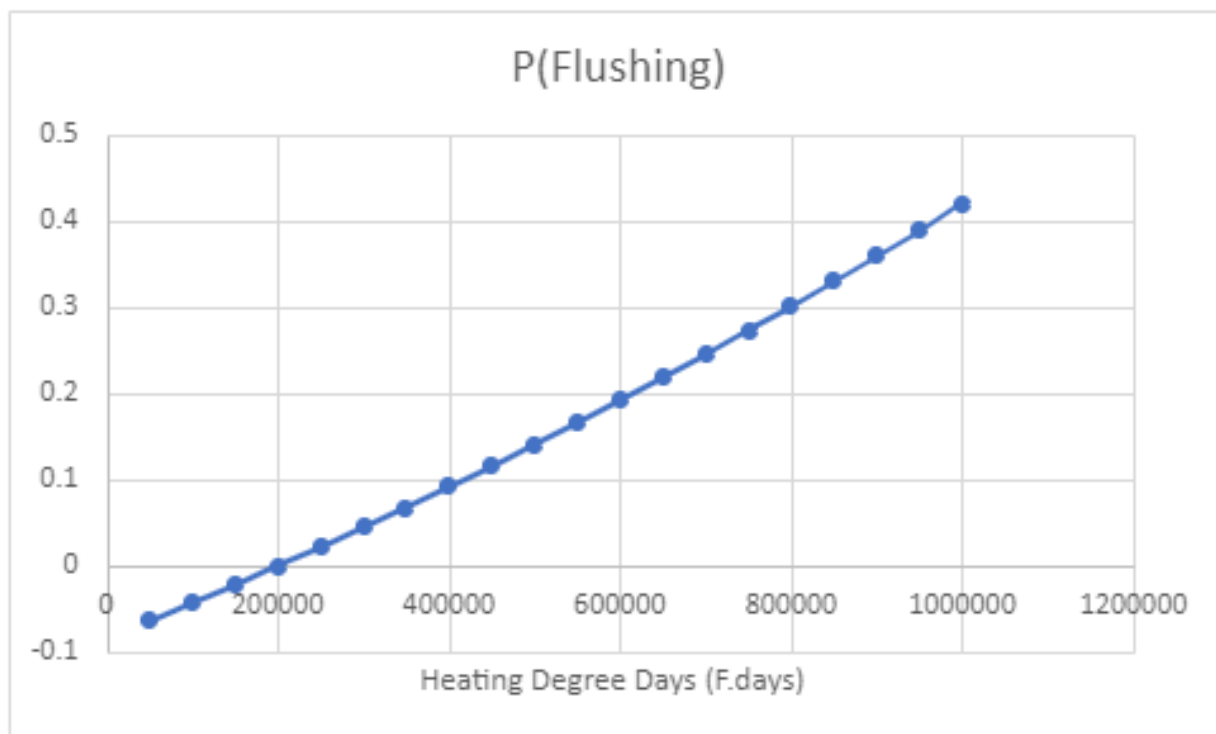
A comprehensive literature review (see Appendix A) revealed multiple methods for simulating asphalt degradation over time, including methods that leverage artificial intelligence and machine learning. As one of the objectives of the study was to simulate disruption with minimized computational requirements, the simulator was configured with a probabilistic model, which linked cumulative heating

degree days with probability of a flushing-related traffic slowdown initiated by NCDOT or other relevant DOTs.

The model assumes that if the trigger atmospheric temperature is 85°F, that flushing would start approximately 1/3 of the typical 20-year lifespan of the asphalt, or at about 6.66 years. This would give a threshold of 85°F * 6.66 years * 365 days/year = 206,833 °F days. A probability function was then developed that assumes that when the road reaches this threshold the probability of flushing becomes non-zero and increases as a power function until at lifespan of 20 years, the probability of flushing is approximately 20%. Figure 4.24 shows the function. The formula for the function is:

$$P(\text{Flushing}) = 3^{((\text{Cumulative Deg Days} - 200000) / 100000 / 25) - 1}$$

Figure 4.24: Probability of Flushing as a Function of Cumulative Heating Degree Days



4.9.2 Disruptions from Heat Events

The following example illustrates how the probabilistic heat event simulation proceeds. In the first quarter of 2040, for a single road segment, the simulator might find that the last maintenance event occurred on 1/1/2027, or thirteen years prior. With increasing maximum temperatures, the cumulative heating degree days at this point are 425,000 °F-days. The probability function says that the probability of an unsafe road due to flushing at this point is 12%. The simulator then uses a random number generator to generate a uniformly distributed random number between 0 and 1, say 0.05. Since the

number is less than 0.12 (i.e., 12%), the road segment is assumed to be unsafe, and a disruption event is recorded for the road segment.

An important note is that the probability model allows for road segments to age beyond the 20-year typical lifespan, with probability of flushing increasing with age.

4.9.3 Disruptions from Heat Events

The literature review and discussions with pavement subject matter experts found multiple actions that can create resilience to flushing. They include:

- **Adjusting binder in asphalt mix:** the primary approach is to design the asphalt mix with a binder that will enable the mix to stand up to expected maximum temperatures. NCDOT uses the so-called Superpave asphalt mix design method to develop asphalt mixtures, where the binder added to the mix is designed to a target design temperature. To adapt to climate change and related increasing temperatures, projected maximum temperatures from global climate models should be used in each pavement design process into the future. Steadily increasing the robustness of the asphalt mix by using higher temperature binder in each successive replacement will likely incur higher costs, but these costs are expected to be manageable particularly as they will allow avoidance of traffic disruption related to flushing.
- **Replacing asphalt more frequently:** as flushing tends to occur as the asset ages, earlier replacement will provide a way to avoid flushing problems and related traffic disruption. This approach will result in higher costs, of course, but these costs are expected to be manageable when compared to disruption costs that may result from flushing. It is worth noting that discussion with NCDOT pavement experts revealed that often replacement occurs more frequently than the 20-year period used to define the flushing probability model, indicating that NCDOT is likely avoiding flushing in its primary route systems already.

4.10 Freight Impact Modeling

Of particular interest in the simulation was the tonnage of freight disrupted by future climate change. Trips were disrupted within the simulation by flood and heat events (as described above in the flood modeling and heat modeling sections). The rationale for estimated freight disruption was to use the reported AADT specifically for trucks and then convert this to a tonnage by using an average tonnage per truck estimate.

4.10.1 AADT Truck Metric

In the same way, total trips disrupted were estimated using the NCDOT AADT metric for each road segment, and freight trip disruption was estimated by using the AADT truck trip estimates provided in the same dataset. This method was determined preferable to a presumptive percentage of total trips because freight was transported on a specific set of roads within the corridor.

The tonnage of freight was estimated by multiplying the number of missed truck trips by the estimated average tonnage of freight in a truck. For this study, an estimate of 20 tons of freight was used per truck. This was taken from the Bureau of Transportation Statistics 2021 report.

4.10.2 Adaptation Approach

The resilience-focused adaptation actions implemented in the adaptation/mitigation scenario described in the Adaptation section of this report largely focused on general improvement of the transportation for all trips. As such, the improvements made such as elevating bridges and culverts proportionally reduced disruption to freight as well. On the roads supporting freight travel, reductions in disruption carried over to freight transportation as well and is reflected in the final results.

4.11 Rail Impact Modeling

Rail disruption was evaluated by simulating flood inundation at the intersection of the rail and road system, namely rail crossings. Within the corridor, there were 528 rail crossings.

While other climate-influenced hazards will likely impact rail operation such as heat causing rail buckling, these hazards were not simulated in this study. Future studies should include these hazards and the infrastructure impacted (i.e., rail track and related infrastructure).

4.11.1 Rail Crossing Flood Frequency Metric

The metric used to express disruption to the rail system was the expected average annual disrupted days (AADD) at each rail crossing. This metric could be converted into an estimate of tonnage of rail cargo disrupted, but this would require sensitive cargo data as well in the assessment. The NCDOT Rail Division agreed that because of the sensitivity of this data, the average annual disrupted days metric were a suitable proxy.

4.11.2 Adaptation Approach

The NCDOT Rail Division agreed that adaptation options, like elevating rail tracks and related infrastructure were likely impracticable. As a result, the only mitigation measure evaluated was the hardening of the rail crossings that are likely to be inundated by floods.

When flooding and inundation occurred at rail crossings, the simulator disabled the crossing and halted rail travel for a recovery period. The duration of the recovery depended on the level of overtopping. The effect of hardening was simulated as reducing the recovery time. The rationale was that the force of overtopping water would cause less damage to the rail infrastructure if the crossing were hardened.

The specific parameters used for rail crossing operations interruption and hardening are provided in Table 4.2.

Table 4.2: Parameters for Rail Crossing Operations Interruption and Hardening

| Storm Size | Recovery Time – Normal Construction (days) | Recovery Time – Hardened (days) |
|-----------------------------|--|---------------------------------|
| 50-year 24-hour | 1 | 1 |
| 100-year 24-hour | 2 | 1 |
| 500-year 24-hour | 5 | 2 |
| 1,000-year 24-hour or above | 10 | 4 |

4.12 Disruption to Disadvantaged Populations

Disadvantaged populations exist throughout the U.S. 74 corridor. A primary concern is the level of access these populations have to sustenance facilities. Within this study, these facilities included gas stations, stores, emergency care, and emergency shelters.

Ideally, disadvantaged populations have access to multiple options for each of these facility types, through multiple redundant routes. The rationale in this study was to investigate the level of accessibility disadvantaged populations had at a detailed scale, thereby allowing for pinpointing road segments that should be improved to increase access. This information can be used by NCDOT planners and engineers for prioritizing future expenditures aimed at increasing robustness of the transportation system.

4.12.1 Approach

The 2019 ACS poverty and minority data — at the census block group level — were used to define the census block groups with disadvantaged populations. The method outlined in the NCDOT community impact assessment guidance method was followed. This method specifies that a disadvantaged population census block group is one with more than 25% of the population at or below the poverty level, and/or 50% of the population or more are in minority groups.

4.12.2 Inaccessibility Index

A sustenance inaccessibility index was developed to quantify the level of access census block group populations had to the road system when flooding occurred (see Figure 4.25).

As described above in the section on MegaBuildings, each road segment in the corridor had a residential building created at its geographic centroid that represented the people who lived on the road. Further, a set of sustenance facilities of type: shop, gas station, emergency care, and emergency shelter —using schools as a proxy— were acquired from the open street map (OSM) buildings dataset. These structures were reported by individuals to this open-source dataset and comprised of an incomplete but valuable approximation of all commercial buildings in the corridor.

Routes from each MegaBuilding to the closest three sustenance facilities of each category were defined. Then, the water crossing assets along these routes (bridges, culverts, pipes) were found. With these relationships established, the sustenance inaccessibility index could be calculated.

The index was then evaluated for each road segment as the product of a redundancy factor and a flood risk factor summed over the four sustenance facility categories.

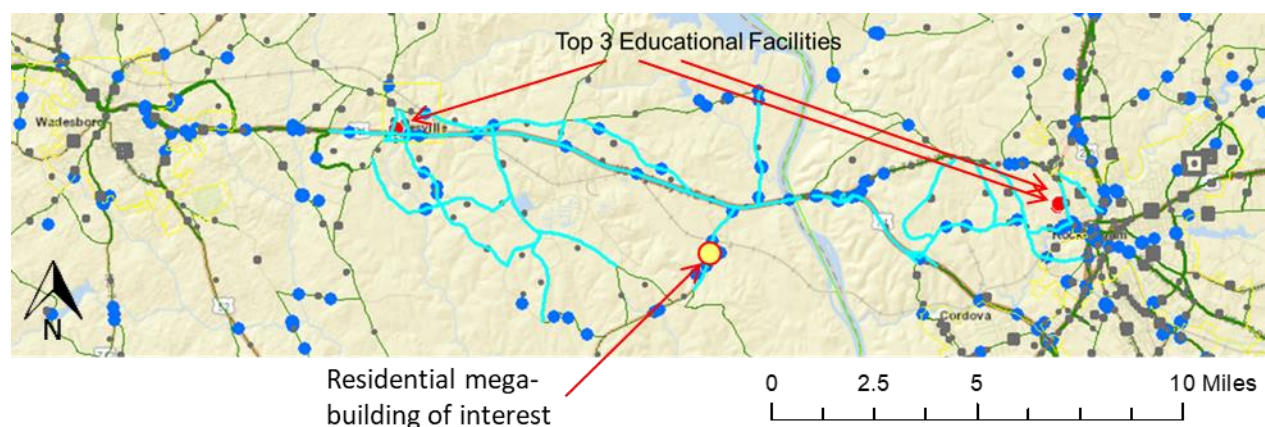
The redundancy factor was defined as the total road length from the MegaBuilding to sustenance facilities divided by the number of road segments. This factor increased as the total road length to sustenance facilities increased and as the number of road segments decreased. Therefore, if a MegaBuilding was far from sustenance facilities and only had single road segments pathways, then inaccessibility is extremely high. Conversely, if the MegaBuilding was close to sustenance facilities and there were comparatively many road segments (implying high redundancy of routes), then inaccessibility is very low.

The second factor was the flood risk factor, which estimated the potential for overtopping the routes had during major flood events. The average overtopping level for the 2020 500-year event was evaluated across all of the water crossing assets on the routes to sustenance facilities. Higher overtopping potential had the effect of increasing the inaccessibility index.

4.12.2.1 Valid Road Segments

The inaccessibility index was evaluated for each valid road segment, where a valid road segment was defined as roads with open access. As mentioned, in the MegaBuildings section above, controlled access roads such as interstates did not have a representative MegaBuilding, and their accessibility was therefore not considered.

Figure 4.25: Sustenance Inaccessibility Index



$$Sustenance\ Inaccessibility\ Index = \sum_{Categories} \frac{1}{N} \sum_{N\ Facilities} \frac{1}{M} \sum_{M\ Routes} \frac{Road\ Length}{Num\ Road\ Segments} * \frac{OT_{500year}}{10}$$

Inaccessibility for disadvantaged populations was quantified with a sustenance inaccessibility index. For each road segment within a disadvantaged population census block group, the closest three sustenance facilities in each of four categories were found. Sustenance facility categories included shops, gas stations, emergency care, and emergency shelter (schools) locations. The figure shows the top three closest schools (red dots) relative to the

disadvantaged road of interest (yellow dot). Multiple routes from the road of interest to each sustenance facility were then found, and the water crossing assets on the routes are found. The flood risk for each water crossing facility was then quantified as the 2020 500-year overtopping level. The final inaccessibility index sums a route-specific metric over the routes available to each sustenance facility. The metric multiplies a redundancy-distance factor (total road length/number of road segments) by a flood risk factor (average overtopping at 500-year storm level / 10). The redundancy-distance factor is large when sustenance facilities are far away and when there are fewer road segments. The result is that the inaccessibility index is highest when there are few routes which are a long distance from the target road and the water crossing assets on the routes are at high flood risk.

4.12.3 Simulating a 500-year Storm Impact on Disadvantaged Populations

The inaccessibility index allowed for ranking disadvantaged population road segments by their level of inaccessibility, and the results in chapter five show the top ten least accessible road segment in each division.

An additional assessment evaluated the top ten most disruptive water-crossing assets (bridges, culverts, drainpipes, and low points in road segments) that are along the path from the least accessible roads to sustenance facilities. This was evaluated by assuming a 2020 500-year storm had occurred and evaluating for each disadvantaged population road segment the stormwater facilities that flooded on the paths to sustenance.

This assessment was done for each sustenance facility type, evaluating the total number of trips disrupted by the water crossing asset in question for people trying to get the sustenance facility type in question. Then, a weighted sum of the disrupted trips was evaluated that applied the following weights to each category of disrupted trips.

- Emergency Shelter: 0.25
- Gas Station: 0.2
- Emergency Care: 0.35
- Retail: 0.20

Chapter five presents the results of this assessment, mapping the top ten most disruptive assets in each division and listing the disrupted trips for the top ten by category along with their joint disrupted trips index. The same set of metrics for all of the assets in the simulation is available through the City Simulator database provided as a deliverable for the project and through the Esri StoryMap.

4.13 Impacts to Critical Facilities

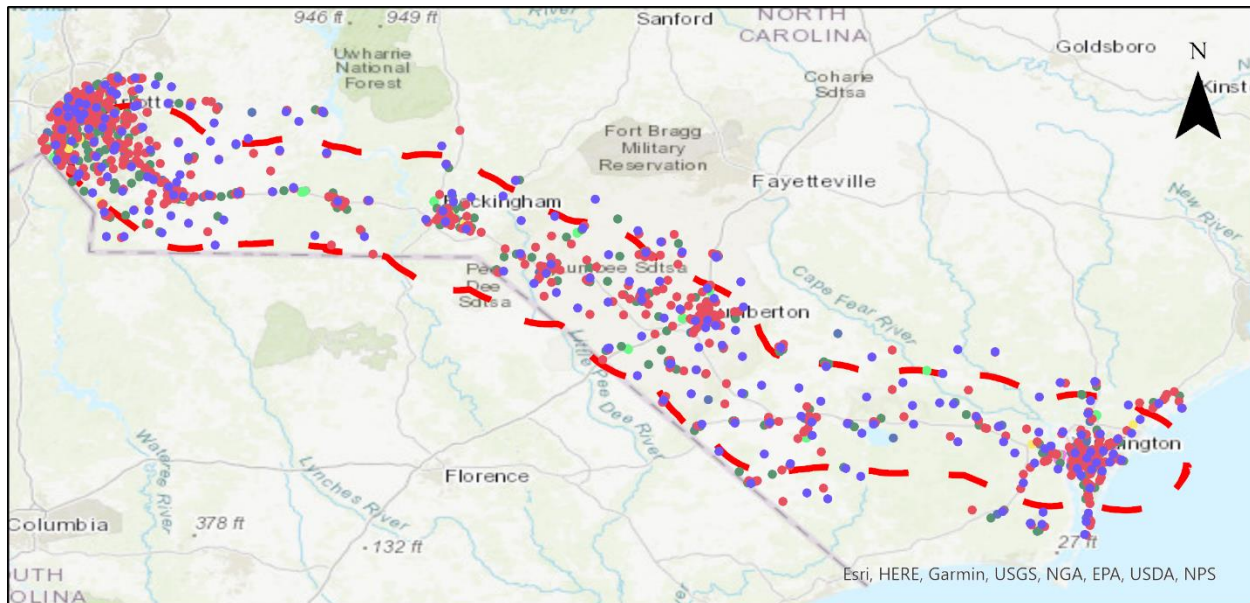
In this study, critical facilities considered included hospitals, emergency care, stores, schools, NCDOT buildings and land, fire stations, and police stations within the study area. These facilities encounter climate change impacts in the sense that the transportation paths providing access to them can become compromised as floods and heat events become more extreme.

The rationale was similar to the approach taken that assessed disadvantaged populations. That is, an inaccessibility index was used to quantify redundant routes and their flood risk to each facility from surrounding streets. The climate change impact to the water crossing assets supporting the routes evaluated the degree to which the facilities will become even less accessible in the future.

4.13.1 Approach

Critical facility locations were found through the open street map buildings (OSM Building) as shown in Figure 4.26. Point locations were downloaded for the full corridor for each of the facility types. A crosswalk was developed to aggregate OSM business and occupancy types to the target categories.

Figure 4.26: Critical Facilities Evaluated



CriticalFacilities_US7410kmBuffer

CriticalFacilityType

- EmergencyShelter
- FireStation
- GasStation
- Hospital
- LawEnforcement
- NCDOTBuilding
- NCDOTLand
- <all other values>



Critical facilities across the corridor were compiled from a combination of the open street map (OSM) publicly available dataset and several GIS datasets provided by NCDOT.

In addition to the OSM data, GIS data specifying the locations of police and fire stations, emergency care, and NCDOT facility and building assets was included. Figure 4.26 presents all facilities used in the assessment.

4.13.2 Inaccessibility Index

The critical facilities were assessed for two factors, remoteness-redundancy and overtopping risk.

Remoteness-redundancy was defined as the length of road within the critical facility’s service area divided by the number of road segments. For critical facilities with short roads and high network density

in their service area, the remoteness-redundancy factor is therefore low. Conversely, for critical facilities with relatively long access routes and low density the factor is high.

Overtopping risk was defined as the average overtopping depth above road deck during the 2020 500-year flood level across all water crossing assets (bridges, culverts, pipes) in the critical facility's service area.

The two factors – remoteness/redundancy and overtopping risk – are similar to the factors used in the disadvantaged population assessment (Section 4.12). The difference in the approach is that the focus is on routes from surrounding residential buildings to the critical facility in question, as opposed to routes from each residential building to multiple sustenance facilities.

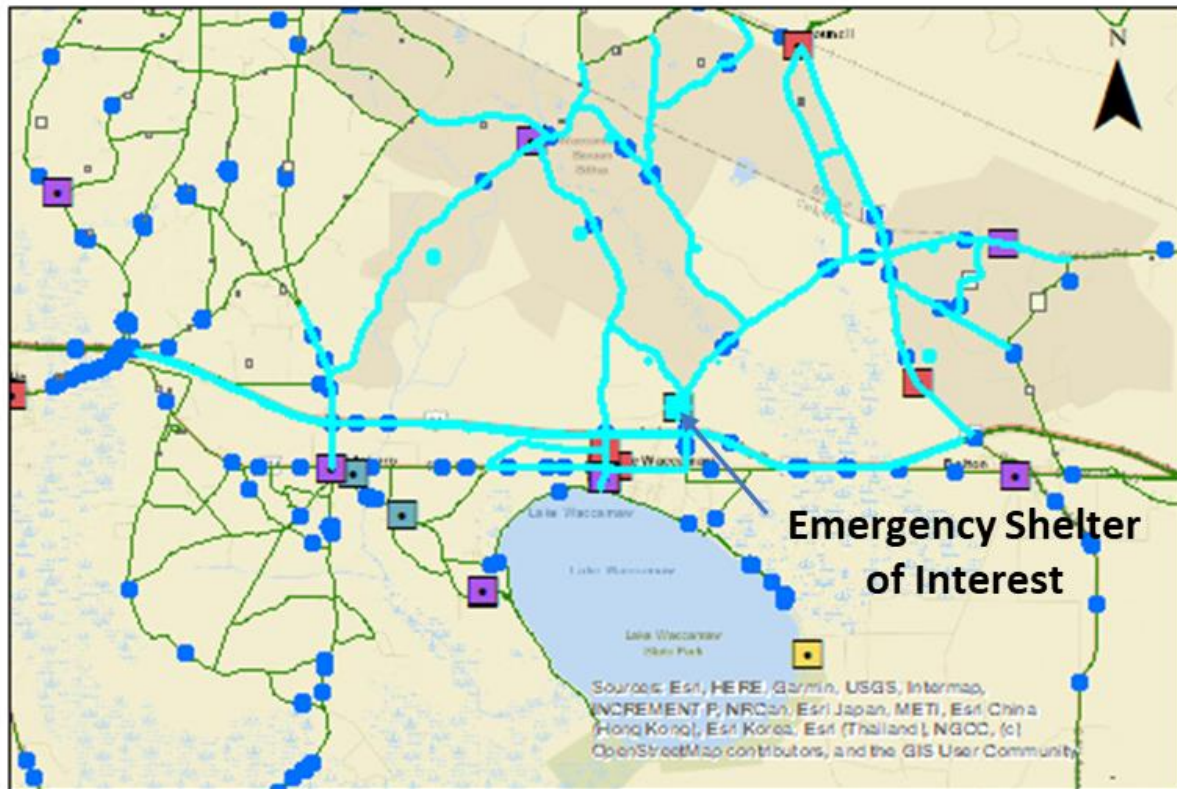
The service area for each critical facility (see Figure 4.27) was defined by selecting nearby residential buildings such that the total number of households in the buildings meets or exceed set threshold for the facility type. The thresholds of households were set as follows:

- Hospital/Emergency Care – 100000 households,
- Emergency Shelter – 5000 households,
- Fire Station – 5000 households,
- Gas Station – 5000 households,
- Law Enforcement – 5000 households,
- NCDOT Building – 1000 households,
- NCDOT Land – 1000 households.

The households' thresholds were estimated based on the prevalence of the facility category in the corridor and the nature of the service being provided. For example, there are many gas stations in the corridor, which implied that gas stations should have a lower number of households being served. Conversely, there were relatively few emergency care facilities in the corridor, implying that these types of facilities are likely serving a much larger population.

The set of residential mega-buildings was selected by progressively expanding a search radius until sufficient households were included to exceed the relevant household threshold. The road network used to transport individuals to/from the critical facility was then identified using the commute paths defined for travel modeling (see Section 4.4).

Figure 4.27: Example Service Area for a Critical Facility



Legend



CriticalFacilities_US74100mmBuffer_WM

CriticalFacilityType

-  EmergencyShelter
-  FireStation
-  Gas Station
-  Hospital
-  LawEnforcement
-  NCDOTBuilding
-  NCDOTLand

An example critical facility service area is shown as selected roads (cyan lines), mega-buildings (cyan squares), and water crossing assets (blue circles). Each critical facility in the corridor had a service area defined in this way to facilitate calculating the critical facilities index.

The water crossing assets on the road network were then identified and their risk estimated as the average overtopping level during the 2020 500-year flood. The total length of road within the service

area network was then found, as well as the number of road segments; these parameters were used to evaluate the remoteness/redundancy factor.

Figure 4.27 shows an example of a service area for a selected emergency shelter (i.e., school). The figure shows the mega-buildings (cyan squares), roads (cyan lines), and water crossing assets (blue circles) used to evaluate the remoteness/redundancy and overtopping risk factors.

To understand relative weights of remoteness/redundancy and overtopping risk, both against each other and across the corridor, each factor was normalized from one to ten, with one indicating low inaccessibility and ten indicating high inaccessibility. These two categorized factors were then added to provide a 1-20 score for each critical facility. The results are presented in Section 5.2.

4.13.3 Opportunities for Improvement

The approach taken above should be considered a first pass at estimating critical facility climate change impact. The method provides multiple opportunities for enhancement. They include:

- Specifying service areas more accurately:
 - Contacting the larger service area entities such as the emergency care facilities to find if they have a specific estimate for the service area or number of households they serve. This data could be used to better calibrate the service area and related transportation network for each facility.
 - Literature review to refine the category-based estimates of households typically served by each category of critical facility. This could also partition the facilities into urban, suburban, and rural, which may serve significantly different numbers of households on average.
- Breaking facilities by travel required to provide service: the method specified above assumes all critical facilities serve a population. While this is true of facilities like hospitals, gas stations and shops, it is not true for all facility types, such as the NCDOT lands and buildings. These facilities are likely accessed by a comparatively minimal number of people. Yet, access to the facility 100% of the time is critical. As such, a closer look that splits the groupings of critical facilities into groups that serve populations that requires travel to the facility and critical facilities that require travel only by service personnel should be undertaken.

4.14 Addressing Future Inflation

The rationale for including inflation in the simulation was to conduct the full simulation in base year (2020) dollars and inflate to future value as a post process. Three percent was used as an inflation rate, as specified by the NCDOT. This was the percentage used on the current STIP. The rate was adopted on December 8, 2021, by the NCDOT Board of Transportation ([NCDOT BOT December 8, 2021, meeting minutes](#)).

4.14.1 Approach

The cost of each maintenance event, storm damage event, and lost productivity were all calculated as present value (PV) estimates — that is in 2020 dollars across the 2020–2060 timeframe. When the

simulation was complete, a future value (FV) for each of these metrics were calculated in each year that used the following formula, where N was the number of years since 2020 and i is the inflation rate.

$$FV = PV * (1 + i)^N$$

4.14.2 Comments on Inflation Approach

Inflation is an uncertain parameter. At the time of this writing (fall 2022), the consumer price index (CPI) has year-on-year increases from eight to nine percent. Though changes in costs for transportation infrastructure capital expenditures had not tracked exactly with consumer prices, if we considered the CPI (a suitable proxy), this creates questions on whether the three percent inflation rate used in the simulation was realistic. Given just a year ago, the year-on-year CPI inflation was considerably lower than three percent, this study assumed an average annual inflation rate of three percent was suitable for the purposes of the study.

Further, the future value approach used only reflects future value of expenditures in the simulation. A net present value (NPV) approach would consider the risk in the investments reflected through a discount rate. In future simulations, a NPV approach is recommended for a more comprehensive assessment of future investments.

5 Vulnerabilities

This chapter presents the vulnerability study findings. These findings were derived from the baseline scenario. In this scenario, no adaptation and mitigation measures were attempted. The transportation system was maintained as planned, with the 2020–2030 STIP projects implemented alongside automated asset maintenance projects governed by the asset condition forecasting model described in Chapter Four. When these projects occurred in the simulation, they did not include future climate change as a design guideline. Rather, they were implemented to simply refurbish and/or replace existing assets, returning them to good condition. Each finding presented below is related to one of the three main study questions that guided configuration of the simulation.

5.1 Study Question 1 Findings: Future Disruption

Eight findings were made in answering the question:

“Which assets (roads, bridges, culverts, and pipes) caused the most (and least) disruption to road and rail traffic if future climate change-influenced events (floods, storms, heat waves, and SLR) took them offline? Which were most likely impacted given their current condition?”

The findings focus on disrupted trips across the corridor and the locations within the corridor where disruption had the highest impact. They also focus on future rain, temperature and sea level changes. Finally, they focus on asset maintenance cost, and how the simulation projects it will change with climate change in the future.

5.1.1 Finding 1.1: Climate change impacts are projected to increase disruption to daily trips 108% by 2060, with riverine and pluvial flood causing the highest percentage of disrupted trips followed by heat and then sea level rise.

Across the corridor, disruption — in the form of disrupted trips — is projected to increase by a total of 108% by 2060. This is largely due to two factors. First, steadily increased usage of the transportation system as populations and business activities increase imply that each successive disaster will have a higher impact farther into the future. For example, I-95 near Lumberton is projected to go from 65,000 trips per day on average in 2020 to 108,000 trips per day by 2060. An equivalently disruptive hurricane in 2060, therefore, will have a much larger impact in terms of disruption than one in 2020.

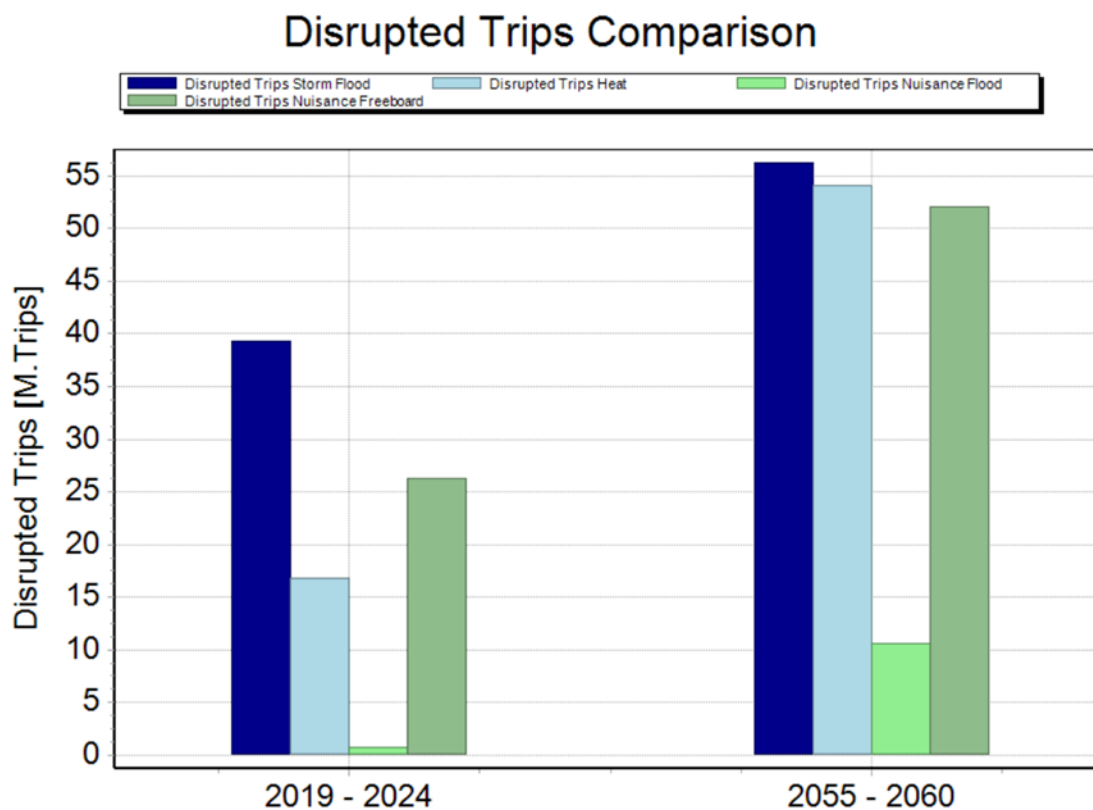
The second factor is that climate models project that future extreme storms will be larger than today’s storms, implying that the same return period storm in 2060 could cause substantially more damage than the storm in 2020.

Figure 5.1 shows projected average annual disrupted trips by cause, where causes include storm/flood, heat, nuisance flooding overtopping roads, and nuisance flooding coming within two feet of road overtopping — a hazardous zone in which the presence of seawater can increase the pace of

deterioration in road condition. The chart compares the average annual disrupted trips during the initial five years of the simulation to disrupted trips in the last five years. The chart shows that disruption increases for all causes across the simulation with the highest increases for heat and nuisance flood. The leading source of disruption is flood, though heat approaches the same level of disruption as flood toward the end of the simulation.

An important note is the simulation considers all of these disruption events as disruptions to travel. For example, a major flood that completely damages a road and stops travel is considered in the same light as nuisance flooding that enters the freeboard zone, or a heat event that slows down travel due to a flushing event. It is recommended that in future studies, the disruptions are partitioned into those that stop travel all together, those that cause inconvenience, and those that hasten transportation asset decay.

Figure 5.1: Average Annual Disrupted Trips at the Beginning of the Simulation and at the End



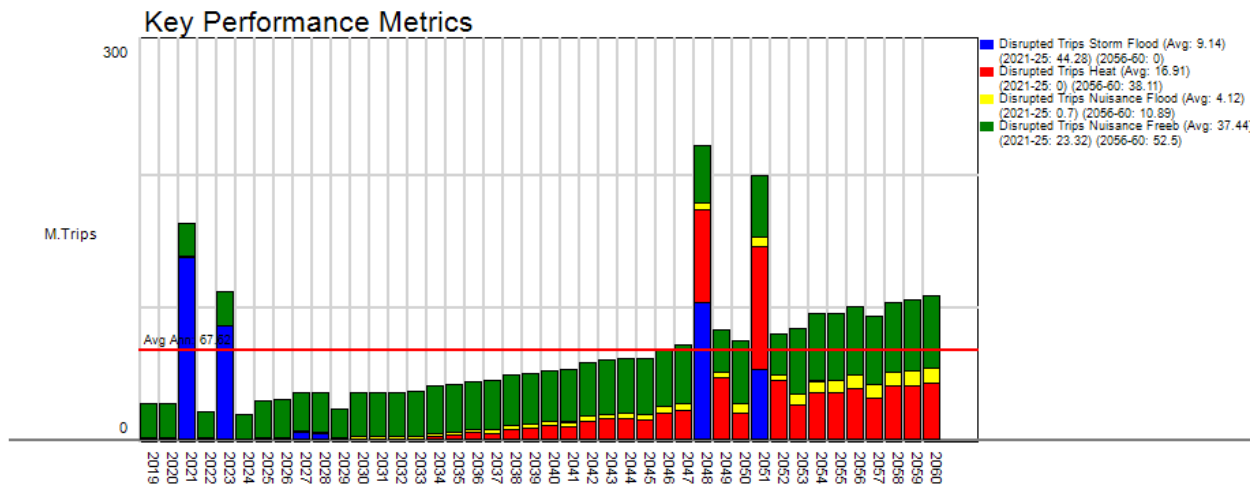
The cause of disruption was tracked as heat events, pluvial and riverine floods, and sea level rise overtopping and within two feet of freeboard.

Another factor considered was chronic versus acute disruption. Figure 5.2 shows the early severity simulation result over time, where “early” means the major storm and flood events occur within the first

five-year period and represent the 95th percentile in terms of severity — close to the worst case — for this five-year period.

As the chart shows, storm and flood events have comparatively high impacts in terms of disrupting trips when compared to other disruptors. But the year after year steadily increasing impacts of heat and SLR cause arguably more disruption over the simulation timeframe. As the simulation approaches mid-century, disruption from heat and SLR is comparable to a major storm or flood event. This oncoming chronic climate change impact should be carefully considered when approaching adaptation and mitigation.

Figure 5.2: Disruption Metrics

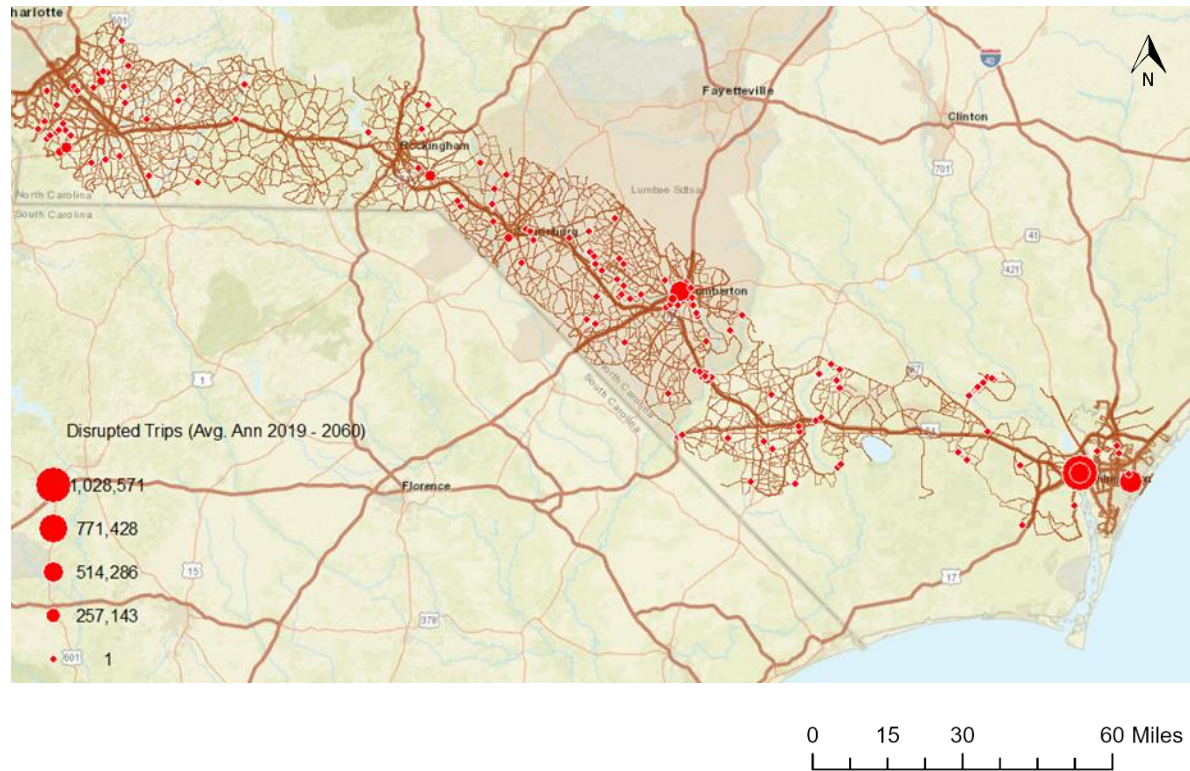


The simulation over time showed how chronic disruption like heat events and sea level rise compared to acute events, like riverine and pluvial floods. Though when the acute events occurred, they had a drastic impact; chronic disruption was far more prevalent.

5.1.2 Finding 1.2: Flood vulnerability occurs across the corridor with the highest disruption locations in the transportation network supporting U.S. 74.

U.S. 74 has several locations that were projected to be vulnerable to future floods, though the highest vulnerability was in the road network connecting to U.S. 74. Figure 5.3 shows the flooding hot spots identified in the simulation, with red circles sized according to the projected average annual trips disrupted at each location. Key locations were in Wilmington and at I-95 near Lumberton.

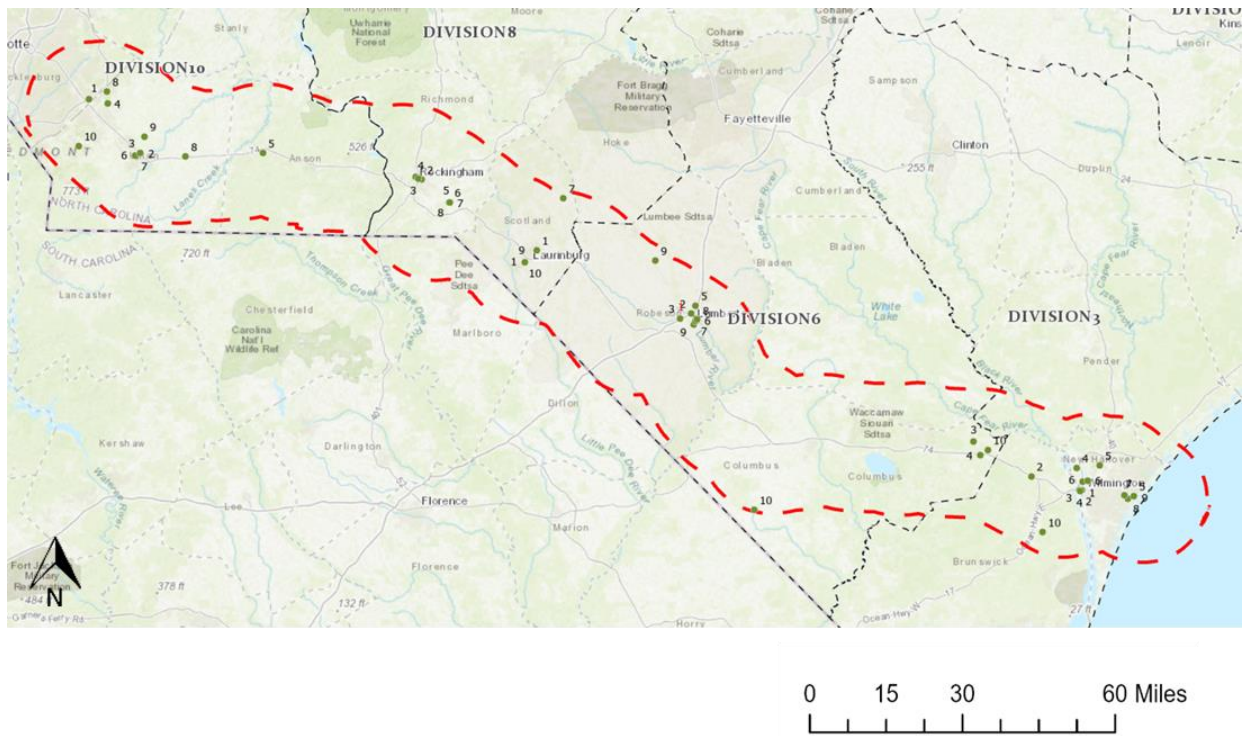
Figure 5.3: Locations with Trip Disruption Greater than 1,000 Average Annual in the U.S. 74 Corridor



Circles are sized according to level of disruption measured in average annual trips disrupted.

Figure 5.4 shows the top ten locations for disruption in each of the NCDOT divisions that cover the corridor. The locations are listed in Table 5.61, with their source ID, rank, division, the street that overtops the asset, the projected average annual trips disrupted and the asset latitude/longitude. The source ID is the NCDOT system ID.

Figure 5.4: Top Ten Disrupted Locations by Division



The rank of each location was labeled on the map. Table 5.1 provides details on the locations.

Table 5.1: Top Ten Disruptive Locations by Division

| Division | Rank | CitySimID | Type | SourceID* | Street | Trips | | |
|----------|------|-----------|---------|-------------|-------------------------|----------------|----------|-----------|
| | | | | | | Disrupted (AA) | Latitude | Longitude |
| 6 | 1 | 1380 | BRIDGE | 770147 | I-95 | 829282 | 34.63228 | -79.0298 |
| 6 | 2 | 1378 | BRIDGE | 770146 | I-95 | 829282 | 34.63219 | -79.02963 |
| 6 | 3 | 1376 | BRIDGE | 770145 | I-95 | 829282 | 34.62768 | -79.03984 |
| 6 | 4 | 1225 | BRIDGE | 770110 | I-74 W | 343246 | 34.44952 | -78.96731 |
| 6 | 5 | 1206 | BRIDGE | 230397 | US-74 | 253392 | 34.4416 | -78.9581 |
| 6 | 6 | 1223 | BRIDGE | 770465 | I-74 E | 253392 | 34.44939 | -78.96748 |
| 6 | 7 | 1210 | BRIDGE | 770466 | US-74 | 253392 | 34.44284 | -78.95989 |
| 6 | 8 | 1215 | CULVERT | 770469 | I-74 E | 141574 | 34.44451 | -78.96202 |
| 6 | 9 | 3141 | PIPE | BP-078-0048 | I-74 E | 138595 | 34.44721 | -78.96493 |
| 6 | 10 | 1361 | BRIDGE | 770125 | NC-72 E | 137503 | 34.61802 | -79.01136 |
| 8 | 1 | 1620 | CULVERT | 760173 | E. Hamlet Ave | 211904 | 34.88275 | -79.69259 |
| 8 | 2 | 3408 | PIPE | BP-083-0067 | U.S. 15-401 / Mccoll Rd | 119797 | 34.74835 | -79.4853 |

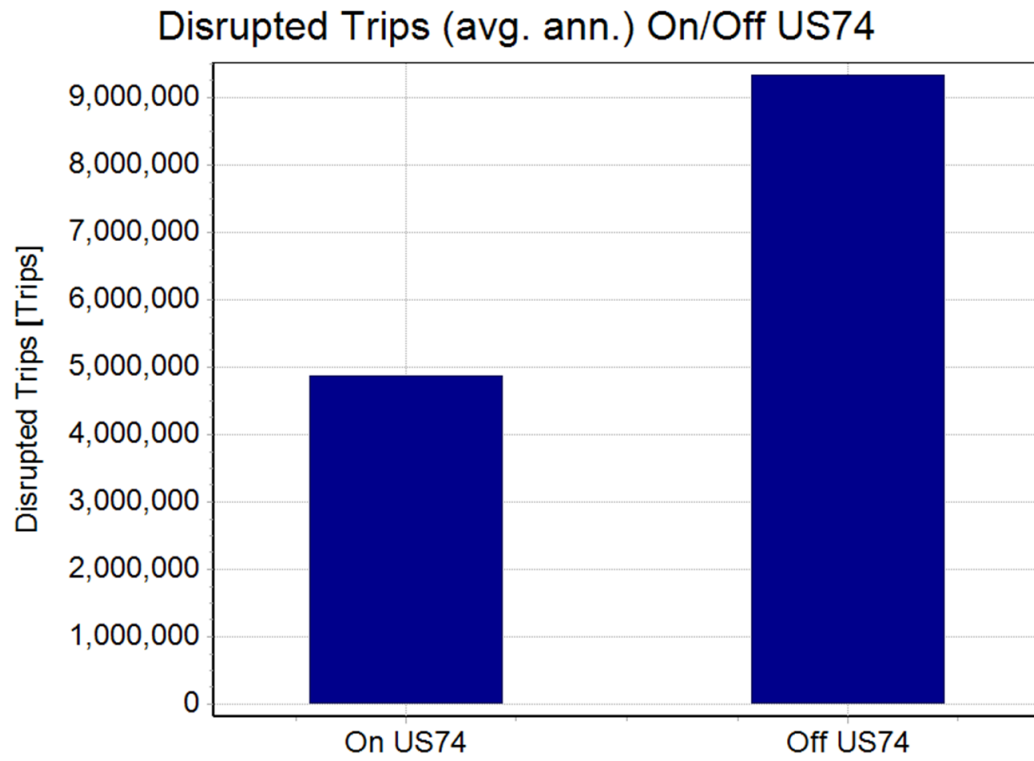
| Division | Rank | CitySimID | Type | SourceID* | Street | Trips Disrupted (AA) | Latitude | Longitude |
|----------|------|-----------|---------|-----------------|-------------------------------|----------------------------|----------|-----------|
| 8 | 3 | 1503 | BRIDGE | 820019 | NC 79 / Gibson Rd | 79050 | 34.78221 | -79.52774 |
| 8 | 4 | 1529 | BRIDGE | 820003 | Old Wire Rd | 50678 | 34.82023 | -79.53048 |
| 8 | 5 | 1816 | BRIDGE | 760050 | Ledbetter Rd | 39526 | 34.98479 | -79.71535 |
| 8 | 6 | 3119 | PIPE | BP-077- 0081 | Hylan Av | 36030 | 34.89847 | -79.72492 |
| 8 | 7 | 1618 | BRIDGE | 760053 | Main St | 35321 | 34.88077 | -79.69586 |
| 8 | 8 | 1448 | BRIDGE | 820044 | Harry Malloy Rd | 21451 | 34.74345 | -79.4196 |
| 8 | 9 | 20 | ROAD | | | 16020 | 34.88293 | -79.69283 |
| 8 | 10 | 1560 | BRIDGE | 820005 | Mcfarland Rd | 15753 | 34.85352 | -79.52454 |
| 3 | 1 | 856 | BRIDGE | 90107 | US-74 | 1310749 | 34.23393 | -77.9694 |
| 3 | 2 | 828 | BRIDGE | 640014 | US-17 | 922196 | 34.2154 | -77.83413 |
| 3 | 3 | 860 | BRIDGE | 90108 | Andrew Jackson Hwy | 674468 | 34.23453 | -77.96968 |
| 3 | 4 | 813 | BRIDGE | 90075 | River Rd | 299750 | 34.19935 | -77.98063 |
| 3 | 5 | 2903 | PIPE | BP-065- 2061 | Eastwood Rd | 270278 | 34.23314 | -77.83938 |
| 3 | 6 | 973 | BRIDGE | 90004 | Andrew Jackson Hwy NE | 180780 | 34.27844 | -78.12568 |
| 3 | 7 | 975 | CULVERT | 640061 | Gordon Rd | 164498 | 34.27707 | -77.8673 |
| 3 | 8 | 2930 | PIPE | BP-065- 2036 | Castle Hayne Rd | 143166 | 34.28236 | -77.92272 |
| 3 | 9 | 39 | ROAD | n/a | Hwy 133/U.S. 421 Hwy NE | 61309 | 34.23641 | -77.95855 |
| 3 | 10 | 3011 | PIPE | BP-071- 2351 | Hwy 210 | 59499 | 34.44179 | -78.20434 |
| 10 | 1 | 3516 | PIPE | BP-090- 0237 | Waxhaw Hwy | 292992 | 34.94374 | -80.65803 |
| 10 | 2 | 2153 | BRIDGE | 890269 | W Lawyers Rd | 168928 | 35.10624 | -80.54847 |
| 10 | 3 | 3515 | PIPE | BP-090- 0233 | Waxhaw Hwy | 155106 | 34.93495 | -80.67712 |
| 10 | 4 | 2110 | BRIDGE | 890270 | Ridge Rd | 125802 | 35.08889 | -80.56689 |

| Division | Rank | CitySimID | Type | SourceID* | Street | Trips Disrupted (AA) | Latitude | Longitude |
|----------|------|-----------|--------|-------------|------------------------------|----------------------|----------|-----------|
| 10 | 5 | 3532 | PIPE | BP-090-0059 | Morgan Mill Rd | 124890 | 35.04092 | -80.50411 |
| 10 | 6 | 1835 | BRIDGE | 890213 | New Town Rd | 109362 | 34.9825 | -80.68048 |
| 10 | 7 | 2168 | BRIDGE | 890268 | W Lawyers Rd | 104313 | 35.10902 | -80.56202 |
| 10 | 8 | 2167 | PIPE | 890468 | W Lawyers Rd | 104313 | 35.109 | -80.56188 |
| 10 | 9 | 2078 | BRIDGE | 890254 | W Unionville Indian Trail Rd | 81392 | 35.07445 | -80.58632 |
| 10 | 10 | 1817 | BRIDGE | 890215 | Billy Howey Rd | 73714 | 34.97618 | -80.68505 |

**Source ID is the NCDOT System ID. Some Source IDs are "n/a" because they are a tracking location at a road low point, as opposed to a water crossing asset like a bridge, culvert, or drainpipe. Only water crossing assets had NCDOT system IDs.*

A key finding was the majority of disruption happened off U.S. 74 in the future. Figure 5.5 shows the projected disrupted trips occurred by whether the disruption was on U.S. 74 or in the connecting transportation network. A large percentage of the off-U.S. 74 disruption was likely on I-95, but other locations throughout the corridor also contributed.

Figure 5.5: Average Annual Storm/Flood Disrupted Trips on U.S. 74 Proper vs. Off-U.S. 74

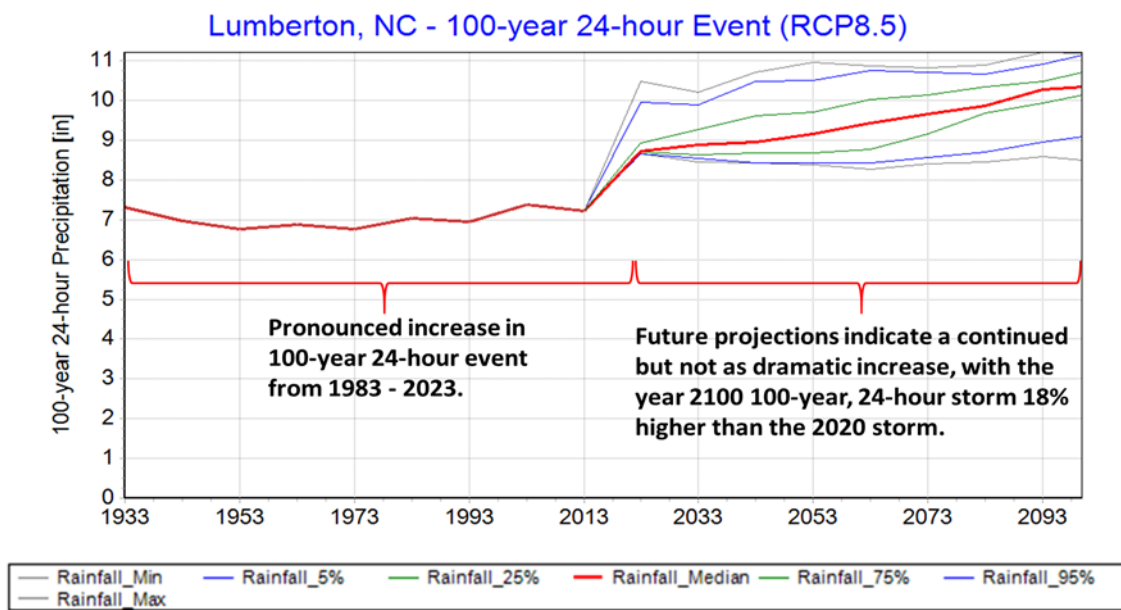


5.1.3 Finding 1.3: Large storms are projected to increase in severity.

Large storms were found to have increased dramatically over the last several decades and were projected to continue increasing into the future. As Figure 5.6 shows, the 100-year 24-hour rain depth was estimated by a sliding 40-year window, from 1922–1952 through 1992–2022 and evaluate the maximum 24-hour rain in each year in the window. A Weibull distribution was then fit to the maxima and the 1% (100-year) event was estimated from the resulting distribution.

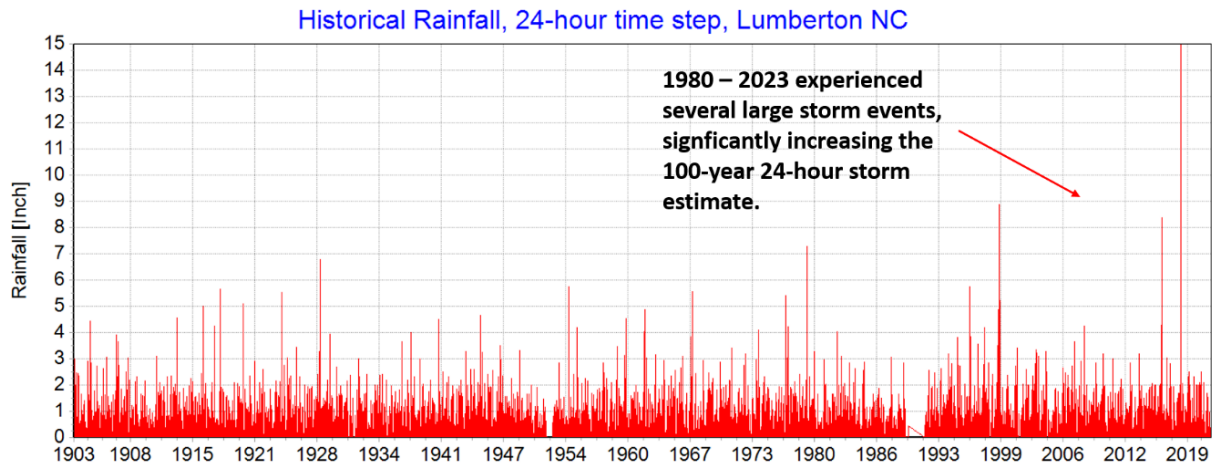
The results show a pronounced increase in the 100-year 24-hour storm over the last 40-year period (ending 2022, see Figure 5.7) and a projected continued increase into the future.

Figure 5.6: 100-Year 24-Hour Storm Event at Lumberton, NC



An ensemble 1922 –2100 daily rainfall projection was created by concatenating historical rainfall at Lumberton with projected rainfall at the same location. Using a sliding 40-year window, the 100-year 24-hour event was estimated in each decade (i.e., 1923-52, 1933-62, etc.) The results showed a pronounced increase in the 100-year 24-hour rain storm depth over the last 40 years, with the ensemble global climate models projecting the increase will continue into the future.

Figure 5.7: Lumberton, NC Historical Rainfall



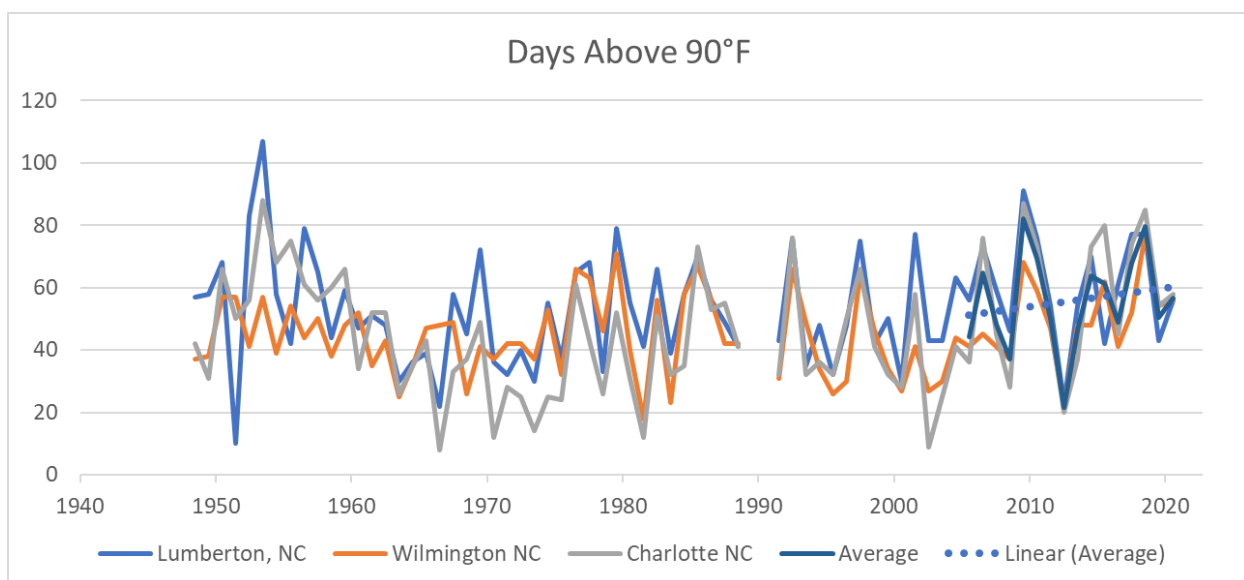
Historical rainfall in Lumberton showed a sharp increase in extreme rainfall events over the past 40 years, when compared to the whole record.

5.1.4 Finding 1.4: Heat is projected to be an increasingly disruptive problem.

The study projected maximum temperatures would rise steadily across the corridor and push the number of days above 90°F to more than three times higher than in 2020. This is projected to increase disruption to road and rail traffic.

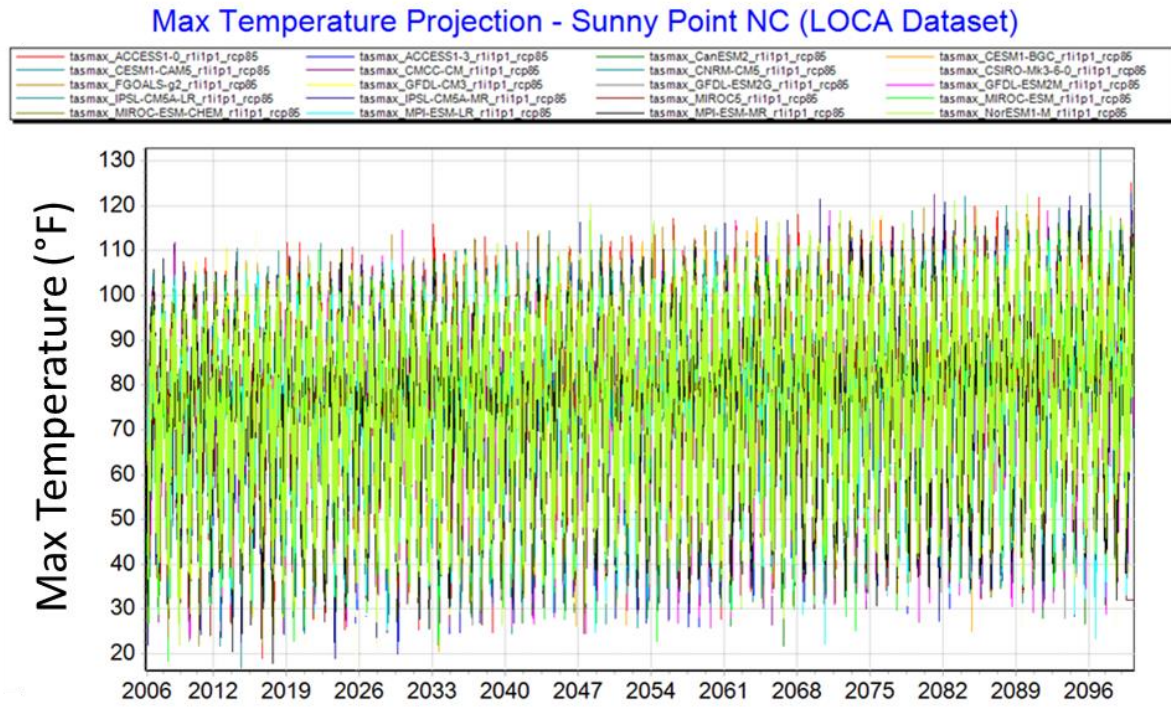
As Figure 5.8 shows, the number of days with maximum temperature above 90°F was near stationary from 1950 – 2005, with an uptick in from 2005 till present. Ensemble projected maximum temperature from the LOCA dataset (RCP8.5) for Sunny Point NC, a point in the eastern end of the corridor, rises steadily over the 21st century. (see Figure 5.9) and results in a projected increase from approximately 50 days per year exceeding 90°F to 150 days (see Figure 5.10).

Figure 5.8. Historical Number of Day Above 90°F



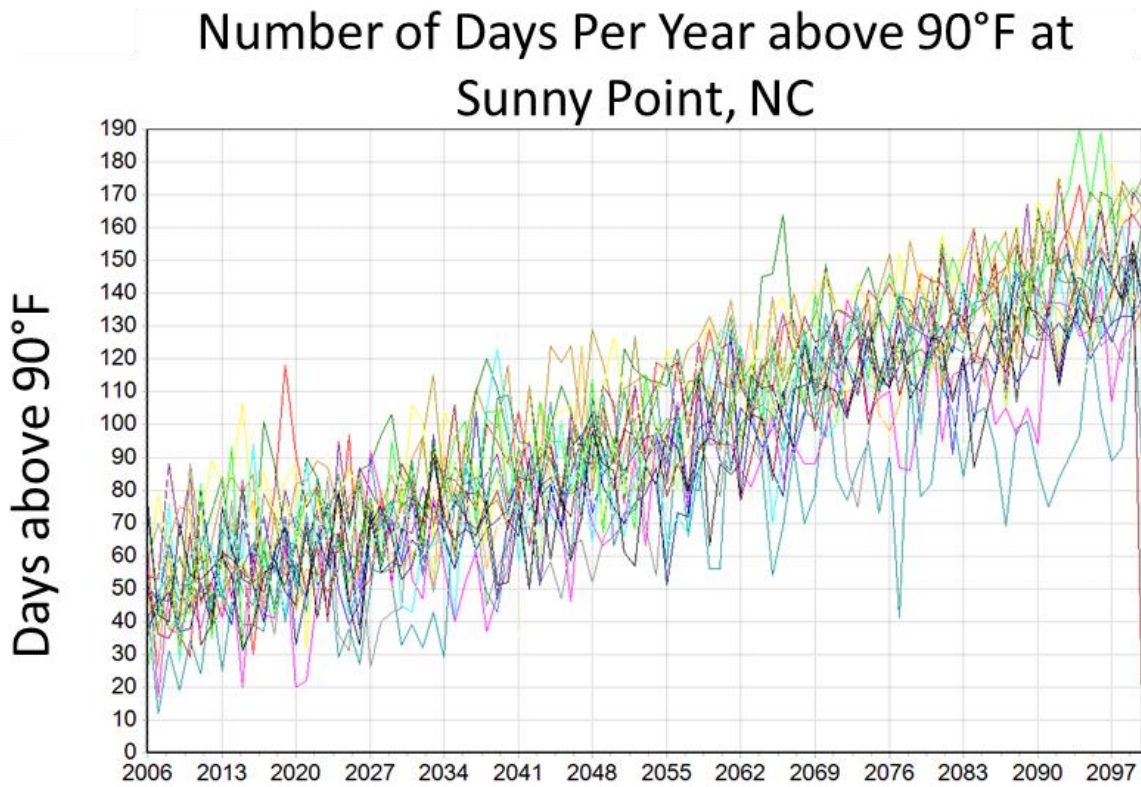
An assessment of the historical number of days with maximum temperature above 90°F at multiple locations across the corridor showed a generally stationary pattern from 1950–2010, with an upward trend from 2000–2020. Interestingly, the Lumberton and Charlotte, NC gauges experienced more extreme heat events in the 1950s than any other times in the record, which showed a historical precedent for extreme heat events.

Figure 5.9: Max Temperature Projection at Sunny Point, NC



The LOCA dataset provided 20 GCM-based projections of maximum temperature at Lumberton, NC. The models generally agreed that temperature will increase steadily into the future.

Figure 5.10: Number of Days per Year Above 90°F at Sunny Point, NC



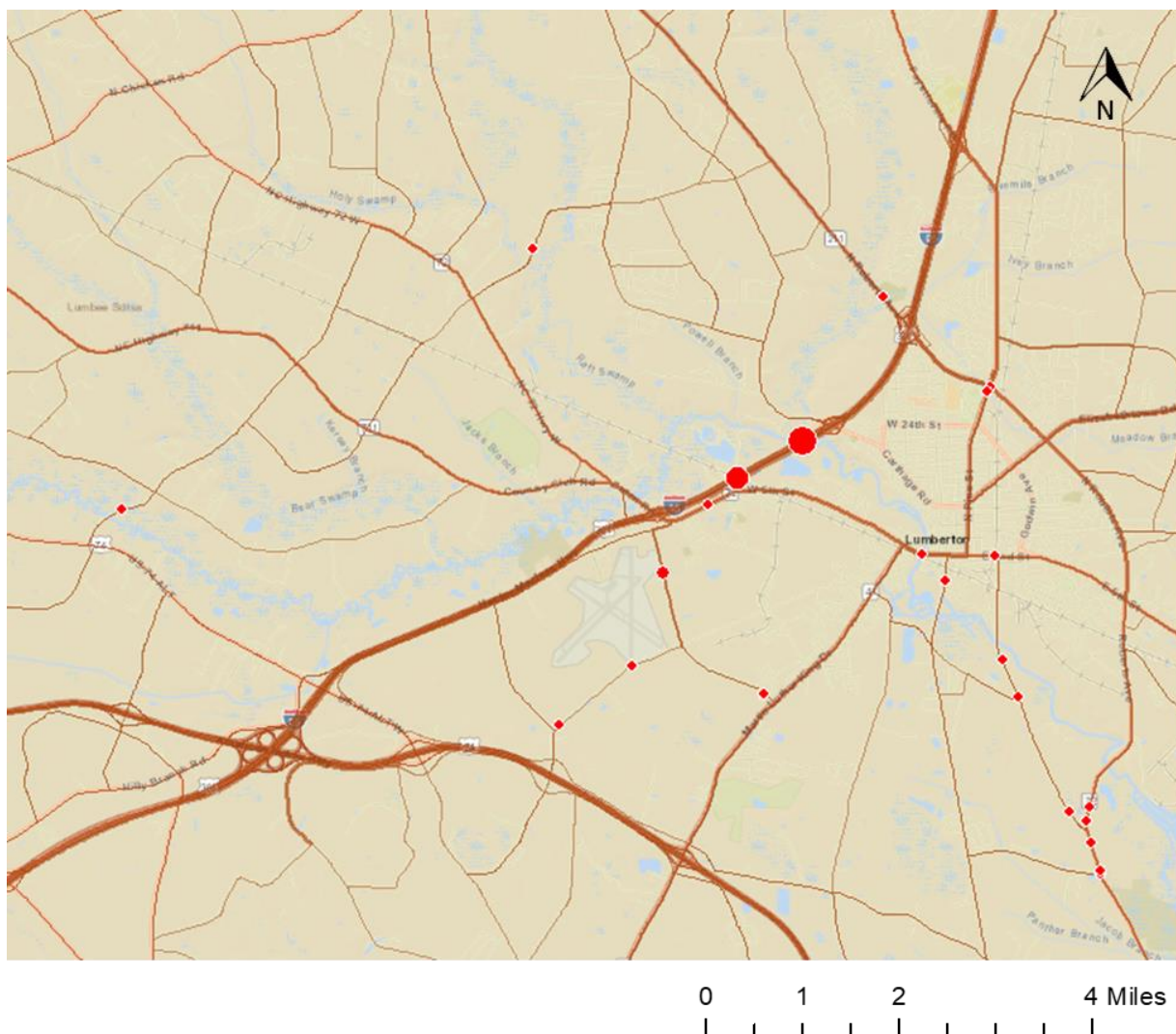
The number of days above 90°F derived from each of the GCM projections in the LOCA dataset for the Lumberton, NC grid cell.

5.1.5 Finding 1.5: I-95 is prone to flood disruption.

I-95 and supporting roads (see Figure 5.11) are projected to be vulnerable to future floods — close to U.S. 74. Recent major storms such as Hurricanes Matthew and Florence overtopped the stretch of I-95 over the Lumber River by several feet, which impacted regional mobility and halted the important transport of freight and state-to-state travelers which I-95 supports.

The simulation showed that with the exception of tidal and surge flood-prone areas in Wilmington, this location was the most impacted in the corridor in terms of future average annual trips disrupted. Given projections that AADT will increase from 65,000 today to 108,000 by 2060, reducing potential for trip disruption in this location is critical.

Figure 5.11: Locations with Potential for Overtopping

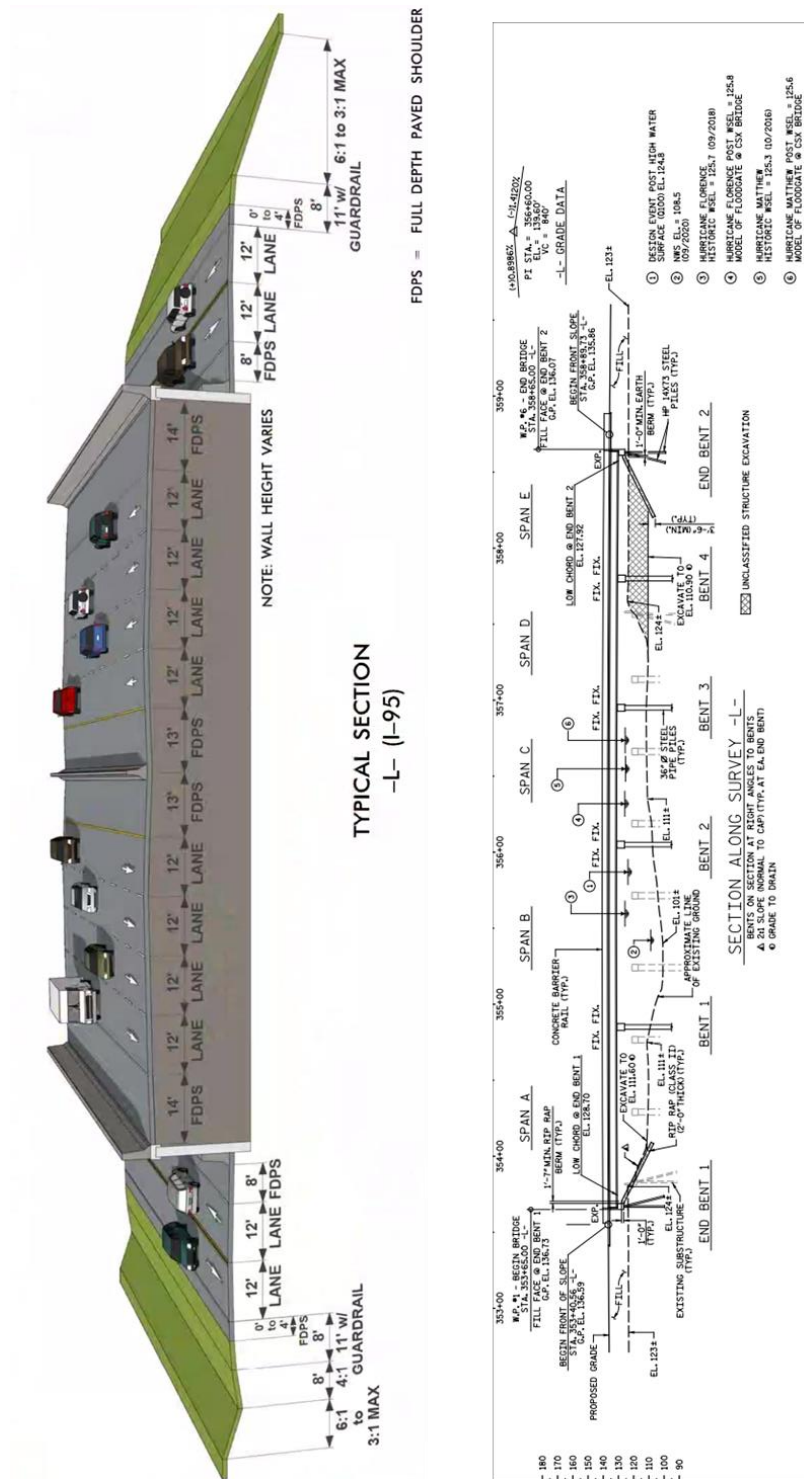


Multiple locations (both on I-95 and on frontage and supporting roads) showed significant potential for overtopping during major storms. I-95 currently supports 65,000 trips per day and is projected to increase to 108,000 trips per day by 2060. As this represents the highest traffic flow in the corridor, reduced disruption through elevation of the infrastructure should be a high priority.

5.1.5.1 *Current Work on I-95*

Design work was underway, which addressed flooding at I-95. As Figure 5.12 shows, the road deck was elevated up to thirteen feet in the area — close to the Lumber River crossing. The figure shows the water surface elevation peak points for several recent major storms, such as Hurricanes Florence and Matthew. The design elevated the road deck several feet above these high marks.

Figure 5.12: Current Work on I-95



Currently, planned work on the flood-prone section of I-95 included the elevation of the road deck up to thirteen feet to ensure water surface elevations (like those associated with Hurricanes Florence and Matthew) were significantly below the road deck.

5.1.6 Finding 1.6: Rail crossings are relatively resilient, with only three potential overtopping locations.

The study found that, generally, rail crossings in the U.S. 74 corridor are fairly flood resilient. The inventory of flood models projected that only three out of the 528 rail crossings in the corridor were potentially impacted by flooding, and this flooding occurred with the 500-year or higher storm.

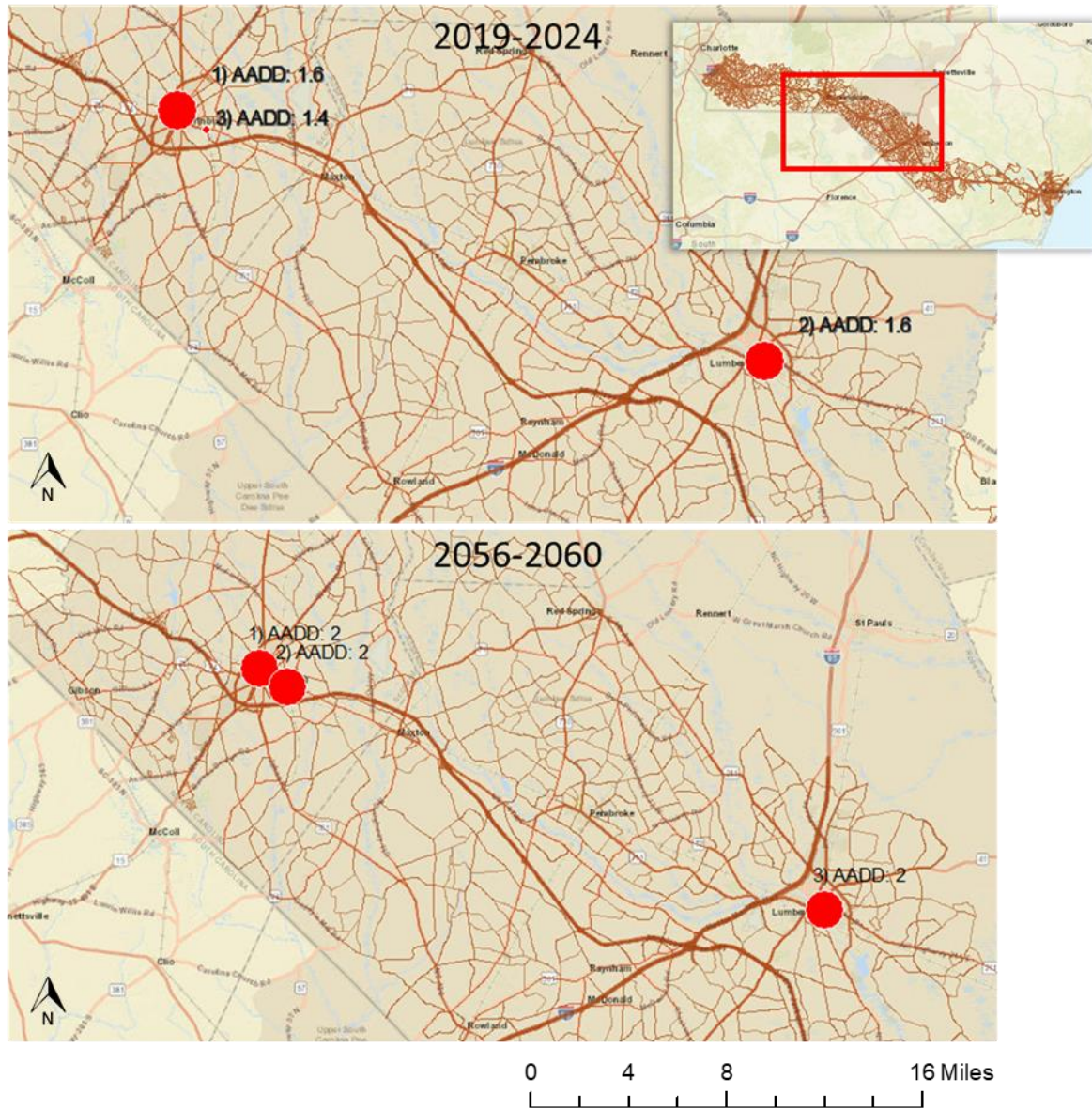
Figure 5.13 and Table 5.2 show the rail crossings, where average annual days disrupted (AADD) exceeded zero during the simulation. The top map shows the early period (2019–2024) and the lower map the late period (2056–2060). Only three rail crossings were overtopped during the simulation of both periods, and the expected AADD over these periods changed from 1.4 to 1.6 days per year to 2.0 days per year.

Table 5.2: Early and Late Period Flood-risk Rail Crossings

| Map Label | CitySimID | Type | SourceID | Street | Days Disrupted (Avg Annual 2019-2024) | Longest Period Disrupted (days) |
|---------------------------------|-----------|--------------|----------|----------------|---------------------------------------|---------------------------------|
| Early Period (2019-2024) | | | | | | |
| 1 | 4303 | RailCrossing | 852657F | N Gill St | 1.6 | 5 |
| 2 | 4655 | RailCrossing | 631438G | E 2nd St | 1.6 | 5 |
| 3 | 4344 | RailCrossing | 852562X | Dixie Guano Rd | 1.4 | 5 |
| Late Period (2056-2060) | | | | | | |
| 1 | 4303 | RailCrossing | 852657F | N Gill St | 2 | 5 |
| 2 | 4344 | RailCrossing | 852562X | Dixie Guano Rd | 2 | 5 |
| 3 | 4655 | RailCrossing | 631438G | E 2nd St | 2 | 5 |

Figure 5.13: Average Annual Days Disrupted at Rail Crossings

Average Annual Days Disrupted at Rail Crossings

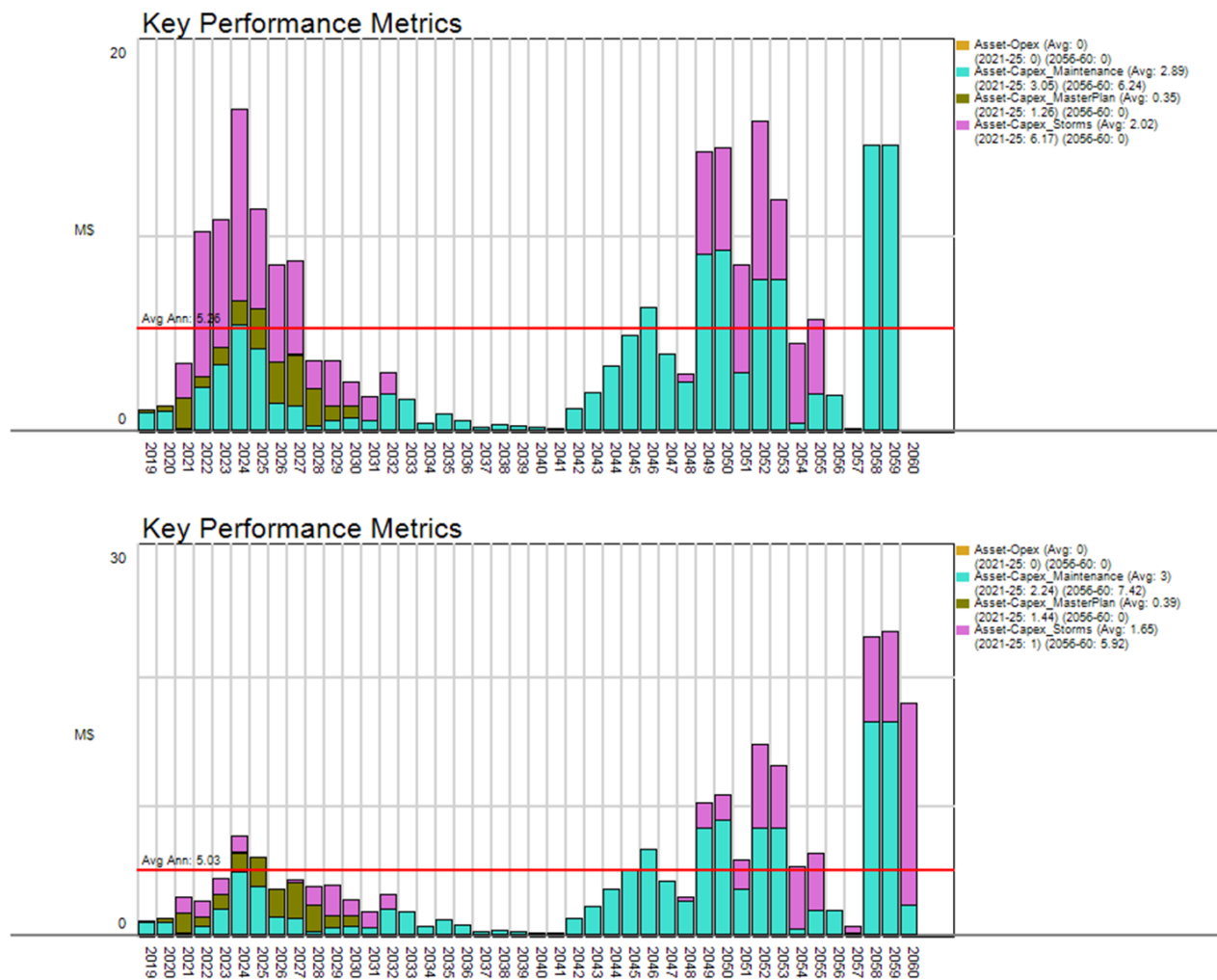


Three of 528 rail crossings in the corridor showed potential for flooding over the course of the simulation. The average annual days disrupted at these locations increased from 1.4–1.6 days per year to 2.0 days per year, when compared the early and late periods (2019–2024 vs. 2056–2060).

5.1.7 Finding 1.7: A 10-year period at the early part of the timeline with a series of storms with return periods like Matthew and Florence will cause average annual \$3.85M in damage (2020 dollars). In the latest 10-year period in the timeline, a series with the same return periods will cause \$5.3M in average annual damage (2020 dollars). The increase is due to extreme storms becoming larger in the future.

Maintenance of the system of bridges, culverts, and pipes will cost on average \$5M per year across the corridor in the coming 40 years. Future floods are projected to drive maintenance costs higher. See Figure 5.14 and Figure 5.15 for projected costs and asset condition for the early storms and late storms scenarios.

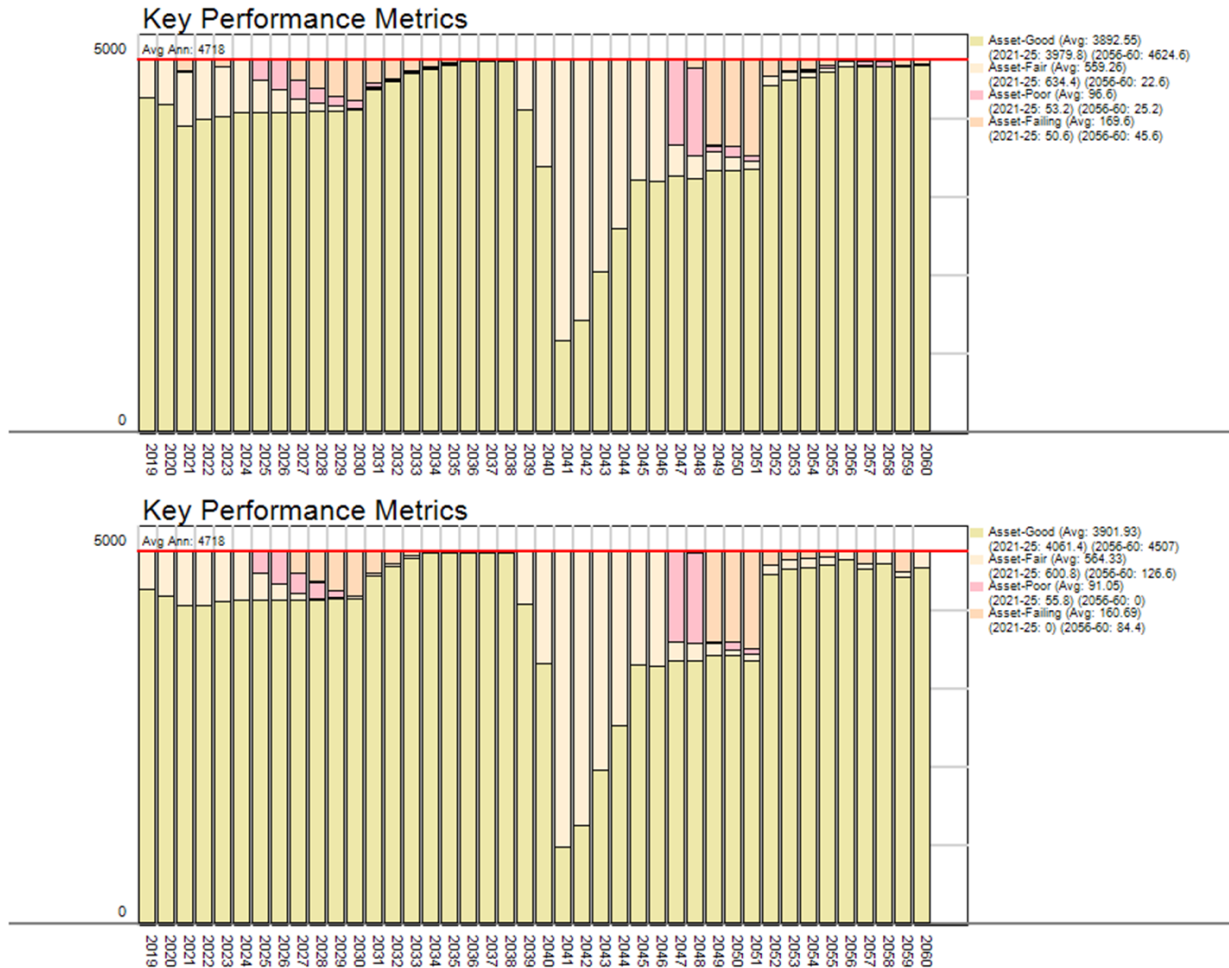
Figure 5.14: Spending on Transportation Asset System



The 95th percentile most severe early timeline (upper chart) held the most severe storms in the 2019-2024 period (upper chart). The 95th percentile most severe late timeline (lower chart) held the most severe storms of the timeline

in the 2056-60 period. The average spending on storm damage (magenta bars) in the first 10 years of the early timeline was \$3.85M, while it was \$5.3M when looking at the 10-year average of the late years in the lower chart.

Figure 5.15: Asset Conditions Across All Assets

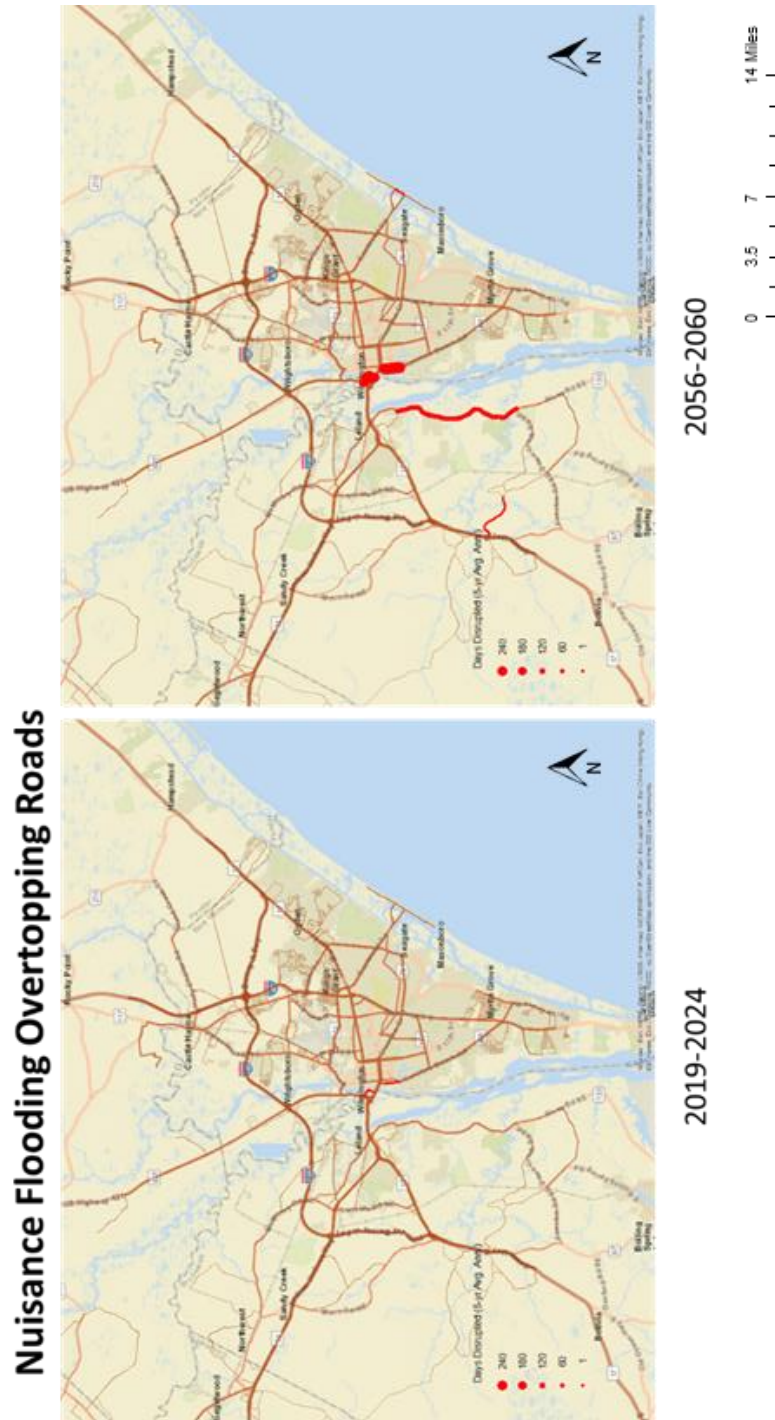


Assets by condition category for the early period forecast (upper chart) and late period forecast (lower chart). Both simulations produced similar distributions of asset condition over time, with a large percentage of good-condition assets present until the 2040s, when many assets started at useful life and moved to failing condition.

5.1.8 Finding 1.8: Coastal roads are projected to be increasingly impacted by tidal overtopping and seawater inundated freeboard.

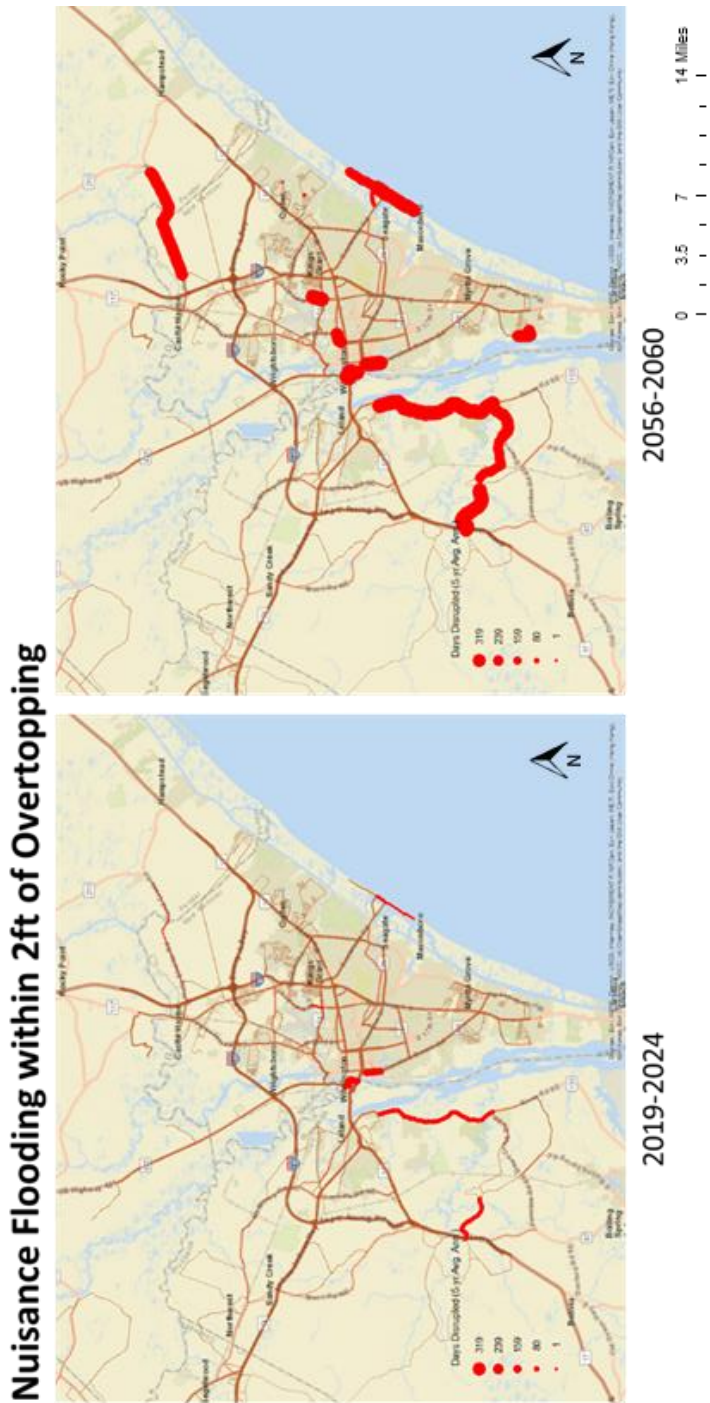
Coastal roads in the Wilmington area were found to be relatively resilient to tidal flooding. Two segments of road were found to experience nuisance flooding in 2022. This was projected to increase to seven road segments by 2060 (see Figure 5.16). A more serious concern was seawater invading the freeboard zone - within two feet of the road deck. With sea water inundation likely to accelerate deterioration of road assets, the projected widespread and regular occurrence of this type of event by 2060 is a reason for concern (see Figure 5.17).

Figure 5.16: Road Segments at Risk of Overtopping for 2025 and 2060



Nuisance flooding was caused by sea level rise and tides, and where seawater overtopped road decks were shown that affected only two sections of road in the 2019–2024 timeframe. By 2056–2060, however, overtopping from nuisance flooding spread to multiple roads, particularly near the Cape Fear and Brunswick River estuaries.

Figure 5.17: Road Segments with Seawater within Two Feet of Overtopping for 2025 and 2060



Nuisance flooding was of concern in the freeboard range of elevation and considered the road deck to be two feet below the road deck in this study. In this zone, infiltrated seawater significantly increased maintenance requirements for roads. This map showed the 2019–2024 levels of water in the freeboard zone and the 2056–2060 levels, where a significant portion of the Wilmington Road system was overwhelmed by seawater.

5.2 Study Question 2 Findings: Critical Facilities

The second question focused on critical facilities asked:

“Which critical facilities (hospitals, emergency care, shops, schools, NCDOT facilities, fire stations, and police stations) were most at risk of cutoff from access? Which assets (roads, bridges, culverts, pipes) were involved?”

The findings focused on identifying the remoteness, redundancy, and flood overtopping risk of the transportation network in each critical facility’s service area and on how these factors are projected to change with climate change.

5.2.1 Finding 2.1: Critical facility risk varies depending on overtopping risk and remoteness/redundancy in the facility service area.

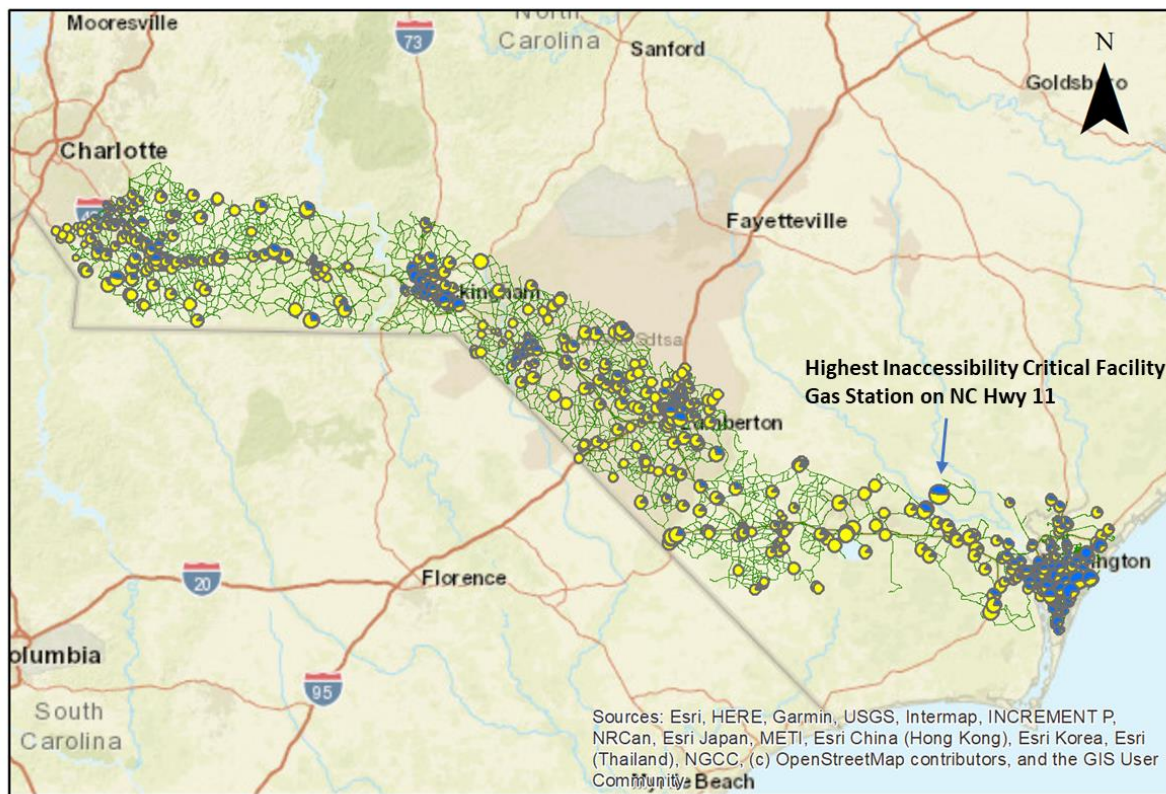
Figure 5.18 presents each critical facility as a pie chart, with blue areas representing overtopping risk and yellow areas representing remoteness/redundancy. The pie charts are sized according to the total inaccessibility risk index, which is a multiplication of the remoteness/redundancy and overtopping risk.

General conclusions from the assessment were:

- Inaccessibility peaks in multiple locations across the corridor with high-ranking facilities in both remote and urban areas. This is due to the inaccessibility index considering both remoteness/redundancy and overtopping risk.
- The highest inaccessibility location is a gas station on NC Highway 11. It has a score of 17 out of 20, with a remoteness/redundancy score of nine and an overtopping risk score of eight.
- Overtopping risk is more of a factor in the parts of the corridor with flood risk determined in Section 5.1. These locations include Wilmington, I-95, Laurinburg, and the Charlotte suburbs. Wilmington overtopping is explained by storm surge potential, while flooding in the other locations is likely due to potential riverine flooding during larger storms like hurricanes.

The remoteness/redundancy, overtopping risk, and inaccessibility indexes are stored in the U.S. 74 City Simulator geodatabase provided as part of the deliverable of this project. Readers can view this data in a standard GIS software package or use the web app, also delivered as part of this project.

Figure 5.18: Critical Facilities by Remoteness/Redundancy and Overtopping Risk



Legend

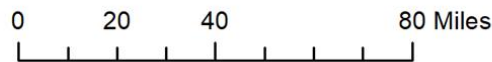
CriticalFacilities_US74100mmBuffer_WM

Inaccessibility_Index



Overtopping_Risk

RemRed_Category



5.2.2 Finding 2.2: Climate change impacts will likely exacerbate inaccessibility for critical facilities.

The climate change impact on critical facilities was projected to be similar to the impacts described above for the larger corridor. Water crossing locations such as bridges, culverts, and pipes will encounter increasingly intense floods that threaten the reduction of accessibility in already remote and low route-redundancy critical facilities. The facilities with large service areas were found to be most at risk, because they often had a single route for access, a route that experienced severe flooding in future decades.

5.3 Study Question 3 Findings: Disadvantaged Populations

The third question focused on disadvantaged populations, asking:

“How were disadvantaged populations impacted by climate disruptions to the transportation system?”

The findings focused on current levels of access for disadvantaged populations to sustenance facilities (gas stations, stores, emergency care, emergency shelters), and how the level of access will change with climate change.

5.3.1 Finding 3.1: Inaccessibility to sustenance facilities currently impacts disadvantaged populations.

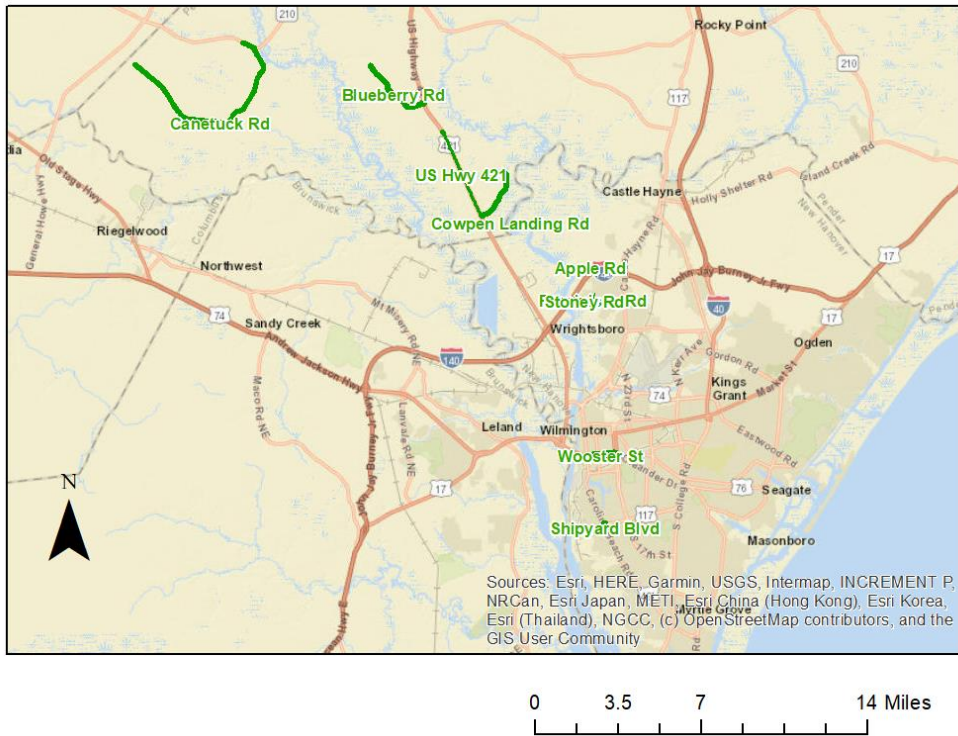
Disadvantaged populations were defined through the NCDOT Title VI-based guidelines as census block groups with high poverty and minority populations. See Sections 4.12 and 4.13 for details on how the populations were defined. Once defined, the roads within the disadvantaged census block groups were evaluated for their level of inaccessibility by an index that integrated the length of travel, road network density and flood risk along routes in nearby sustenance facilities. Sustenance facilities were defined as stores, emergency health care, emergency shelters, and gas stations.

Figure 5.19 – 5.27 and Table 5.3 – 5.6, present the top ten roads in terms of low accessibility for each NCDOT division in green and the top ten disrupting water-crossing assets (bridges, culverts, drainpipes, and road low points).

The tables provide information on each water crossing assets, which includes the type of asset, the NCDOT ID, the number of trips disrupted during a 2020 500-year storm event for each sustenance category, the joint disrupted trips index, and the ranking by division and county.

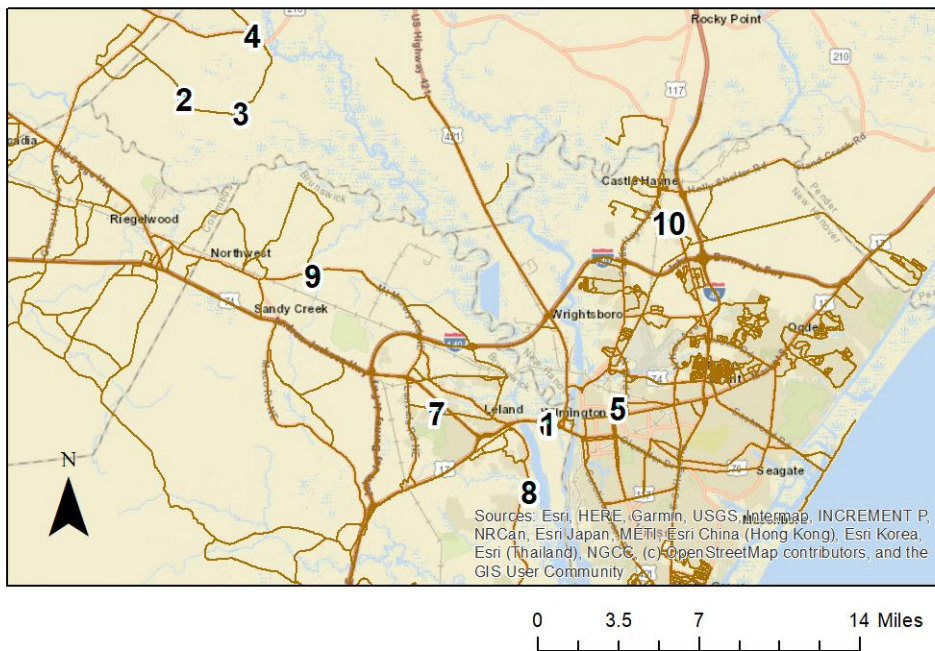
As the figures and table show, inaccessibility is a concern even in the early period assessment. Disrupted trips appear in all divisions, with a maximum joint disruption index of over eight million trips in certain locations in Division 3. Division 3 was the most prone to disruption from flood reducing inaccessibility. This was because of its proximity to the coast, which had a denser water crossing road network, higher population density, and potentially higher population increase into the future.

Figure 5.19: Top Ten Least Accessible Disadvantaged Population Streets



The green road segments are the top ranked inaccessible road segments in disadvantaged areas in the division.

Figure 5.20: Division 3 –Disadvantaged Population Streets and Supporting Water Crossing Assets

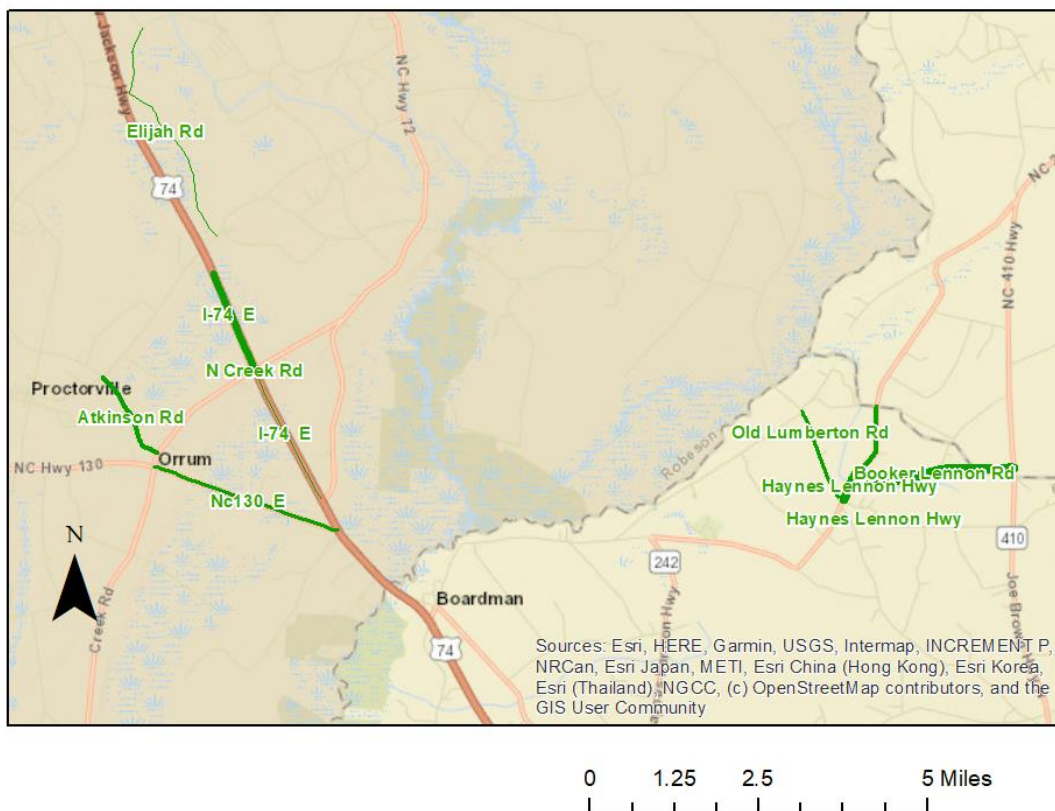


Rank of disruption of bridges, culverts, drainpipes, low road points within the division.

Table 5.3: Division 3 - Disadvantaged Population Streets and Supporting Water Crossing Assets

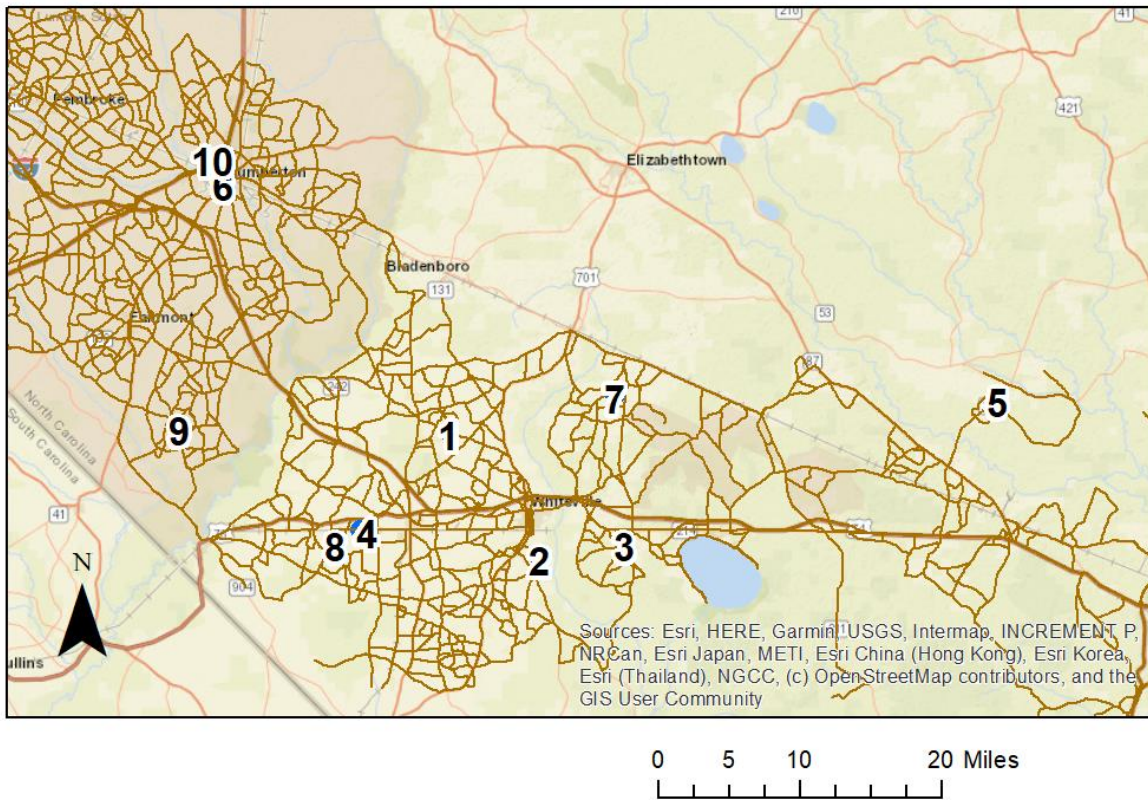
| | | Disrupted Trips for Disadvantaged Populations during 500-year storm | | | | | Rank in Division |
|---------|----------|---|----------|---------|----------|---------|------------------|
| SubType | SourceID | Educational | Fuel | Medical | Retail | Joint | |
| BRIDGE | 90108 | 2752560 | 14469120 | 7300080 | 14469120 | 8307360 | 1 |
| BRIDGE | 700215 | 260640 | 19301760 | 5080320 | 16403400 | 8164134 | 2 |
| BRIDGE | 700020 | 260640 | 19301760 | 5080320 | 16403400 | 8164134 | 3 |
| BRIDGE | 700144 | 253440 | 18027000 | 4837680 | 15140520 | 7633026 | 4 |
| CULVERT | 640137 | 1167120 | 6539760 | 5968080 | 6539760 | 4669524 | 5 |
| BRIDGE | 90107 | 2211840 | 4795200 | 4740480 | 4795200 | 3890448 | 6 |
| BRIDGE | 90181 | 1940400 | 4450320 | 4395600 | 4450320 | 3581172 | 7 |
| BRIDGE | 90075 | 455760 | 4712400 | 4657680 | 4712400 | 3393468 | 8 |
| ROAD | n/a | 369600 | 3788640 | 1398360 | 3338100 | 1840269 | 9 |
| CULVERT | 640064 | 168360 | 3404580 | 855480 | 2942760 | 1463838 | 10 |

Figure 5.21: Division 6 – Top 10 least accessible Disadvantaged Population Streets



The green road segments are the top ranked inaccessible road segments in disadvantaged areas in the division.

Figure 5.22: Division 6 –Disadvantaged Population Streets and Supporting Water Crossing Assets

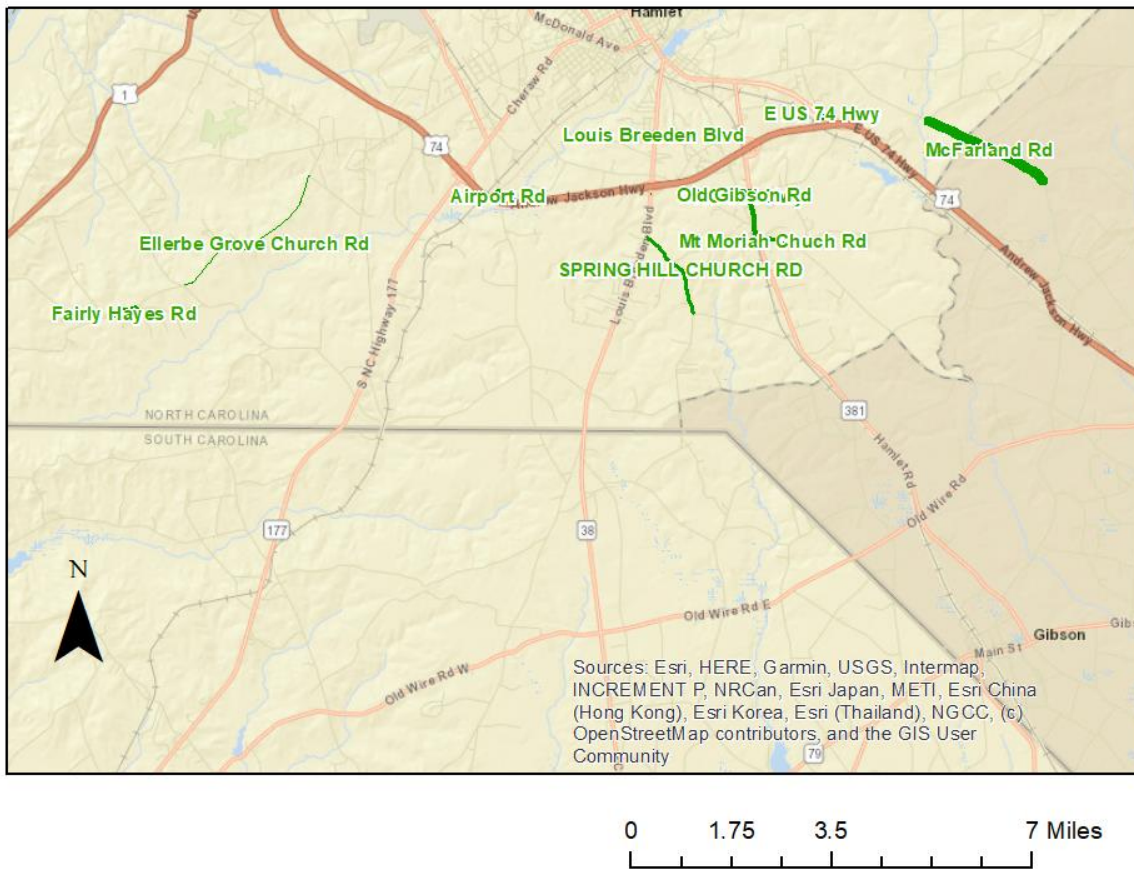


Rank of disruption of bridges, culverts, drainpipes, low road points within the division.

Table 5.4: Division 6 - Disadvantaged Population Streets and Supporting Water Crossing Assets

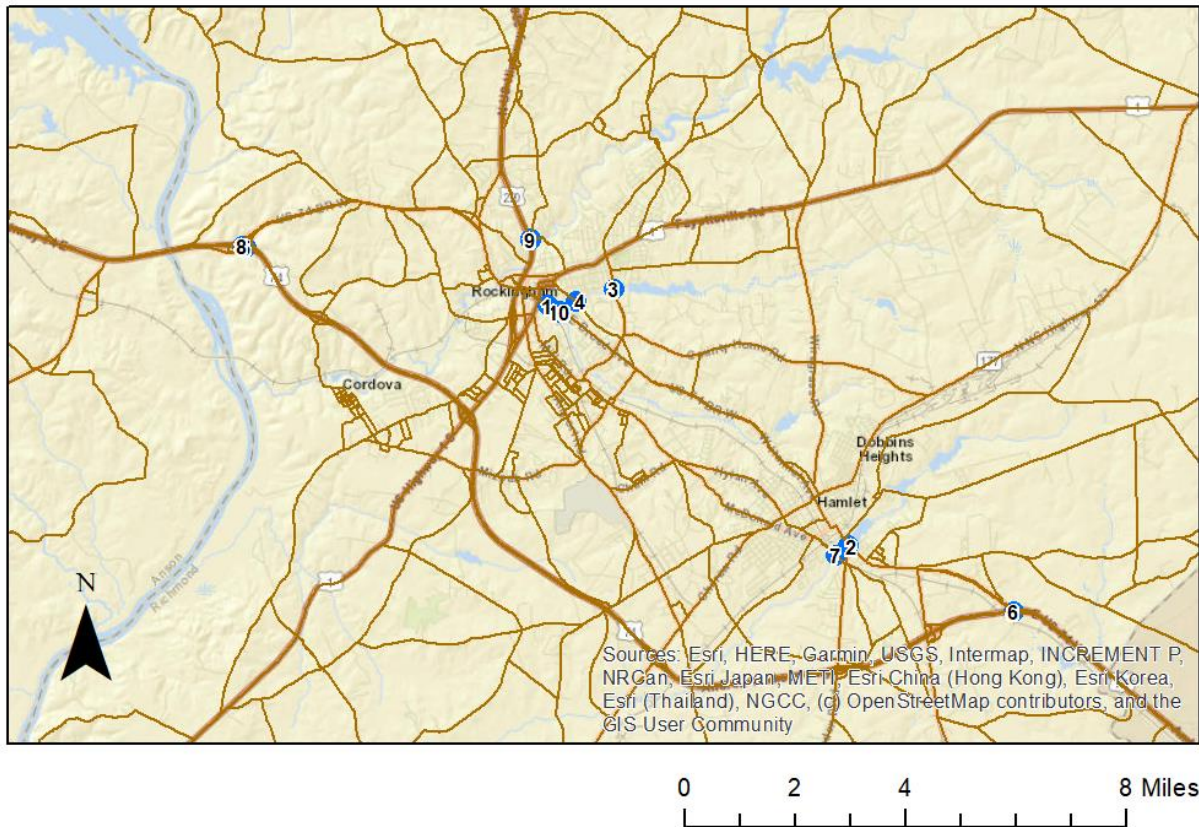
| | | Disrupted Trips for Disadvantaged Populations during 500-year storm | | | | | Rank in Division |
|---------|----------|---|----------|----------|----------|----------|------------------|
| SubType | SourceID | Educational | Fuel | Medical | Retail | Joint | |
| BRIDGE | 230201 | 253440 | 24777720 | 13389120 | 21745080 | 12966858 | 1 |
| BRIDGE | 230002 | 197280 | 18537120 | 6096240 | 15833880 | 8265510 | 2 |
| BRIDGE | 230211 | 237600 | 18788400 | 5434560 | 16085160 | 8131950 | 3 |
| BRIDGE | 230141 | 1756080 | 17136000 | 5996880 | 14292000 | 8108928 | 4 |
| BRIDGE | 80055 | 563040 | 18559440 | 5147280 | 15687720 | 8007354 | 5 |
| CULVERT | 770122 | 1761840 | 13128120 | 8178480 | 11934720 | 7718760 | 6 |
| BRIDGE | 230232 | 125280 | 18067680 | 4709520 | 15195960 | 7572582 | 7 |
| BRIDGE | 230285 | 30960 | 15132600 | 4217040 | 12288240 | 6353460 | 8 |
| BRIDGE | 770114 | 311040 | 12130200 | 4487040 | 9261360 | 5463468 | 9 |
| CULVERT | 770212 | 1013040 | 7079400 | 2574000 | 6671520 | 3570768 | 10 |

Figure 5.23: Division 8 – Top 10 least accessible Disadvantaged Population Streets



The green road segments are the top ranked inaccessible road segments in disadvantaged areas in the division.

Figure 5.24: Division 8 – Disadvantaged Population Streets and Supporting Water Crossing Assets



Rank of disruption of bridges, culverts, drainpipes, low road points within the division.

Table 5.5: Division 8 - Disadvantaged Population Streets and Supporting Water Crossing Assets

| | | Disrupted Trips for Disadvantaged Populations during 500-year storm | | | | | Rank in |
|---------|----------|---|---------|---------|---------|---------|----------|
| SubType | SourceID | Educational | Fuel | Medical | Retail | Joint | Division |
| CULVERT | 760175 | 3342960 | 8676360 | 8999280 | 8577720 | 7007418 | 1 |
| CULVERT | 760173 | 5749200 | 7918920 | 8022960 | 7781040 | 6996276 | 2 |
| CULVERT | 760169 | 1443600 | 5079240 | 5402160 | 4834440 | 3992670 | 3 |
| BRIDGE | 760163 | 1740240 | 4770360 | 5093280 | 4662360 | 3871134 | 4 |
| CULVERT | 760223 | 863280 | 3072600 | 2444400 | 2856600 | 2114370 | 5 |
| BRIDGE | 760214 | 2021040 | 2256840 | 2316960 | 2178720 | 2094372 | 6 |
| BRIDGE | 760053 | 1712880 | 2040840 | 2144880 | 1933560 | 1877130 | 7 |
| BRIDGE | 760221 | 835920 | 2462040 | 1810800 | 2222280 | 1668510 | 8 |
| CULVERT | 760171 | 514800 | 1935000 | 1874880 | 1792080 | 1440720 | 9 |
| ROAD | n/a | 557160 | 1446060 | 1499880 | 1429620 | 1167903 | 10 |

Figure 5.25: Division 10 – Top 10 Least Accessible Disadvantaged Population Streets, Part A

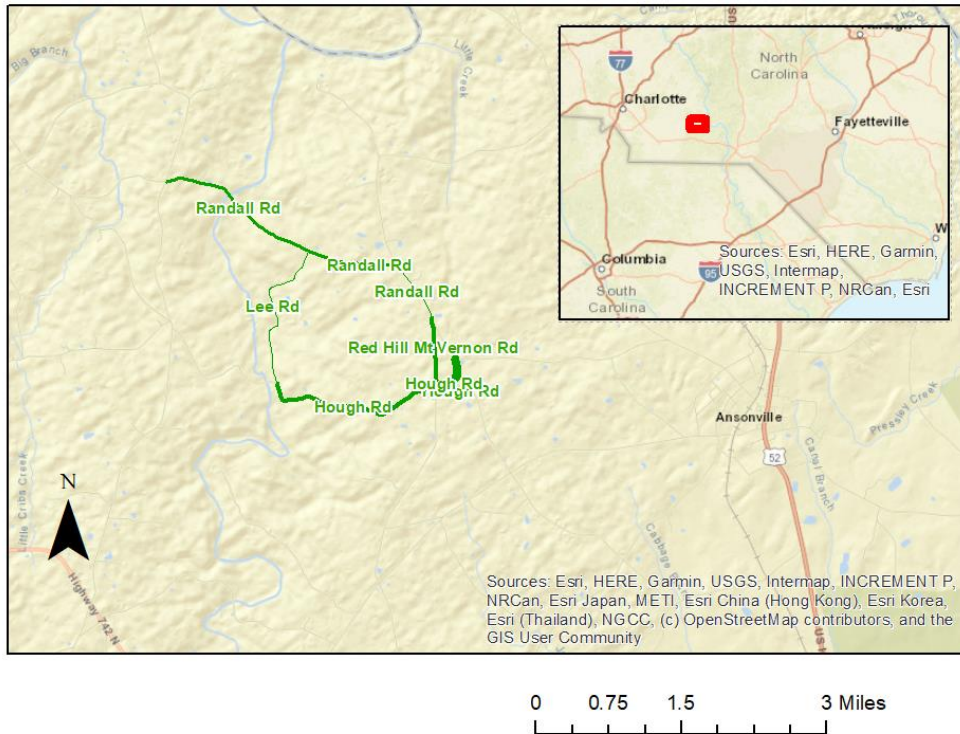


Figure 5.26: Division 10 – Top 10 Least Accessible Disadvantaged Population Streets, Part B

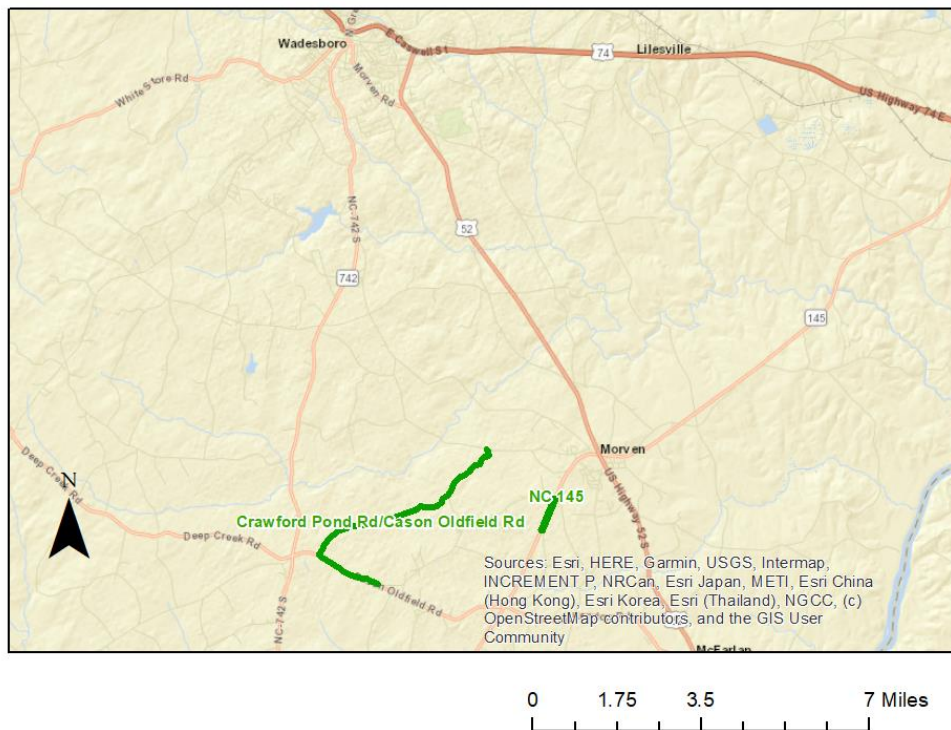
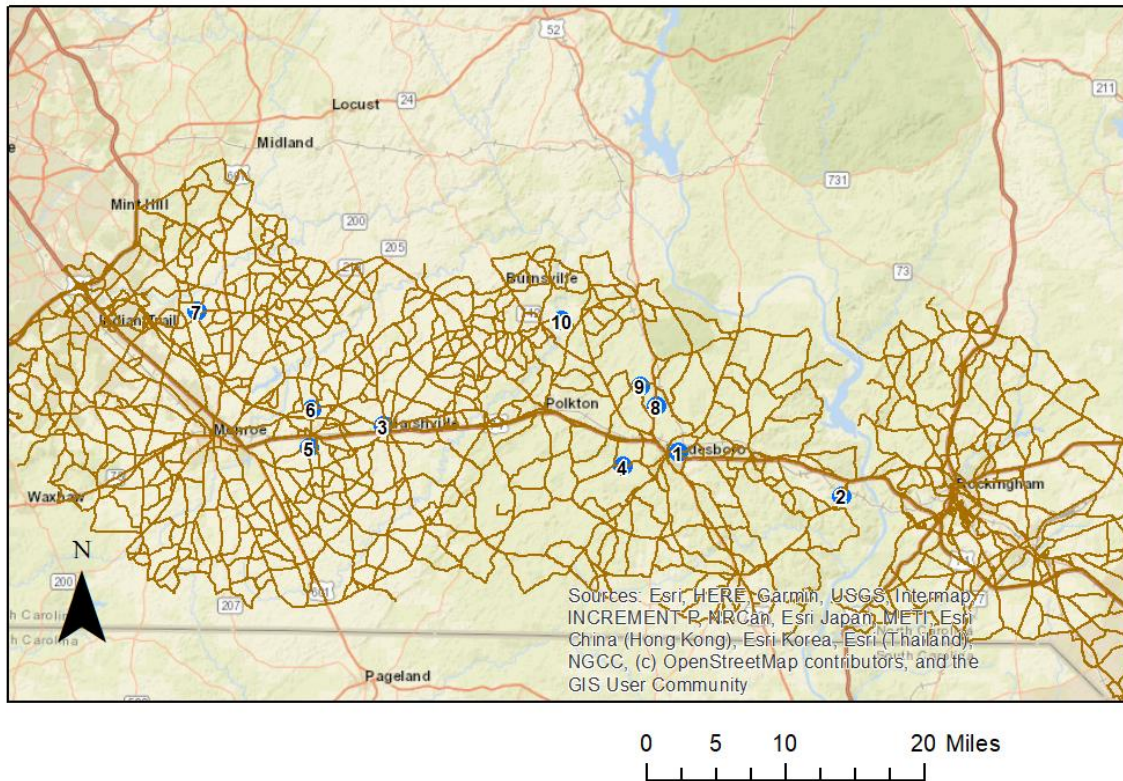


Figure 5.27: Division 10 –Disadvantaged Population Streets and Supporting Water Crossing Assets



Rank of disruption of bridges, culverts, drainpipes, low road points within the division.

Table 5.6: Division 10 - Disadvantaged Population Streets and Supporting Water Crossing Assets

| | | Disrupted Trips for Disadvantaged Populations during 500-year storm | | | | | Rank in Division |
|---------|----------|---|---------|---------|---------|---------|------------------|
| SubType | SourceID | Educational | Fuel | Medical | Retail | Joint | |
| CULVERT | 30031 | 2531520 | 4043520 | 3427920 | 4536720 | 3321864 | 1 |
| CULVERT | 30330 | 693360 | 2744640 | 2575440 | 2532600 | 2003562 | 2 |
| BRIDGE | 890417 | 802800 | 1974960 | 1127160 | 1707840 | 1246374 | 3 |
| CULVERT | 30326 | 797760 | 1635480 | 1453680 | 1391040 | 1243980 | 4 |
| BRIDGE | 890082 | 383760 | 2099160 | 748080 | 2426400 | 1141560 | 5 |
| BRIDGE | 890074 | 313200 | 2266560 | 664200 | 2033640 | 1069128 | 6 |
| BRIDGE | 890270 | 198720 | 2495160 | 450360 | 2142000 | 1027638 | 7 |
| CULVERT | 30043 | 174240 | 1878480 | 808920 | 1848600 | 979668 | 8 |
| BRIDGE | 30161 | 100800 | 1994400 | 658440 | 1706760 | 910548 | 9 |
| BRIDGE | 30304 | 210240 | 2066040 | 524520 | 1713960 | 906444 | 10 |

5.3.2 Finding 3.2: Climate change is likely to exacerbate inaccessibility for disadvantaged populations.

These two disruption-focused metrics presented in Finding 3.1 — average annual trips and days disrupted — were calculated for the early period of the simulation (2019–2024). Also presented in the tables for finding 3.1 above are the projected changes in disruption by the end of the simulation (2056–2060). Both the early period estimates and the late period estimates were 95th percentile – or near worst case – estimates of disruption in their respective five-year periods.

As Figure 5.19, Figure 5.20, Figure 5.21, Figure 5.22, Figure 5.23, Figure 5.24, Figure 5.25, Figure 5.26 and Figure 5.27 and Table 5.3, Table 5.4, Rank of *disruption of bridges, culverts, drainpipes, low road points within the division*.

Table 5.5, and Table 5.6 show, inaccessibility is a concern for disadvantaged populations across the corridor. Expected SLR compounded with storm surge, riverine, and pluvial flooding at the coast is projected to lead to significant increases in flood risk in Division 3, while isolated disadvantaged populations in rural areas of Divisions 6, 8, and 10 experienced increasing flood risk from pluvial and riverine sources.

The projected increases in average annual trips disrupted ranged from five percent to more than eight times the disruption. This is because of both increased flood risk and increased travel on flood-prone roads, as population increased into the future.

6 Adaptation and Mitigation

6.1 Rationale

The simulator was used to test reducing the vulnerabilities identified in the previous chapter with adaptation and mitigation actions. These actions included the elevation of bridges and the roadways that overtopped culverts, hardened rail crossings, elevating roads at the coast, and increased redundant routes in inaccessible areas.

The study used a scenario-based approach, where a portfolio of actions were introduced in a single resilience-focused scenario. This scenario was simulated, and the subsequent performance metrics were compared to the same metrics evaluated in the vulnerability assessments' baseline run scenario.

Resilience-focused improvements were pursued on all future projects in the corridor, both documented STIP projects and automated maintenance projects initiated by asset condition decay. The type of improvement implicitly varied with the asset type. For example, if the asset was a bridge and a replacement was projected, then the improvement was to design and construct the asset with a higher protection level than the level used to design the current asset.

In the baseline scenario, a 2020 50-year event protection level was assumed as the design criterion – implying that any new bridge, culvert, or drainpipe is designed so that the road deck is above the water surface elevation projected to occur during a 2020 50-year flood event.

In the resilience-focused scenario, the protection level was increased to the 2020 500-year level. This increase resulted in increased cost as a percentage of asset replacement cost, as summarized in Table 6.1 below. For this study, it was assumed that all current assets are designed to the 50-year protection level in the baseline scenario, and that in the resilience-focused scenario the protection level was at 500-year, which increased cost for replacement by 50%.

Table 6.1: Protection Level and Percent of Replacement Cost

| Protection Level | Percent of Replacement Cost |
|--------------------|-----------------------------|
| 50-year 24-hour | 100% |
| 100-year 24-hour | 125% |
| 500-year 24-hour | 150% |
| 1,000-year 24-hour | 200% |
| All Storms | 250% |

An initial simulation of the resilience-focused scenario increased the protection level to the 500-year, while other factors such as the scheduling of maintenance events remained the same as the baseline scenario. In this initial scenario run, the level of investment was not limited, and return on investment (ROI) was not used as a guide. Often, this approach led to a reactive approach to improving resilience by only replacing and improving assets in the wake of storms.

Further, as many of the assets in the transportation system were installed around the same time, the approach led to “clumping” of maintenance projects, where years of relatively little spending were followed by heavy-spending years. The findings on asset spending above underscored this effect. (See Finding 1.7 which shows relatively little asset spending in the 2030s followed by high very high spending requirements in the 2040s and 2050s.)

A sensitivity assessment was then conducted to refine the resilience-focused scenario to reduce post-disaster spending and achieve the highest resilience ROI given limited spending per year. Figure 6.1 summarizes the resilience-focused scenario runs. The subsequent sections summarize the results of the initial resilience-focused run and sensitivity analysis.

Figure 6.1: Base Run and Resilience-Focus

| Base Run | Resilience-focus | | | | | |
|---|--|---|---------------|--------------------|--|---|
| <ul style="list-style-type: none"> • Ground-truthed Maintenance • Current Plans (2020-2030) • No Adaptation • No Mitigation | <ul style="list-style-type: none"> • Same as Base Run • Add resilience actions at each opportunity • Elevate Bridges/Culverts to 2020 500-year WSEL • Harden Rail Crossings • Increase Route Redundancy | <table border="0"> <tr> <td style="vertical-align: top;">Timing</td> <td style="vertical-align: top;">Highest ROI</td> </tr> <tr> <td> <ul style="list-style-type: none"> • All at start • Annual Steady Improvement • Post-Disaster </td> <td> <ul style="list-style-type: none"> • Limitless Spend • Current Spend + 10% • Current Spend + 25% </td> </tr> </table> | Timing | Highest ROI | <ul style="list-style-type: none"> • All at start • Annual Steady Improvement • Post-Disaster | <ul style="list-style-type: none"> • Limitless Spend • Current Spend + 10% • Current Spend + 25% |
| Timing | Highest ROI | | | | | |
| <ul style="list-style-type: none"> • All at start • Annual Steady Improvement • Post-Disaster | <ul style="list-style-type: none"> • Limitless Spend • Current Spend + 10% • Current Spend + 25% | | | | | |

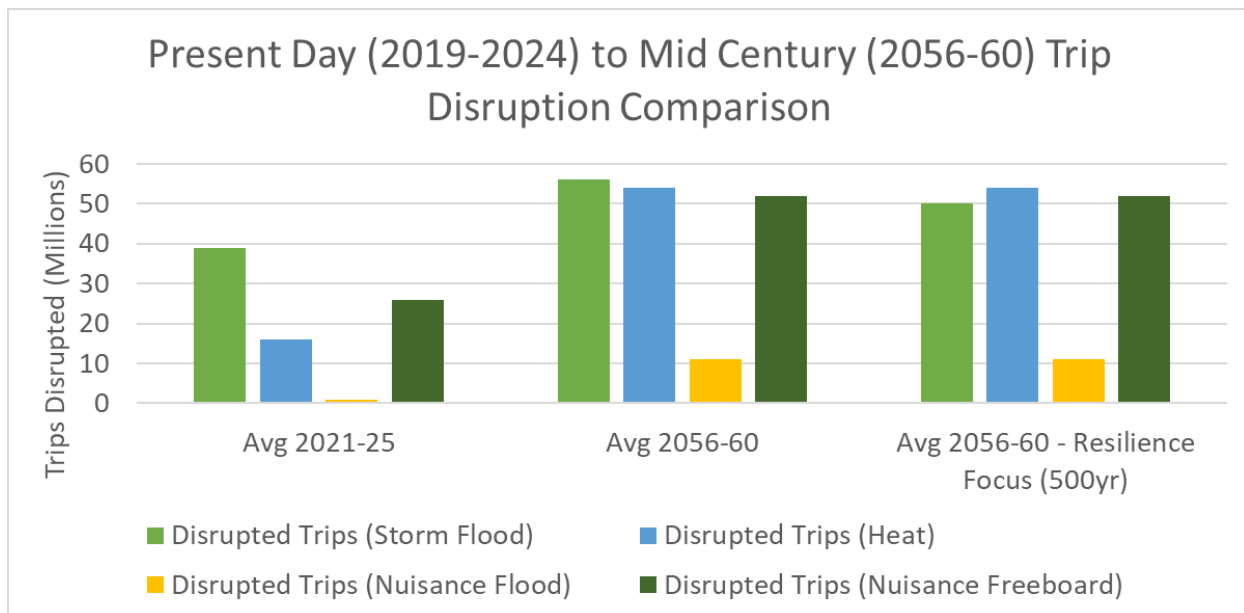
6.2 Resilience-Focus Scenario

6.2.1 Improved Protection Level from 50-Year Storm to 500-Year Storm

Increasing the protection level from 50-year to 500-year in all future projects resulted in a substantial reduction of disruption in the corridor. Figure 6.2 summarizes the reduction. The chart on the left shows the baseline result for disruption by stressor for the early and late periods in the simulation. The chart on the right shows the same result when the protection level rose from the 50-year storm to the 500-year storm for each asset maintenance event — either post-storm damage or initiated by maintenance because of failing condition.

Figure 6.2 shows that an increase in the protection level to 500-year storm lowered average annual trips disruption in the 2056–2060 period, with a drop from 56 million trips to 50 million disrupted trips.

Figure 6.2: Present Day to Mid-Century Trip Disruption Comparison

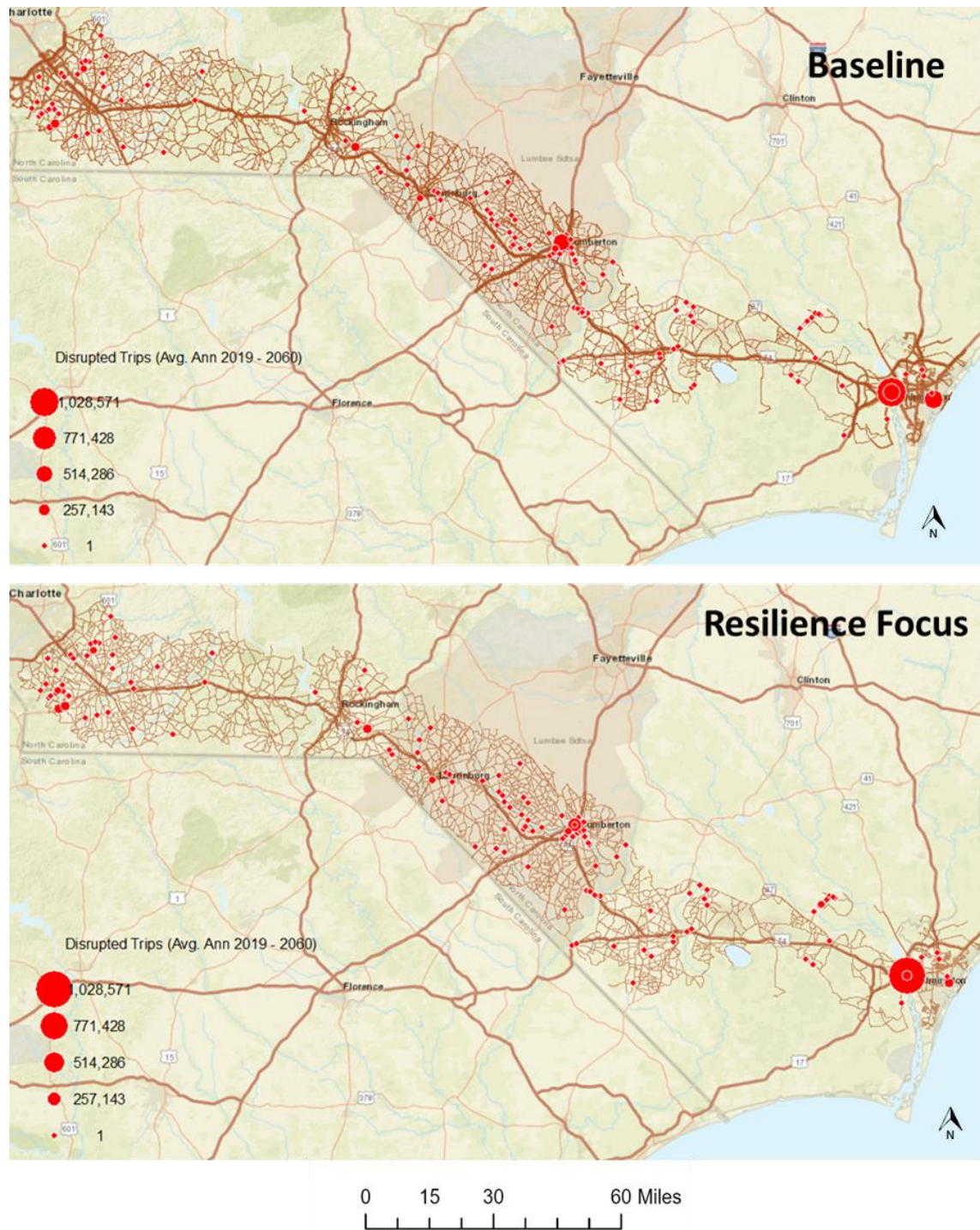


This chart compares disrupted trip levels by cause for the baseline and the resilience-focused scenarios. Overall, the resilience-focused actions of elevated roadways and bridges and hardened rail crossings reduced disruption from floods and storms by twelve percent in the late period.

An important note is that this assessment focused generally on adaptation and mitigation actions that controlled flooding. For this reason, the improvements from the resilience-focused scenario improved the disruption because of flood and storm metrics, while having no substantial impact on heat-related and SLR-related disruption. Future studies should evaluate more adaptation actions that address these impacts.

Figure 6.3 compares the result from the baseline disrupted trips (presented in the chapter five) with the result from the resilience-focused scenario. Overall, the reduction in disruption was clear across the corridor. Locations like I-95 experienced substantially less disruption, while other locations reduced to zero projected disruption.

Figure 6.3: Comparison of Baseline and Resilience-Focused Scenarios



The resilience-focused scenario increased the protection level of all assets in the system from 50-year to 500-year storms based on 2020 estimates. This resulted in a substantial reduction of disruption across the corridor. There were a few locations with increased disruption, which was because of the combined effect of increasingly large storms combined with higher trip rates in the future.

6.2.2 Balance Between Improvements and Increased Risk and Level of Service

Despite protecting assets to the 500-year level, significant damage was found to still occur in the transportation system and grow in the future. This disruption is due to a steady, heightened demand on the road system by travelers and an increased intensity in storms. By the end of the simulation, the 95th percentile storms were substantially larger than in the early period, which meant that even if the transportation assets had been improved up to the 2020 500-year storm, the assets will continue to be damaged, disrupting trips.

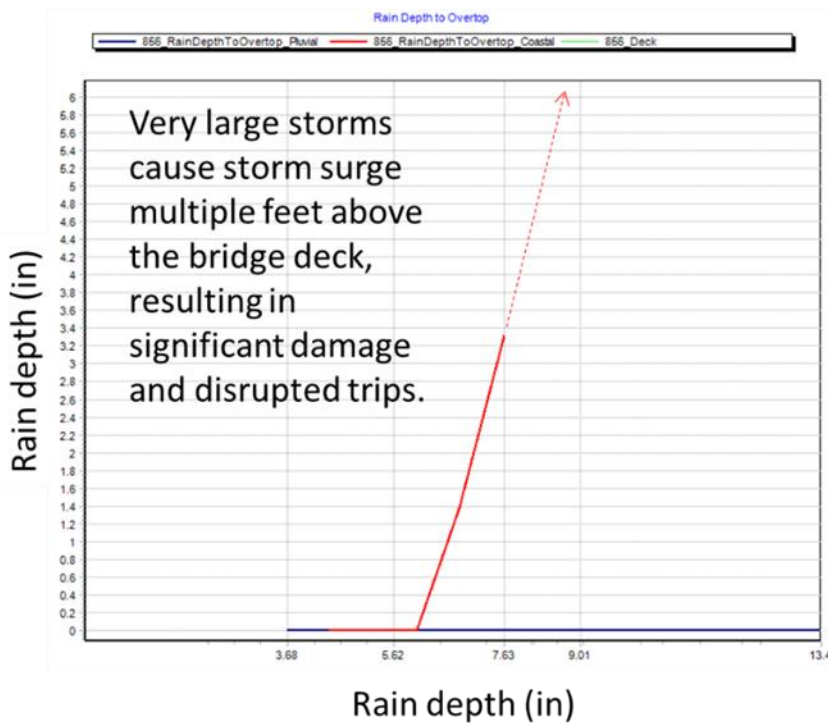
A key location where this effect happened was on the Andrew Jackson Hwy over Alligator Creek near Wilmington. Figure 6.4 shows a zoom-in to this location. The deck elevation of this stretch of highway was 7.48 feet NAVD88, while the projected storm surge of a 2020 100-year event was 11.0 feet NAVD88.

The simulation projected that when large storm events occur around mid-century, the high level of overtopping will likely destroy the road deck, resulting in a recovery period of 180 days. As this highway transports thousands of trips per day now and will potentially carry approximately 60% more by 2060, the long-duration recovery event had a larger impact event on disrupted trips than a similar event that happens in 2020, regardless of the protection level.

An important recommendation noted from this assessment was that an overview into the coastal flood model projections will be valuable. As Figure 6.4 shows, the flood response curve of this bridge was very steep and covered from the 2020 10-year to 100-year events. Therefore, the simulator was required to extrapolate, the overtopping level of storms larger than the 2020 100-year event.

The dashed line in the chart shows the linear extrapolation. If a 500-year or 1,000-year storm occurs, the extrapolated overtopping will rise to ten to fifteen feet. This is unlikely because of storm surge dynamics and bears a closer review.

Figure 6.4: Detail of U.S. 74/U.S. 76 (Andrew Jackson Hwy) Crossing Alligator Creek Near Wilmington, NC



U.S. 74/U.S. 76 (Andrew Jackson Hwy) over Alligator Creek near Wilmington projected 3.2ft of overtopping during a 100-year storm, caused by storm surge. Given projected storms were larger than the 2020 100-year event, and that traffic was projected a strong increase on this road by 2060, the resilience-focused approach of an assets protection level improvement to the 2020 500-year level was essentially ineffective for this specific asset.

6.2.3 Varied Asset Improvement Timing to Increase Resilience

The initial resilience-focused scenario ran similarly to the baseline in terms of scheduling. That is, the 2020–2029 STIP projects were implemented along with asset condition-based maintenance events. This approach largely ignored resilience as a priority for scheduling asset improvement, beyond any focus on resilience built into the STIP.

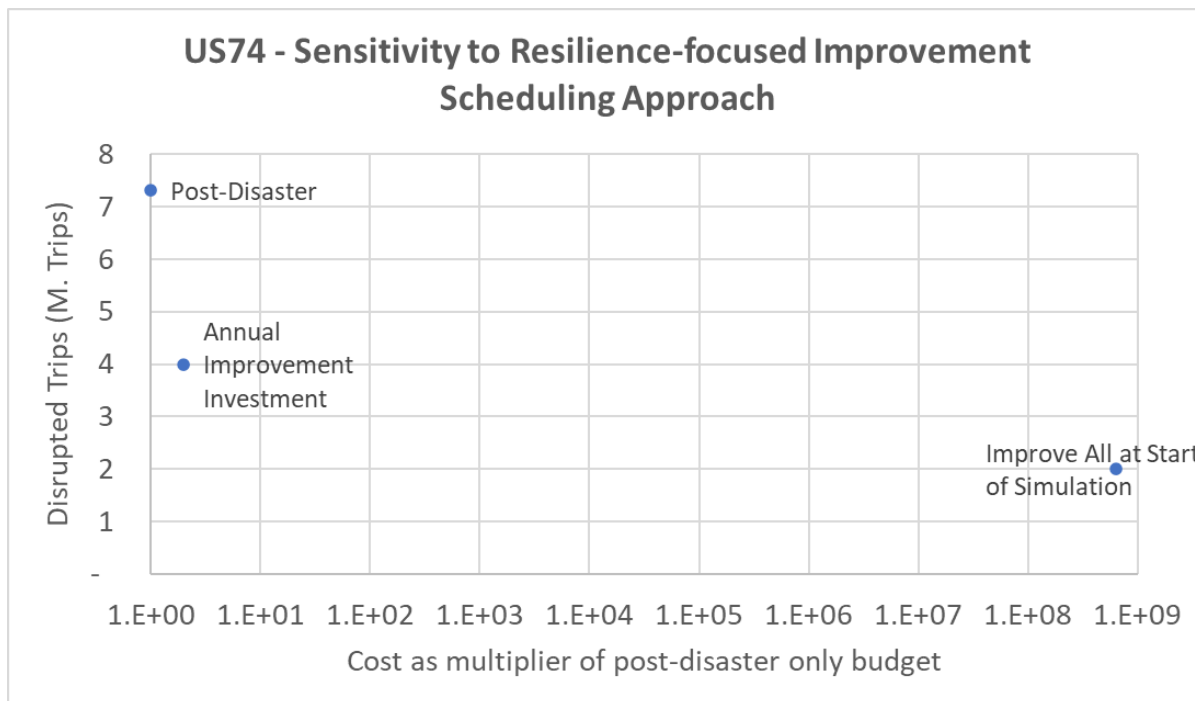
A sensitivity analysis was conducted that focused on adjusting the scheduling of resilience-focused projects to explore methods to reduce disruption further. The three schemes compared were:

- **Post-disaster** — This was the initial resilience-focused scenario, where improvements only occurred post-disaster, or when an asset condition initiated maintenance.
- **Annual Improvement Investment** — This followed a set annual expenditure on improvements of \$2M (or approximately 50%) of the current average maintenance budget. The budget was used to improve as many of the highest flood-risk assets as possible each year.
- **Improve all assets at start of simulation** — This unrealistic approach aimed to quantify the attainable minimum level of disruption and assumed no limit of funds in the first year of the simulation.

Figure 6.5 shows that the attainable minimum level of disruption. Post-disaster and maintenance triggered improvements result in approximately 7.2M trips disrupted per year. If the whole system is improved in the start year, the resulting disrupted trips were around 2M trips, a 73% reduction in disrupted trips. However, this approach required spending essentially the full replacement cost of the corridor, plus an additional 50% for resilience-focus (or about \$3.2B dollars) in a single year, an impracticable approach.

The highest benefit approach was executing annual improvements, which required an increase in the average annual budget by 50% but reduced disrupted trips to 4M, which is a 45% decrease compared to the post-disaster only approach.

Figure 6.5: Sensitivity to Scheduling of Improvement Projects



The sensitivity analysis focused on how an effect changed the timing of asset improvement ranged from the disaster-triggered scheduling of the initial assessment to a system that improved all assets in the first year.

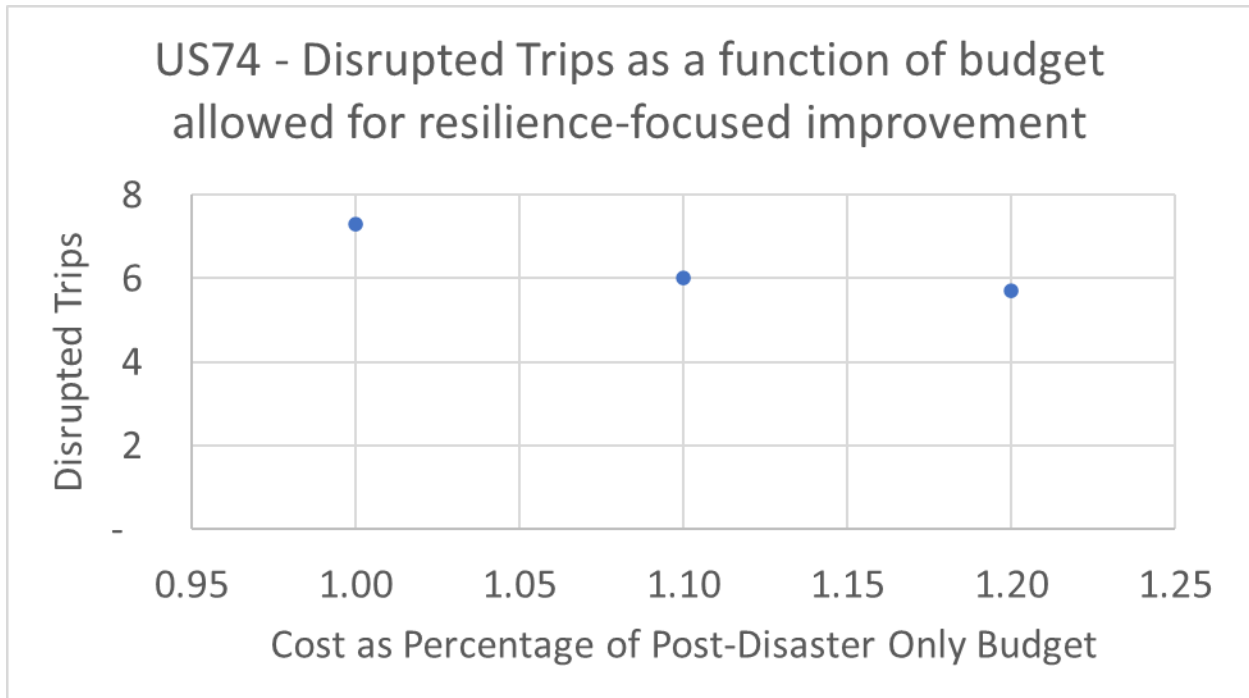
6.2.4 Highest ROI Targets

Even the 50% increase in budget required for an annual resilience-focused improvement approach possibly may be considered too costly. Another sensitivity analysis was aimed at the assessing the maximum reduction in disruption given a set budget. The simulation was configured with a set annual budget based on a percentage increase compared to the current average annual budget. Ten and twenty percent increases were attempted and their corresponding reductions in disruption are shown in Figure 6.6.

The results showed approximately 18% and 29% reduction in disruption when the budget increased to ten percent and 20%, respectively, compared to current average annual expenditures.

The general conclusion from both sensitivity assessments was that the more funding the NCDOT allocated to a resilience focus to their regular maintenance and capital expenditure programs, the more they avoided unpredictable storm-caused expenditures. A pro-active annual improvement investment approach is essential in terms of increasing resiliency.

Figure 6.6: Disrupted Trips as a Function of Budget Allowed for Resilience-Focused Improvement



A sensitivity to budget increase analysis showed that the budget increased for annual maintenance by ten percent and 20%, resulted in nineteen percent and 29% reductions in disruption, respectively.

7 Recommendations and Next Steps

The study revealed vulnerabilities throughout the U.S. 74 corridor with future climate change. Also, multiple opportunities for adaptation and mitigation were revealed in the assessment of adaptation and mitigation options. They are listed below and categorized into one of four groupings: increased information, policy and planning, general infrastructure improvement, and physical countermeasures to climate change.

7.1 Increased Information and Awareness

- NPV Asset Investment Calculations.
- Add Benefit to Cost Ratio to Assessment.
- Increase sensors on U.S. 74 and supported transportation infrastructure.
- Expansion of Rain-on-Grid Flood Models to whole corridor.
- Improve Compound Flood Modeling.
- Inclusion of Real-Storm Models in Simulation.
- On-going cost calibration between SAP and Digital Twins.
- Simulator Training for NCDOT staff.

7.2 Policy and Planning

- Adjust maintenance schedules and maximized preparedness.
- Integrate Master Planning across NCDOT/MPOs/Municipalities.
- Upgrade design guidelines with climate change and asset lifespan awareness — projected design levels matched preferably to lifespan of the asset. For example, if the asset is projected to provide a service life of 75 years, then the design guidelines should match to storms levels 75 years after the install date of the planned asset.
- Introduce periodic vulnerability assessments and evaluate efficacy and update projections. For example, repeat this study on a five-year basis.
- Require future planning studies and engineering design processes include climate change influence.
- Adjust to a climate-infrastructure interaction model.
- Incorporate additional natural hazards and their impacts in vulnerability studies, such as wildfires and drought.
- Incorporate carbon footprint and net-zero assessment into studies.

7.3 Incorporate habitat and natural system concerns into future studies. General Infrastructure Improvement

- Prioritize Improvement Scheduling to Maximize Resilience.

- Improve Alternate Routes.
- Avoid Disaster Response-Driven Capital Improvement.
- Increased Inspection Rates to Identify Potential Problems.
- Improved Simulation of How Floods Impact- Road Structure Below Deck.
- Defined and Adopted Resilience-focused Standards.

7.4 Physical Countermeasures to Climate Change

- Harden Roads.
- Road Elevation.
- Harden Rail Crossings.
- Harden Freeboard Areas Against SLR Impacts.

8 Further Reading

The study included integrated climate science, flood modeling, agent-based travel modeling, economical modeling and GIS-based digital twin technology in a dynamic simulation. While the study stretched the bounds in terms of the level and details of this integration, further work was conducted both within NCDOT and externally that improved our ability of potential climate change impacts and an action plan. The following list of resources provides a broader perspective on recent studies and research. The reader is encouraged to these resources for their knowledge on the topics studied.

2022 - NOAA – Sea Level Rise Technical Report: Download and FAQs ([noaa.gov](https://oceanservice.noaa.gov/hazards/sealevelrise/sealevelrise-tech-report-sections.html))
<https://oceanservice.noaa.gov/hazards/sealevelrise/sealevelrise-tech-report-sections.html>

2018 – National Climate Assessment 4 – Vol II. Impacts, Risks, and Adaptation in the United States.
<https://www.globalchange.gov/nca4>

2016 – Kipp, Max. Nationwide (USA) Pluvial Flood Modeling via Telemac2D
<https://www.nrc.gov/docs/ML2106/ML21064A445.pdf>

2007 – Bourne, Stephen. Microsoft PowerPoint –ARC TAZ Disaggregator.ppt ([ampo.org](https://www.ampo.org/assets/604_arctazdisaggregator.pdf))
https://www.ampo.org/assets/604_arctazdisaggregator.pdf

2022 – NASA [SVS: CMIP5: 21st Century Temperature and Precipitation Scenarios \(nasa.gov\)](https://svs.gsfc.nasa.gov/4110)
<https://svs.gsfc.nasa.gov/4110>

2019 – Paul Chinowsky, Jacob Helman, Sahil Gulati, James Neumann, Jeremy Martinich. [Impact of Climate Change on Operation of the US Rail System](#). Transport Policy, 2019.

2018 – Extreme heat causes pavement buckling issues across the state –Radio Iowa
<https://www.radioiowa.com/2018/05/29/extreme-heat-causes-pavement-buckling-issues-across-the-state/>

Appendices

Appendix A. Data

This chapter provided links to the datasets used in the study, where possible. Where the data was not served for download, a reference was provided for further reading on the dataset.

A.1 Weather

A.1.1 Historical Rainfall and Temperature

- Menne, Matthew J., Imke Durre, Bryant Korzeniewski, Shelley McNeill, Kristy Thomas, Xungang Yin, Steven Anthony, Ron Ray, Russell S. Vose, Byron E. Gleason, and Tamara G. Houston (2012): Global Historical Climatology Network - Daily (GHCN-Daily), Version 3. NOAA National Climatic Data Center. doi:10.7289/V5D21VHZ

A.1.2 Projected Future Rainfall and Temperature

- 2022 – NASA SVS: CMIP5: 21st Century Temperature and Precipitation Scenarios – <https://svs.gsfc.nasa.gov/4110>
- https://cida.usgs.gov/thredds/dodsC/cmip5_bcsd/future_2.html
- https://cida.usgs.gov/thredds/dodsC/loca_future.html

A.1.3 Eco-Regions

- US EPA Ecoregions Site – <https://www.epa.gov/eco-research/ecoregion-download-files-region>

A.2 Flood Models

A.2.1 Riverine: HEC-RAS1D

[Flood Risk Information System \(nc.gov\)](#)

A.2.2 Pluvial: Rain-on-Grid

NCEM Rain on Grid models (enquire with NCEM for access)

A.2.3 Coastal: ADCIRC Plus WHAFIS

NCDOT coastal data (enquire with NCDOT for access)

A.2.4 Pluvial: Atkins Pluvial

- 2016 – Kipp, Max. Nationwide (USA) Pluvial Flood Modeling via Telemac2D <https://www.nrc.gov/docs/ML2106/ML21064A445.pdf>

A.3 Sea Level

A.3.1 Mean Sea Level Projection

- 2022 – NOAA – [Sea Level Rise Technical Report: Download and FAQs \(noaa.gov\)](https://oceanservice.noaa.gov/hazards/sealevelrise/sealevelrise-tech-report-sections.html)
<https://oceanservice.noaa.gov/hazards/sealevelrise/sealevelrise-tech-report-sections.html>

A.3.2 Tidal Dynamics

- NOAA Water Levels Server –
<https://tidesandcurrents.noaa.gov/stations.html?type=Water+Levels>

A.4 Transportation Infrastructure

A.4.1 Assets

- NCDOT’s NBIS Geodatabase (enquire with NCDOT for access)
- NCDOT’s Non-NBIS Geodatabase (enquire with NCDOT for access)

A.4.2 Routes

- NCDOT’s Linear Referencing System (LRS) Dataset (enquire with NCDOT for access)

A.4.3 Geographic Divisions

- NCDOT Division layer (enquire with NCDOT for access)

A.4.4 Railroads

- NCDOT Rail Crossing Layer (enquire with NCDOT for access)

A.5 Asset Costing

A.5.1 Historical Opex and Capex

- NCDOT’s SAP Asset cost tracking system (enquire with NCDOT for access)
- NCDOT Project Bid Spreadsheet (enquire with NCDOT for access)

A.5.2 Expenditure Models

- NCDOT Board of Transportation – December 2021 Meeting Minutes – Inflation Rates

A.6 Travel Demand Models

A.6.1 RPO/MPO

- Charlotte Regional TPO 2050 Transcad model – (enquire with Charlotte MPO for access)

- Wilmington MPO 2045 Transcad model (enquire with Wilmington MPO for access)

A.6.2 NCDOT

- NCDOT Statewide 2045 Transcad model (enquire with NCDOT for access)

A.7 Demographics and Disadvantage Populations

A.7.1 Population/Jobs/Household

- ACS – TIGER/Line Geodatabase with Selected Geographic and Statistical Data –
- <https://www.census.gov/geographies/mapping-files/time-series/geo/tiger-data.html>

A.7.2 Poverty/Minority

- ACS – TIGER/Line Geodatabase with Selected Geographic and Statistical Data
- <https://www.census.gov/geographies/mapping-files/time-series/geo/tiger-data.html>

A.8 Land Use and Buildings

A.8.1 Buildings and Buildings

- Parcels and Building Footprints were merged into a single-related feature dataset for each county prior to the start of the project. The data was a part of Atkins' National Building Database. The source data for this dataset included:
 - Parcels – NC OneMap's NC Statewide Parcel Geodatabase.
<https://www.nconemap.gov/pages/parcels>
 - Building Footprints – NC Floodplain Mapping Program.
[NC Buildings Footprints \(2010\) | NC OneMap](#)

A.8.2 Parcels

- See buildings discussion

Appendix B. Heat Modeling

This appendix is an extension of the section in chapter 4 on heat modeling. It includes a citing of each literature reviewed as well as the abstract/website text for each citing. For ease of reading, the section on heat modeling in chapter 4 is repeated here and the literature review notes follow.

In each quarter, the heating degree days for each road segment was evaluated since the last maintenance event on the road segment. For example, if the last maintenance event occurred 10 years before the current time step in the simulation and the average atmospheric temperature was 90°F, the heating degree days are 10 years * 365 days/year * 90°F = 328,500 °F-days. The simulator includes projected maximum temperature from the LOCA dataset (see section above on climate stressor projections) and the latest maintenance event on each road segment. These were used to evaluate the heating degree days for the road.

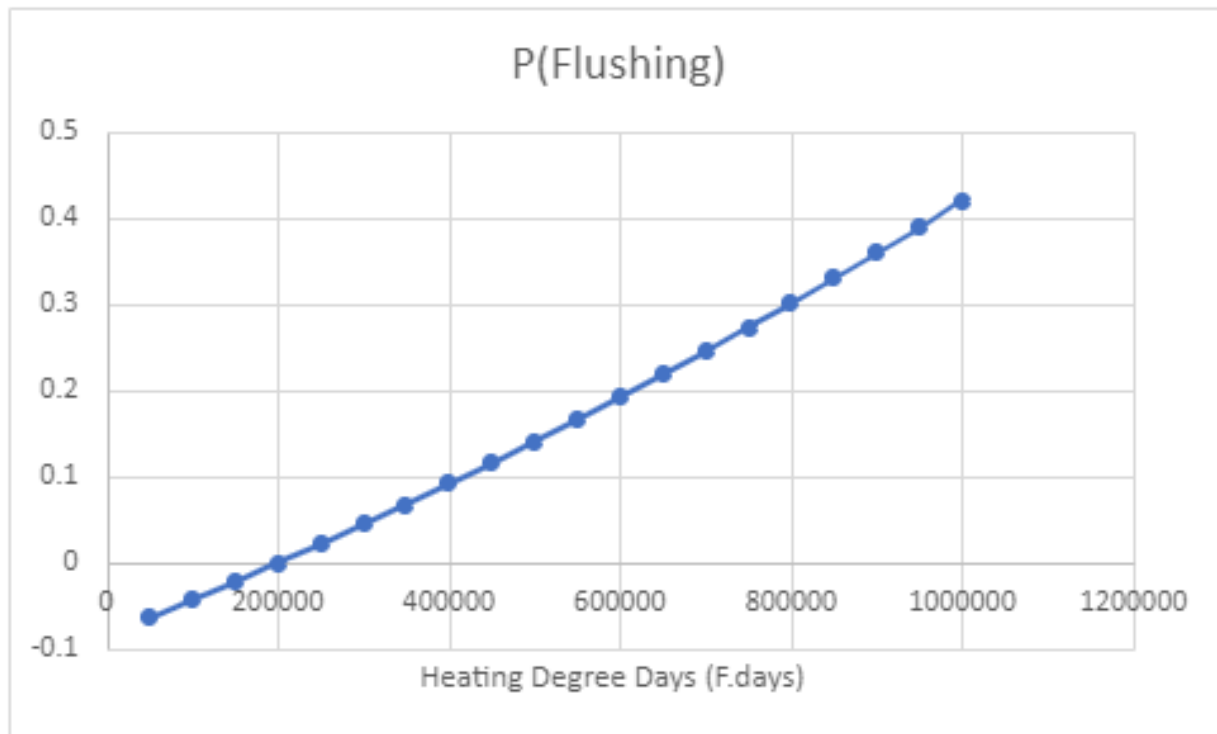
A comprehensive literature review (see Appendix A) revealed multiple methods for simulating asphalt degradation over time, including methods that leverage artificial intelligence and machine learning. As one of the objectives of the study was to simulate disruption with minimized computational requirements, the simulator was configured with a probabilistic model, which linked cumulative heating degree days with probability of a flushing-related traffic slowdown initiated by NCDOT or other relevant DOTs.

The model assumes that if the trigger atmospheric temperature is 85°F, that flushing would start approximately 1/3 of the typical 20-year lifespan of the asphalt, or at about 6.66 years. This would give a threshold of 85°F * 6.66 years * 365 days/year = 206,833 °F days. A probability function was then developed that assumes that when the road reaches this threshold the probability of flushing becomes non-zero and increases as a power function until at lifespan of 20 years, the probability of flushing is approximately 20%.

Figure 4.24 shows the function. The formula for the function is:

$$P(\text{Flushing}) = 3 \wedge ((\text{Cumulative Deg Days} - 200000) / 100000/25) - 1$$

Figure 8.1: Probability of Flushing as a Function of Cumulative Heating Degree Days



Note that the relationship used allows for extrapolation, so road segments that go beyond 20 years are estimated to have higher than 20% probability of having slow down events.

Adaptation & Mitigation

Literature mentions

Sealing

Adding polymer to bitumen

Cooling via leaf canopy and building shadow

Cooling with water

Proposed Improvement to Heat Modeling Approach

Additional discussions with Atkins pavement subject matter experts provided a possibly enhancement to the basic heat model implemented in the simulator. This method is recorded here and is recommended for use in future studies.

The method focuses on adding more variables, primarily expected traffic condition. In the current simulation, the heat model assumes that the road is performing at design level (i.e., design AADT). But, future traffic levels may vary substantially from design levels, particularly with growing population increasing levels, or adaptation/mitigation reducing AADT. As such, including measured or estimated travel in the heat model will provide more accurate estimates of flushing potential.

The flow chart below illustrates the proposed model. The primary differences between the current heating degree days only model and the proposed are:

Each road's AADT will be used to classify if the road is low or high volume.

The volume will be used to assign a binder that was/will be used in the Asphalt mix.

NCDOT likely uses the "superpave" asphalt mix design method, as most DOTs use. These mixes include a binder for increasing the roads' ability to stand up to heavy and repeated traffic in high temperatures. The numeric part of the binder name (eg. PG64) refers to the design temperature in Celsius. The temperature is actually a 7-day maximum temperature average. That is, when designing the mix, the 7-day historic average maximum temperature is found, and the mix is designed to accommodate this temperature. The 7-day max atmospheric temperature is then converted to pavement temperature, which is significantly higher than atmospheric. The binder number chosen should be higher than the resulting pavement temperature.

During the simulation, two items will be checked:

Exceedance of design AADT – where simulated AADT increases in the model as the simulation proceeds

Exceedance of design temperature – where the past 7-day avg max pavement temperature will be evaluated from the 7-day avg max atmospheric temperature.

The simulation will accumulate exceedance of design trips and temperature each day and multiply them to make a combined cumulated exceedance index.

When the accumulated combined index goes above a threshold, the probability of flushing will go above zero as with the first heat model.

The proposed model will use the assumed 1/3 of 20 year life span and evaluate the threshold as the value of the combined index given constant 85F and the design AADT on the road of interest.

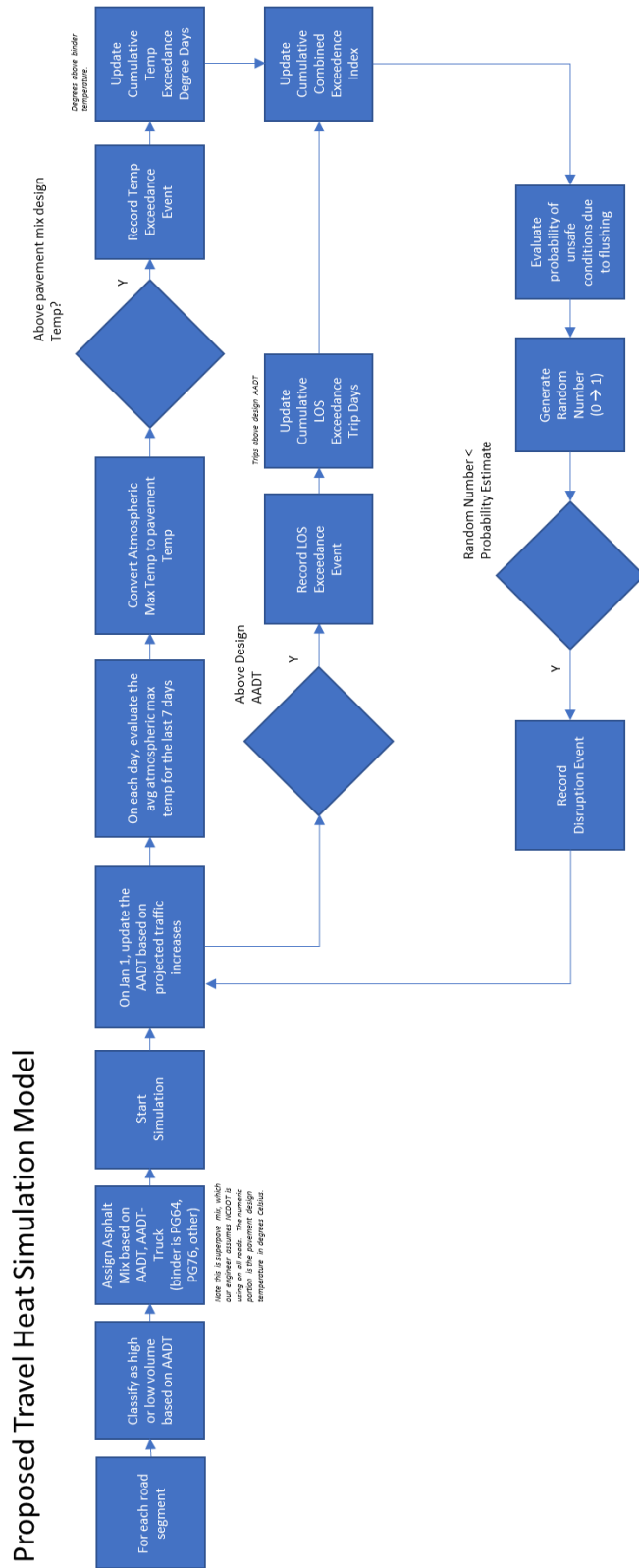
If a random number falls below the probability, then the simulation will assume a disruption occurs, and a disruption event will be recorded.

Notes:

This model will provide higher accuracy than the temperature-only model, primarily because it includes road usage in the calculation.

This model will essentially estimate the heating component the same as the first model, but it will add the component of increasing usage of roads over time, which is a new factor.

Figure B-2: Proposed Heat Model Flow Chart



Heat Modeling Literature Review

Links to literature reviewed (note that abstracts are provided below)

http://www.scielo.org/co/scielo.php?script=sci_arttext&pid=S0123-21262015000200006

<https://www.ntnu.no/ojs/index.php/BCRRA/article/download/2743/2806/11505>

https://www.researchgate.net/publication/279467078_Maintenance_Solutions_for_Bleeding_and_Flushed_Pavements_Surfaced_with_a_Seal_Coat_or_Surface_Treatment/figures?lo=1

<https://www.ayresassociates.com/the-long-and-short-of-it-lifespans-of-paved-roadways/>

<https://www.ncbi.nlm.nih.gov/pmc/articles/PMC6416576/>

<https://aip.scitation.org/doi/pdf/10.1063/1.5042946>

https://onlinepubs.trb.org/onlinepubs/nchrp/docs/NCHRP09-54_InterimReport-Submitted6-16-15.pdf

<https://journals.sagepub.com/doi/abs/10.3141/2507-03>

<https://www.tandfonline.com/doi/full/10.1080/14680629.2016.1266739>

<https://www.tandfonline.com/doi/full/10.1080/14680629.2016.1266739?scroll=top&needAccess=true>

https://scholar.google.com/scholar?q=asphalt+road+failure+prediction+model+with+temperature&hl=en&as_sdt=0&as_vis=1&oi=scholar#d=gs_qabs&t=1666777647114&u=%23p%3DYukmUkNQLsAJ

<https://static.tti.tamu.edu/tti.tamu.edu/documents/0-6746-01-1.pdf>

<https://journals.sagepub.com/doi/full/10.1177/0361198118822501>

<https://www.ntnu.no/ojs/index.php/BCRRA/article/download/2725/2788>

<https://ops.fhwa.dot.gov/publications/fhwahop20062/fhwahop20062.pdf>

<https://www.hindawi.com/journals/jat/2022/7783588/>

<https://www.tandfonline.com/doi/abs/10.1080/10298436.2013.828839>

<https://www.tandfonline.com/doi/full/10.1080/16742834.2019.1608791>

<https://transportgeography.org/contents/applications/climate-change-transport-infrastructure/climate-change-impacts-transportation/>

https://ops.fhwa.dot.gov/weather/q1_roadimpact.htm

<https://www.bloomberg.com/news/articles/2022-08-18/the-world-s-roads-and-highways-aren-t-built-for-a-hotter-climate>

<https://www.plsofflorida.com/how-do-potholes-form/>

<https://www.washingtonpost.com/climate-environment/2022/07/20/heat-wave-road-railway-buckling/>

<https://www.roadbotics.com/2022/06/08/hot-weather-effects-on-roads/>

https://www.researchgate.net/publication/230320048_Quantifying_the_effects_of_high_summer_temperatures_due_to_climate_change_on_buckling_and_rail_related_delays_in_south-east_United_Kingdom

<https://rmets.onlinelibrary.wiley.com/doi/10.1002/met.1910>

<https://www.ncbi.nlm.nih.gov/pmc/articles/PMC6416576/>

<https://heatisland.lbl.gov/sites/default/files/cuhi/docs/211420-mallick-doc.pdf>

https://www.tac-atc.ca/sites/default/files/conf_papers/shafieem-climate_change_and_asphalt_binder_selectio.pdf

<https://urldefense.com/v3/https://www.pavemax.com/how-hot-weather-affects-concrete-asphalt/>

[https://www.pavemax.com/how-hot-weather-affects-concrete-asphalt/;!!OepYZ6Q!5y2nKpmUtvDDjoh8-4tSiR2KJD0Vx6gcDK0SRAnhAByFvJT2yOdrafWltIPBXD3_gsjE33JkxpXYKG6XLUVrD4ZRYtk_6sjXgQ\\$](https://www.pavemax.com/how-hot-weather-affects-concrete-asphalt/;!!OepYZ6Q!5y2nKpmUtvDDjoh8-4tSiR2KJD0Vx6gcDK0SRAnhAByFvJT2yOdrafWltIPBXD3_gsjE33JkxpXYKG6XLUVrD4ZRYtk_6sjXgQ$)

https://www.ipcc.ch/apps/njlite/srex/njlite_download.php?id=6159

http://www.scielo.org.co/scielo.php?script=sci_arttext&pid=S0123-21262015000200006

Abstract

This article presents the results of the analysis of the effect of aging on the properties of asphalt and asphalt mixtures. The objective of this study was to compare the properties of the original asphalt and aged asphalt and the dynamic modulus of asphalt mixtures. The long-term aging was simulated by using Pressure Asphalt Vessel (PAV). Marshall and RAMCODES methodologies were used to determine the formula of work; values of dynamic modulus of designed mixtures were obtained by the indirect tensile test, using the Nottingham Asphalt Tester (NAT). The results showed an increase in the rigidity of the aged asphalt. Also, an increase of the stability and a decreased flow in the mixtures made with this type of binder was found. The dynamic modulus values of the mixtures containing aged asphalt showed an increase up to three times compared with those elaborated with original asphalt mixtures.

<https://www.ntnu.no/ojs/index.php/BCRRA/article/download/2743/2806/11505>

ABSTRACT: The various causes/categories of pavement cracking and generalized criteria for identification of potential deficiencies are presented in conjunction with case histories that relate to investigations of pavement distress. Asphalt binder properties, such as viscosity and penetration are shown to relate well with thermal and combined thermal/load stress conditions. Although slightly more involved testing procedures are required, criteria have been developed for different yearly ESALS to identify a paving mixture's resistance to top-down cracking. Dissipated creep strain energy parameters are obtained from indirect tension tests to define an energy ratio for separating cracked from uncracked pavements. It is difficult to interpret Falling Weight Deflectometer (FWD) data from cracked pavements unless special procedures are followed. At high pavement temperatures the influence of cracks will diminish and allow for improved determination of moduli for underlying pavement layers and foundation/subgrade soils. These analyses are enhanced when asphalt viscosity relationships with resilient moduli are used to assign E1 values for backcalculation. Relationships or procedures for estimation of any pavement layer or subgrade modulus are very beneficial in simplifying the interpretation or backcalculation of other layer moduli. Where possible, laboratory test parameters that relate directly to the behavior of paving mixtures should be integrated in the design and performance models for asphalt pavements. Realistic, multiple/simplified, methods for design and/or evaluation of pavement performance are desirable over one specific approach since comparable results are an indication of reliability.

https://www.researchgate.net/publication/279467078_Maintenance_Solutions_for_Bleeding_and_Flushed_Pavements_Surfaced_with_a_Seal_Coat_or_Surface_Treatment/figures?lo=1

Maintenance Solutions for Bleeding and Flushed Pavements Surfaced with a Seal Coat or Surface Treatment

Abstract and figures



No abstract

The abstract for this research item is not available.



Figure content uploaded by [Sanjaya Senadheera](#) Author content

Content may be subject to copyright.

<https://www.ayresassociates.com/the-long-and-short-of-it-lifespans-of-paved-roadways/>

The Long and Short of It: Lifespans of Paved Roadways

By Ayres | February 8, 2022 | No Comments



By Matthew Barr, PE

Across the country, one-third of our highways and major streets are in poor condition, according to TRIP, a nonprofit transportation research group.



About the Expert:

Matthew Barr, PE, has been the design engineer and project manager for various highway and bridge projects since he joined Ayres in 1989. He is responsible for project engineering of major roadway and bridge replacement reconstruction projects, including staff management, subconsultant and agency coordination, concept development, engineering design, public involvement, report writing, and plan preparation.

Persistent potholes and recurring ruts wreak havoc with our commutes, impose financial burdens from automobile repairs, inflict significant injury, prompt contentious lawsuits, and account for roughly one-third of deaths occurring annually on American roads.

<https://www.ncbi.nlm.nih.gov/pmc/articles/PMC6416576/>

Influence of Overheating Phenomenon on Bitumen and Asphalt Mixture Properties

[Michał Sarnowski](#), [Karol J. Kowalski](#), [Jan B. Król](#), and [Piotr Radziszewski](#)

[Author information](#) [Article notes](#) [Copyright and License information](#) [Disclaimer](#)

[Go to:](#)

Abstract

In the course of manufacturing, transport and installation, road bitumens and asphalt mixtures can be exposed to the impact of elevated process temperatures exceeding 240 °C. This mainly applies to the mixtures used for road pavements and bridge deck insulation during adverse weather conditions. The heating process should not change the basic and rheological properties of binders and the asphalt mixtures that to a degree cause the degradation of asphalt pavement durability. The work involved analyzing the properties of non-modified bitumens and SBS polymer modified bitumens, heated at temperatures of 200 °C, 250 °C and 300 °C for 1 h. Next, the asphalt mixtures were heated in the same temperatures. Based on the developed Overheating Degradation Index (ODI) it was demonstrated that polymer-modified bitumens were characterized by higher overheating sensitivity $A_{(ODI)}$ than non-modified bitumens, which was confirmed by mixture test results. Overheating limit temperatures $T_{(ODI)}$ were determined, which in the case of polymer-modified bitumens are up to 20 °C lower than for non-modified bitumens. When the temperature increases above $T_{(ODI)}$, loss of viscoelastic properties occurs in the material which causes, among other effects, a loss of resistance to fatigue cracking.

<https://aip.scitation.org/doi/pdf/10.1063/1.5042946>

The Effect of Temperature Changes on Mechanistic Performance of Hotmix Asphalt as Wearing Course with Different Gradation Types

Senja Rum Harnaeni^{1, 3, a}, F. Pungky Pramesti², Arif Budiarto² and Ary Setyawan² ¹ Doctoral Program in Civil Engineering, Faculty of Engineering, Universitas Sebelas Maret, Surakarta, Indonesia ² Civil Engineering Department, Universitas Sebelas Maret, Surakarta, Indonesia ³ Civil Engineering Department, Universitas Muhammadiyah Surakarta, Surakarta, Indonesia ^aCorresponding author: srh289@ums.ac.id

Abstract. The performance of hot mix asphalt serves as wearing course with different aggregate gradation types, namely dense graded and gap graded, is empirically determined using Marshall test. Based on data bitumen penetration, bitumen softening point, volume of bitumen, volume of aggregate and volume of voids, the mechanistic performance of bitumen (for example : bitumen stiffness) and hot mix asphalt (such as asphalt mix stiffness and fatigue life asphalt mix) in relation with temperature changes can be predicted. This mechanistic performance of hot mix asphalt are solved by Shell nomograph that can be simulated by software BANDS 2.0. The mixture consists of Asphalt Concrete-Wearing Course (AC-WC) and Hot Rolled Sheet-Wearing Course (HRS-WC) by considering their different gradations, in addition to its widely using as wearing course in Indonesia. The study was initiated by testing bitumen and asphalt mixture materials, including asphalt penetration 60/70 according to Bina Marga (2010) specification of coarse aggregate and fine aggregate. Subsequently, preparation of gradation mixture for AC-WC and HRS-WC based on Bina Marga (2010) was carried out, followed by Marshall Test with five variations of bitumen content on each asphalt mixture to determine optimum bitumen content. Based on the result of optimum bitumen content, specimens were made to determine the Marshall properties of the two diverse gradation asphalt mixtures using Marshall Test. Furthermore, by using data bitumen penetration, bitumen softening point and Marshall test, i.e. volume of bitumen, volume of aggregate and volume of voids, the mechanistic performance of hot mix asphalt was measured. It indicated the difference of Marshall properties between the dense graded and gap graded mixture. The first asphalt mixture has greater stability, VFWA (Void Filled With Asphalt) and MQ (Marshall Quotient) in compared with the second mixture. On the contrary, the second mixture has higher values of flow, VIM (Void In the Mix) and VMA (Void in Mineral Aggregate). The results of BANDS 2.0 simulation, mechanistic performance of hot mix asphalt shows that temperature changes influence bitumen stiffness, asphalt mix stiffness and fatigue life asphalt mix. The higher the temperature, the lower the bitumen stiffness and asphalt mix stiffness and the higher the fatigue life asphalt mix. At the same temperature, asphalt mix stiffness of dense graded mixture is higher than gap graded mixture. The other way for fatigue life asphalt mix.

https://onlinepubs.trb.org/onlinepubs/nchrp/docs/NCHRP09-54_InterimReport-Submitted6-16-15.pdf

INTERIM REPORT to the NATIONAL COOPERATIVE HIGHWAY RESEARCH PROGRAM (NCHRP)

Project NCHRP 09-54

Long-Term Aging of Asphalt Mixtures for Performance Testing and Prediction

from Y. Richard Kim, Ph.D., P.E., F.ASCE Cassie Castorena, Ph.D. Farhad Yousefi Rad, Michael Elwardany
North Carolina State University Shane Underwood, Ph.D. Arizona State University Mike J. Farrar, Ronald
R. Glaser Western Research Institute

June 2015

<https://journals.sagepub.com/doi/abs/10.3141/2507-03>

Prediction of Field Aging Gradient in Asphalt Pavements

[Xue Luo](#) —, [Fan Gu](#), and [Robert L. Lytton](#)[View all authors and affiliations](#)

Volume 2507, Issue 1

<https://doi.org/10.3141/2507-03>

Abstract

The aging of asphalt pavements is a key factor that influences pavement performance. Aging can be characterized by laboratory tests and prediction models. Common aging prediction models use the change of physical or chemical properties of asphalt binders based on regression techniques or aging reaction kinetics. The objective of this study was to develop a kinetics-based aging prediction model for the mixture modulus gradient in asphalt pavements to study long-term in-service aging. The proposed model was composed of three submodels for baseline modulus, surface modulus, and aging exponent to define the change of the mixture modulus with pavement depth. The model used kinetic parameters (aging activation energy and preexponential factor) of asphalt mixtures and combined the two reaction rate periods (fast-rate and constant-rate). Laboratory-measured modulus gradients of 29 field cores at different ages were used to determine the model parameters. The laboratory testing condition was converted to the field condition at a given age and corresponding temperature by introducing the rheological activation energy to quantify the temperature dependence of field cores at each age. The end of the fast-rate period or the beginning of the constant-rate period was accurately identified to model these two periods and to determine the associated parameters separately. The results showed that the predictions matched well with the measurements and the calculated model parameters were verified. The proposed aging prediction model took into account the major factors that affect field aging speed of an asphalt pavement, such as the binder type, aggregate type, air void content, pavement depth, aging temperature, and aging time.

<https://www.tandfonline.com/doi/full/10.1080/14680629.2016.1266739>

Long-term ageing of asphalt mixtures

Fan Yin

,

Edith Arámbula-Mercado

,

Amy Epps Martin

,

David Newcomb

&

Nam Tran

Pages 2-27 | Received 13 Aug 2015, Accepted 27 Oct 2015, Published online: 02 Jan 2017

Abstract

Ageing of asphalt mixtures occurs during production and construction and continues throughout the service life of the pavement. Although this topic has been studied extensively, recent changes in asphalt mixture components, production parameters, and plant design have raised a need for a comprehensive evaluation that considers the impacts of climate, aggregate type, recycled materials, WMA technology, plant type, and production temperature. In this study, field cores were acquired from seven field projects at construction and several months afterwards, and raw materials were also collected for fabricating laboratory specimens that were long-term oven aged (LTOA) in accordance with selected protocols. The resilient modulus and Hamburg wheel tracking tests were conducted on both specimen types to evaluate the evolution of mixture stiffness and rutting resistance with ageing. The concepts of cumulative degree days and mixture property ratio were proposed to quantify field ageing and its effect on mixture properties. Test results indicated that the LTOA protocols of two weeks at 140°F (60°C) and five days at 185°F (85°C) produced mixtures with equivalent in-service field ageing of 7–12 months and 12–23 months, respectively, depending on climate. Finally, among the

factors investigated in the study, WMA technology, recycled materials, and aggregate absorption exhibited a significant effect on the long-term ageing characteristics of asphalt mixtures, while production temperature and plant type had no effect.

https://scholar.google.com/scholar?q=asphalt+road+failure+prediction+model+with+temperature&hl=en&as_sdt=0&as_vis=1&oi=scholart#d=gs_qabs&t=1666777647114&u=%23p%3DYukmUkNQLsAJ

Prediction Models of Shear Parameters and Dynamic Creep Instability for Asphalt Mixture under Different High Temperatures

by

Junxiu Lv

^{1,2} and

Xiaoyuan Zhang

^{3,*}

¹

The Architectural Design & Research Institute of Zhejiang University Co., Ltd., Hangzhou 310028, China

²

School of Transportation, Southeast University, Nanjing 210096, China

³

School of Civil Engineering and Architecture, Zhejiang Sci-Tech University, Hangzhou 310018, China

*

Author to whom correspondence should be addressed.

Academic Editor: Giulio Malucelli

Polymers **2021**, *13*(15), 2542; <https://doi.org/10.3390/polym13152542>

Received: 13 July 2021 / Revised: 25 July 2021 / Accepted: 28 July 2021 / Published: 31 July 2021

(This article belongs to the Special Issue **Polymer Processing and Surfaces II**)

Citation Export

Abstract

This study mainly investigates the prediction models of shear parameters and dynamic creep instability for asphalt mixture under different high temperatures to reveal the instability mechanism of the rutting for asphalt pavement. Cohesive force c and internal friction angle φ in the shear strength parameters for asphalt mixture were obtained by the triaxial compressive strength test. Then, through analyzing the influence of different temperatures on parameters c and φ , the prediction models of shear strength parameters related to temperature were developed. Meanwhile, the corresponding forecast model related to confining pressure and shear strength parameters was obtained by simplifying the calculation method of shear stress level on the failure surface under cyclic loading. Thus, the relationship of shear stress level with temperature was established. Furthermore, the cyclic time F_N of dynamic creep instability at 60 °C was obtained by the triaxial dynamic creep test, and the effects of confining pressure and shear stress level were considered. Results showed that F_N decreases exponentially with the increase in stress levels under the same confining pressure and increases with the increase in confining pressure. The ratio

between shear stress level and corresponding shear strength under the same confining pressure was introduced; thus, the relationship curve of F_N with shear stress level can eliminate the effect of different confining pressures. The instability prediction model of F_N for asphalt mixture was established using exponential model fitting analysis, and the rationality of the model was verified. Finally, the change rule of the parameters in the instability prediction model was investigated by further changing the temperature, and the instability forecast model in the range of high temperature for the same gradation mixture was established by the interpolation calculation.

<https://static.tti.tamu.edu/tti.tamu.edu/documents/0-6746-01-1.pdf>

1. Report No. FHWA/TX-17/0-6746-01-1 | 2. Government Accession No. | 3. Recipient's Catalog No.
4. Title and Subtitle VALIDATION OF ASPHALT MIXTURE PAVEMENT SKID PREDICTION MODEL AND DEVELOPMENT OF SKID PREDICTION MODEL FOR SURFACE TREATMENTS
5. Report Date Published: April 2017 | 6. Performing Organization Code
7. Author(s) Arif Chowdhury, Emad Kassem, Sand Aldagari, and Eyad Masad
8. Performing Organization Report No. Report 0-6746-01-1
9. Performing Organization Name and Address Texas A&M Transportation Institute The Texas A&M University System College Station, Texas 77843-3135
10. Work Unit No. (TRAIS) | 11. Contract or Grant No. Project 0-6746
12. Sponsoring Agency Name and Address Texas Department of Transportation Research and Technology Implementation Office 125 E. 11th Street Austin, Texas 78701-2483
13. Type of Report and Period Covered Technical Report: November 2012–December 2016
14. Sponsoring Agency Code
15. Supplementary Notes Project performed in cooperation with the Texas Department of Transportation and the Federal Highway Administration. Project Title: Validation of TxDOT Flexible Pavement Skid Prediction Model URL: <http://tti.tamu.edu/documents/0-6746-01-1.pdf>
16. Abstract Pavement skid resistance is primarily a function of the surface texture, which includes both microtexture and macrotexture. Earlier, under the Texas Department of Transportation (TxDOT) Research Project 0-5627, the researchers developed a method to predict asphalt pavement skid resistance based on inputs including aggregate texture before and after polishing, gradation of asphalt mixture, and traffic levels. In this study, the researchers validated and revised the skid prediction model for asphalt pavements and developed a skid prediction model for seal coat surfaces. The researchers investigated and examined the surface friction characteristics of 70 test sections of asphalt mixtures and surface-treated roads in Texas. The test sections covered a wide range of mixtures and aggregate types. The researchers measured pavement macrotexture and microtexture of these sections and revised the traffic calculation. Historical skid numbers were obtained from TxDOT's Pavement Management Information System database and measured using a skid trailer. Aggregate texture and angularity was quantified using the aggregate image measurement system. Statistical methods were used to develop a prediction model for skid numbers, and the predicted values were compared to the measured ones in the field. The revised model describes the skid resistance of asphalt pavements as a function of aggregate characteristics, mixture gradation, and traffic level. The researchers incorporated aggregate angularity as an additional parameter in the model. Similarly, the researchers developed a skid prediction model for seal coat surfaces using the same parameters. A Microsoft Access– based Visual Basic desktop application was developed to automatically calculate the predicted skid numbers by incorporating the skid prediction models. Using this standalone application, one can input the basic aggregate characteristics and traffic data to predict the pavement's skid resistance during its service life.
17. Key Words Skid Resistance, Asphalt Mixture, Surface Treatment, Aggregate Texture, Aggregate Angularity
18. Distribution Statement No restrictions. This document is available to the public through NTIS: National Technical Information Service Alexandria, Virginia, <http://www.ntis.gov>
19. Security Classif. (of this report) Unclassified
20. Security Classif. (of this page) Unclassified | 21. No. of Page 168 | 22. Pric

<https://journals.sagepub.com/doi/full/10.1177/0361198118822501>

Establishment of Prediction Models of Asphalt Pavement Performance based on a Novel Data Calibration Method and Neural Network

[Linyi Yao](#), [Qiao Dong](#) —, [...], [Jiwang Jiang](#), and [Fujian Ni](#), [+1 -1View all authors and affiliations](#)

[Volume 2673, Issue 1](#)

<https://doi.org/10.1177/0361198118822501>

Abstract

This paper aims to develop models to forecast the deterioration of pavement conditions including rutting, roughness, skid-resistance, transverse cracking, and pavement surface distress. A data quality control method was proposed to rebuild the performance data based on the idea of longest increasing or decreasing subsequences. Neural network (NN) was used to develop the five models, and principal component analysis (PCA) was applied to reduce the dimension of traffic variables. The influence of different input variables on the model outputs was discussed respectively by comparing their mean impact values (MIV). Results show that the proposed NN models demonstrated great potential for accurate prediction of pavement conditions, with an average testing R-square of 0.8692. The results of sensitivity analysis revealed that recent pavement conditions may influence the future pavement conditions significantly. Rutting and roughness were sensitive to pavement age and maintenance type. The materials of original pavement asphalt layer were highly relevant to the prediction of pavement roughness, skid-resistance, and pavement surface distress. Moreover, traffic loads obviously affected the pavement skid-resistance and transverse cracking. Pavement and bridge had different effect on surface distress. The material of the base has a remarkable impact on the initiation and development of transverse cracks. Disease treatment in terms of pavement cracking—such as sticking the cracks, excavating and filling the cracks—shows a high MIV in the prediction model of transverse cracking and pavement surface distress.

<https://ops.fhwa.dot.gov/publications/fhwahop20062/fhwahop20062.pdf>

1. Report No. FHWA-HOP-20-062
2. Government Accession No.
3. Recipient's Catalog No.
4. Title and Subtitle Integrated Modeling for Road Condition Prediction – Phase 3 Evaluation Report
5. Report Date December 2020
6. Performing Organization Code
7. Author(s) Robert Sanchez, Michelle Neuner, Tracy Gonzalez
8. Performing Organization Report No.
9. Performing Organization Name and Address
10. Work Unit No. (TRAVIS) Leidos, Inc. 11251 Roger Bacon Drive Reston, VA 20190
11. Contract or Grant No. DTFH61-16-D-00053L, Task 693JJ318F000084
12. Sponsoring Agency Name and Address U.S. Department of Transportation Federal Highway Administration 1200 New Jersey Avenue, SE Washington, DC 20590
13. Type of Report and Period Covered Evaluation Report; 3/26/2018–9/25/2020
14. Sponsoring Agency Code
15. Supplementary Notes Road Weather Management Program; the government's task order manager: Jawad Paracha
16. Abstract The Integrated Modeling for Road Condition Prediction (IMRCP) is a prototype system and demonstration deployment that provides a framework for the integration of road condition monitoring and forecast data to support decisions by travelers, transportation operators, and maintenance providers. The system collects and integrates environmental and transportation operations data, collects forecast weather data, initiates road weather and traffic forecasts, generates advisories and warnings, and provides the results to other applications and systems. The model could ultimately become a practical tool for transportation agencies to support traveler advisories, maintenance plans, and operational decisions at both strategic and tactical levels. The purpose of the evaluation is to explore IMRCP operational impacts and usefulness at its deployment site of Kansas City Scout (KC Scout). The evaluation examined whether the speeds and speed forecasts were accurate and whether the traffic and weather information was useful to KC Scout operators. The findings could inform others who may be considering similar deployments and provide the Federal Highway Administration (FHWA) with information to help determine next steps for IMRCP.
17. Key Words Prediction; Road Weather Management Program (RWMP); transportation system management and operations (TSMO); evaluation; weather-responsive traffic management (WRTM); traffic modeling; road condition; weather; road weather; Integrated Modeling for Road Condition Prediction (IMRCP)
18. Distribution Statement No restrictions.

19. Security Classif. (of this report) Unclassified

20. Security Classif. (of this page) Unclassified

21. No. of Pages 82

22. Price n/a Form DOT F 1700.7 (8-72) Reproduction of completed page authorized

<https://www.hindawi.com/journals/jat/2022/7783588/>

An Overview of Pavement Degradation Prediction Models

Amir Shtayat,¹Sara Moridpour,¹Berthold Best,²and Shahriar Rumi¹

Academic Editor: Seyed Ali Ghahari

Received17 Sept 2021

Revised25 Dec 2021

Accepted27 Dec 2021

Published31 Jan 2022

Abstract

Pavement management systems (PMSs) have a primary role in determining pavement condition monitoring and maintenance strategies. Moreover, many researchers have focused on pavement condition evaluation tools, starting with data collection, followed by processing, analyzing, and ultimately reaching practical conclusions regarding pavement condition. The analysis step is considered an essential part of the pavement condition evaluation process, as it focuses on the tools used to find the most accurate results. On the other hand, prediction models are important tools used in pavement condition evaluation to determine the current and future performance of the road pavement. Therefore, pavement condition prediction has an effective and significant role in identifying the appropriate maintenance techniques and treatment processes. Moreover, pavement performance indices are commonly used as key indicators to describe the condition of pavement surfaces and the level of pavement degradation. This paper systematically summarizes the existing performance prediction models conducted to predict the condition of asphalt pavement degradation using pavement condition indexes (PCI) and the international roughness index (IRI). These performance indices are commonly used in pavement monitoring to accurately evaluate the health status of pavement. The paper also identifies and summarizes the most influencing parameters in road pavement condition prediction models and presents the strength and weaknesses of each prediction model. The findings show that most previous studies preferred machine learning approaches and artificial neural networks forecasting and estimating the road pavement conditions because of their ability to deal with massive data, their higher accuracy, and them being worthwhile in solving time-series problems.

<https://www.tandfonline.com/doi/abs/10.1080/10298436.2013.828839>

Using a multi-phase model to predict flushing of sprayed seal pavements

[Sachi Kodippily](#)

,

[Theunis F.P. Henning](#)

&

[Jason M. Ingham](#)

Pages 267-278 | Received 23 Sep 2012, Accepted 16 Jul 2013, Published online: 16 Aug 2013

Abstract

Flushing is a pavement defect that has a negative effect on the structural integrity and performance of a pavement surface. The aim of this study was to develop a model to predict the occurrence and progression of flushing on sprayed seal pavements. Data analysis and model development were performed using data sourced from New Zealand's Long-Term Pavement Performance programme. The developed model consists of two phases to model (1) the probability of flushing initiating on a pavement and (2) the progression of flushing. The probability of flushing initiation was modelled using a logistic model format, and the progression of flushing was modelled using a linear model format. Testing of the developed model revealed that the logistic model predicted the probability of flushing initiation at 76% accuracy, whereas the linear model had statistically robust predictions of flushing. The developed model is recommended for use in sprayed seal pavement management processes.

<https://www.tandfonline.com/doi/full/10.1080/16742834.2019.1608791>

A case study of environmental characteristics on urban road-surface and air temperatures during heat-wave days in Seoul

[Yoo-Jun KIM](#)

[Baek-Jo KIM](#)

[Yoon-Sook SHIN](#)

[Hui-Won KIM](#)

[Geon-Tae KIM](#) &

[Seon-Jeong KIM](#)






Pages 261-269 | Received 03 Jan 2019, Accepted 21 Feb 2019, Published online: 30 Apr 2019

ABSTRACT

High road-surface temperature due to heat waves can lead to dangerous driving conditions such as tire blowouts and deformation induced by thermal stress on the roads. In this study, a Mobile Observation Vehicle dataset, with high spatial and temporal resolutions for the heat-wave episode that occurred on 16–17 August 2018, is used to understand environmental characteristics on urban road-surface and air temperatures in Seoul. This study demonstrates that the magnitude of urban road-surface temperature is dependent on the differences in incoming solar radiation due to screening of high-rise buildings in the Gangnam area, and is associated with the topographical features in the Gangbuk area. The road-surface temperature in the section of darker-colored asphalts was higher than that of lighter-colored asphalts, with a mean difference of 6.8°C, and both surface and air temperatures on the iron plate were highest, with means of 51.7°C and 35.1°C, respectively. In addition, during the water-sprinkling period, road-surface temperature was cooled by about 8.7°C (19%) compared with that in the period without water-sprinkling, but there was no significant change in air temperature. The current results could be practically used to improve road-surface temperature prediction models for civil engineers or road managers.

<https://transportgeography.org/contents/applications/climate-change-transport-infrastructure/climate-change-impacts-transportation/>

Climate Change and its Potential Impacts on Transportation

| | Operations | Infrastructures |
|---|---|---|
| Heat waves  | <ul style="list-style-type: none"> • Limits on periods of construction activity. • More energy for reefer transportation and storage. | <ul style="list-style-type: none"> • Thermal expansion of piers. • Pavement integrity and softening. • Deformation of rail tracks. |
| Rising sea levels  | <ul style="list-style-type: none"> • Frequent interruptions of coastal low-lying road and rail due to storm surges. • Flooding of terminal areas. | <ul style="list-style-type: none"> • More frequent flooding of infrastructure (and potential damage) in low lying areas. • Erosion of infrastructure support. • Changes in harbor facilities to accommodate higher tides and surges. |
| Intensity of precipitation  | <ul style="list-style-type: none"> • Increase in weather related delays and disruptions. | |
| Increasing hurricane intensity  | <ul style="list-style-type: none"> • Frequent interruptions of air services. • Frequent and extensive evacuations of coastal areas. • Debris on road and rail infrastructures. | <ul style="list-style-type: none"> • Greater probability of infrastructure failure. • Greater damage to port infrastructures. • More significant flooding on hinterland infrastructures. |
| Increase in arctic temperatures  | <ul style="list-style-type: none"> • Longer shipping season. • More ice-free ports in northern regions. • Availability of trans-arctic shipping routes. | <ul style="list-style-type: none"> • Damage to infrastructure because of the thawing of the permafrost. |

© GTS

Climate Change and its Potential Impacts on Transportation

Source: adapted from National Research Council (2008) Potential impacts of climate change on U.S. Transportation. Transportation Research Board.

Elements associated with climate change have an array of potential impacts on transport operations and infrastructures.

https://ops.fhwa.dot.gov/weather/q1_roadimpact.htm

How Do Weather Events Impact Roads?

[Home](#)

Weather acts through visibility impairments, precipitation, high winds, and temperature extremes to affect driver capabilities, vehicle performance (i.e., traction, stability and maneuverability), pavement friction, roadway infrastructure, crash risk, traffic flow, and agency productivity. The table below, summarizes the impacts of various weather events on roadways, traffic flow, and operational decisions.

Table: Weather Impacts on Roads, Traffic and Operational Decisions

| Road Weather Variables | Roadway Impacts | Traffic Flow Impacts | Operational Impacts |
|--|--|---|--|
| Air temperature and humidity | N/A | N/A | Road treatment strategy (e.g., snow and ice control) Construction planning (e.g., paving and striping) |
| Wind speed | Visibility distance (due to blowing snow, dust) Lane obstruction (due to wind-blown snow, debris) | Traffic speed Travel time delay Accident risk | Vehicle performance (e.g., stability) Access control (e.g., restrict vehicle type, close road) Evacuation decision support |
| Precipitation (type, rate, start/end times) | Visibility distance Pavement friction Lane obstruction | Roadway capacity Traffic speed Travel time delay Accident risk | Vehicle performance (e.g., traction) Driver capabilities/behavior Road treatment strategy Traffic signal timing Speed limit control Evacuation decision support Institutional coordination |
| Fog | Visibility distance | Traffic speed Speed variance Travel time delay Accident risk | Driver capabilities/behavior Road treatment strategy Access control Speed limit control |
| Pavement temperature | Infrastructure damage | N/A | Road treatment strategy |
| Pavement condition | Pavement friction Infrastructure damage | Roadway capacity Traffic speed Travel time delay Accident risk | Vehicle performance Driver capabilities/behavior (e.g., route choice) Road treatment strategy Traffic signal timing Speed limit control |

| | | | |
|--------------------|-----------------|-------------------|-----------------------------|
| Water level | Lane submersion | Traffic speed | Access control |
| | | Travel time delay | Evacuation decision support |
| | | Accident risk | Institutional coordin |

<https://www.bloomberg.com/news/articles/2022-08-18/the-world-s-roads-and-highways-aren-t-built-for-a-hotter-climate>

The World's Roads Aren't Ready for a Hotter Climate

Global warming is damaging the vast web of asphalt and concrete we use to move around. Fixing the problem won't be cheap.



As average temperatures rise and heat waves become more frequent and intense, it's become clear that infrastructure and in particular roads are vulnerable to accelerating global warming.

Photographer: Robert Michael/Picture Alliance/Getty Images

By

William Ralston

August 18, 2022 at 4:00 AM EDT

The historic heat wave that's smothered western Europe this summer has caused transportation chaos. Railroad tracks warped, airport runways failed and key roads buckled. On July 18, the busy A14 highway in Cambridge, England, was shut down after developing a bizarre ridge that, while enticing to skateboarders, would be calamitous to fast-moving cars and their passengers.

<https://www.plsofflorida.com/how-do-potholes-form/>

How do Potholes form in Warm Climates?

Posted by Parking Lot Services In **Asphalt Repair, Blog, Parking Lot, Parking Lot Design, Parking Lot Planning, Parking Lot Services of Florida, Parking Lot Striping, Paving**

Understanding how potholes form is important when keeping your parking lot well-maintained.

Potholes are an all too common occurrence in many parking lots. These parking lot potholes can easily form in warm climates due to a variety of reasons. Potholes create significant safety concerns while also decreasing the curb appeal of your business. Scheduling **parking lot maintenance** is a great way to stay proactive to ensure your parking lot is safe and functions well for years.

How Do Potholes Form?

Pavement is always constructed to avoid the accumulation of water. However, water can eventually find its way underneath the pavement due to cracks or separations within the asphalt. These cracks can appear due to heavy traffic or extreme heat. Water can easily drain into these cracks and wash out the layers of stone or dirt that support the pavement. Eventually, an air gap is created within the sub-base of the asphalt pavement.

Over time, the top layer of the pavement will begin to sag, and it will collapse and crumble, which results in creating a pothole. Ultimately, this is how potholes form, as they can create significant liability concerns for your business.

Potholes make it more difficult to drive across a parking lot while also greatly decreasing the visual appeal of your property. Reaching out to professionals to fix potholes is essential in keeping your parking lot looking great and extending its lifespan.

<https://www.washingtonpost.com/climate-environment/2022/07/20/heat-wave-road-railway-buckling/>

With extreme heat, we can't build roads and railways as we used to

Buckled roads, warped train tracks and expanded bridges are a stark reminder, experts say, of the need to adapt quickly to a warming planet



By [Allyson Chiu](#)

July 20, 2022 at 6:00 a.m. EDT

Water is sprayed on the taxiways at the Schiphol airport in Amsterdam to prevent the deformation of the asphalt, due to a heat wave in July 2019. (Robin van Lonkhuijsen/AFP/Getty Images)

Listen

6 min

Comment

Gift Article

Share

Roads and airport runways buckling. Train tracks warping. Bridges swelling.

These are just some of the damaging effects extreme heat has had on critical infrastructure in recent years, as heat waves have become more frequent and intense — a stark reminder, experts say, of the need to adjust quickly to a warming planet.

10 steps you can take to lower your carbon footprint

“Most of our physical infrastructure was built using the temperature records of the mid-20th century,” [Costa Samaras](#), principal assistant director for energy with the White House’s Office of Science and Technology Policy, wrote in an email. “That is not the climate we have now.”

Samaras added: “Melting roads and runways are no longer a hypothetical — and we know with increased emissions it’s only going to get hotter.”

The latest scramble to adapt came this week as heat waves smothered parts of the United States and Europe, sending temperatures in many historically temperate areas skyrocketing. In London, for instance, parts of a Victorian-era bridge were wrapped in silver insulation foil to protect the metal from cracking.

Meanwhile, [steel train tracks warped and buckled, and airport runways were damaged by the heat](#), causing widespread travel disruptions.

[Britain’s freakish heat demolished records. Here’s what happened.](#)

“When reality and future conditions start shifting away from what was used in the design, our infrastructure becomes more prone to failure and may also suffer from a reduced service life,” [Amit Bhasin](#), a professor and director of the Center for Transportation Research at the University of Texas at Austin, wrote in an email.

But experts stressed that solutions should not focus solely on improving infrastructure. “The bottom line is: we are not going to only build our way out of this,” Samaras said. “We must decarbonize our energy uses and learn how to remove carbon we’ve already added to the atmosphere.”

As concrete buckles and roads flood, states are responding slowly to the new climate reality

What infrastructure is at risk?

Heat can impact all types of physical infrastructure, but roads, runways and railways may be among the most vulnerable, said [Ladd Keith](#), an assistant professor of planning and chair of sustainable built environments at the University of Arizona’s College of Architecture, Planning and Landscape Architecture.

Paved surfaces, such as roads and runways, are typically made of asphalt or concrete, materials that can be affected, in some cases dramatically and quickly, by heat.

“Asphalt is a temperature-sensitive material, so when it gets hot, it gets really soft,” said [Jo Sias](#), a professor of civil and environmental engineering at the University of New Hampshire.

While many descriptions of extreme heat’s effect on asphalt include the word “melting,” that isn’t entirely accurate, said [Steve Muench](#), a professor of civil and environmental engineering at the University of Washington. Instead, he said, the effect is more similar to what you could do to Play-Doh or clay.

Asphalt also tends to age faster at higher temperatures, which can reduce its life span, Bhasin said.

For roadways that use concrete, expansion caused by unusually hot weather can be a major problem. These thoroughfares are paved with slabs and designed with space in between to account for expansion (when it’s hot) or contraction (when it’s cold), Muench said. But when temperatures are much higher than usual and if improper maintenance has led to debris getting into the spaces, the slabs can run out of room to expand, eventually causing “concrete pavement blowups or buckling,” he said.

Expanding is also an issue for the steel used to construct train tracks, Sias said. “All of a sudden, the individual rails, they don’t have enough room to expand, so they’ll just buckle. Then, you get those curves in the railway lines, which obviously are not good.”

Repair work is carried out on a highway in Germany after it was damaged in the heat in July 2019. (Rainer Jensen/Picture-alliance/DPA/AP Images)

What is the tipping point?

The answer often depends on location and design. “There may not always be a magic number at which the infrastructure will go from ‘working’ to ‘failed,’” Bhasin said.

Physical infrastructure is traditionally designed based on the historical conditions of a particular location, Keith said. That means the point at which extreme heat starts to affect surfaces varies depending on the past climate of that location.

“Any kind of prolonged extreme heat outside of that past climate will push the physical infrastructure into dangerous territory,” he said.

What can be done?

It’s important to be prepared to make immediate repairs, Sias said. Public agencies should know that extreme weather can cause damage and have the supplies on hand to react promptly.

“In terms of predicting where things like buckling are going to happen, it’s very, very difficult to do,” she said. “There’s no real models or anything that will tell you, ‘Okay, this joint is going to buckle, but this one’s not.’ ”

Still, there are some “relatively mundane engineering things” that can be done to lower the chances of negative impacts, Muench said.

For example, concrete slabs used for road pavement can be made smaller. “The shorter the slab is, the less length change it undergoes during heating and cooling,” he said. “If you can reduce that length change, then the likelihood of something like a blowup would be less.”

Modifications can also be made to an asphalt mixture that makes it stiffer in higher temperatures and more resistant to cracking at lower temperatures, he said.

It may also be helpful to plant trees along roadways to create shade, or to use “cool pavement,” which is in lighter colors and slightly more reflective than what is traditionally used, Keith said.

As temperatures rise, this research could help cities stay cool

But he and other experts emphasized that broader changes and, in particular, efforts to adjust infrastructure design, are critical for adapting to future extreme weather.

A [2017 study](#) that assessed extreme climate impacts on infrastructure in Europe noted that heat waves would account for about 92 percent of total hazard damage in the transport sector by the 2080s, with much of the effects expected on roads and railways.

“We need to think longer term and more holistically about heat,” Keith said. “We need to make sure that every time that we have a roadway project or a railway project of the future, that we’re making sure to design it for the climate that we’re pushing ourselves into and not the one that we’re currently in or the one that we’ve had been in the past.”

A holistic approach, Bhasin added, should also include taking steps to understand and mitigate the causes for these extreme temperature events.

“If not, we may continue in a downward spiral,” he said.

<https://www.roadbotics.com/2022/06/08/hot-weather-effects-on-roads/>

Wisconsin

In June 2021, Wisconsin handled multiple reports of buckling due to heat waves:

WEAU [informed citizens of buckling on Highway 53 Bypass and Clairemont Ave](#) in Eau Claire after temperatures hit the mid-90s, setting new records at several weather-reporting stations across Wisconsin, including Eau Claire. This year, the state started facing high temperatures a month earlier, as heat hit in May.



Buckling on Clairemont Ave.; Photo credit: Eau Claire Police Dept.

NBC15 shared an [instance of buckling in Madison, WI](#).

Elsewhere in Wisconsin, pavement buckling forced an onramp to Interstate 90 in Columbia Co. in south-central Wisconsin [to briefly close for repairs](#), while Interstate 41 near Neenah [also had pavement buckling](#).



Photo Credit: Eau Claire Police Department

A week later, [additional buckling was reported by Channel 3000](#) in the Portage area record-breaking streak of May heat.



Example of buckling on Highway 16 in Portage, Wis.; Photo credit: PORTAGE DAILY REGISTER ARCHIVES

High temperatures hit many other areas hard, this year and last.

Washington

KUOW in the Puget Sound [reported multiple instances of buckling on I-5](#). Luckily, construction crews were already dispatched and were redirected to address the buckling issue immediately.



Buckling in Everson, Washington, June 2021; Photo credit: WSDOT

Media outlet, KREM, reported [Heat-related road woes: Pavement buckles on Highway 195 south of Rosalia](#) WSDOT East said the road is peeling in the westbound lanes. Crews will sand the road to keep it from peeling back further. Chelan County Public Works said it received reports of oil coming up on county roads.



Photo credit: WSDOT

Utah

KSL TV5 reported [major buckling in Salt Lake City, UT due to 100+ degree temperatures](#) last July. The concrete contracts and expands, but never back to its original volume. Rocks and grit get in the joints which keeps the concrete from moving back and forth. Then heat expands the concrete and it buckles.

Oregon

KOIN News covered a [buckling that took place right outside someone's front door](#).

Dayton residents Tiffany and Andrew Prather shared that they suddenly noticed the entire house shaking. After investigating the situation, they found a buckled road outside their property.

<https://www.researchgate.net/publication/230320048> Quantifying the effects of high summer temperatures due to climate change on buckling and rail related delays in south-east United Kingdom

Quantifying the effects of high summer temperatures due to climate change on buckling and rail related delays in south-east United Kingdom

June 2009

[Meteorological Applications](#) 16(2):245 - 251

Follow journal

DOI:

[10.1002/met.114](https://doi.org/10.1002/met.114)

[K. Dobney](#)

[C. J. Baker](#)



[Andrew David Quinn](#)



[Lee Chapman](#)

Abstract

Extreme high temperatures are associated with increased incidences of rail buckles. Climate change is predicted to alter the temperature profile in the United Kingdom with extreme high temperatures becoming an increasingly frequent occurrence. The result is that the number of buckles, and therefore delays, expected per year will increase if the track is maintained to the current standard. This paper uses a combination of analogue techniques and a weather generator to quantify the increase in the number of buckles and rail related delays in the south-east of the United Kingdom. The paper concludes by assigning a cost to the resultant rise in delays and damage before making recommendations on how these effects can be mitigated. Copyright © 2008 Royal Meteorological Society

<https://rmets.onlinelibrary.wiley.com/doi/10.1002/met.1910>

The impact of high temperatures and extreme heat to delays on the London Underground rail network: An empirical study

[Sarah Greenham, Emma Ferranti, Andrew Quinn, Katherine Drayson](#)

First published: 22 June 2020

<https://doi.org/10.1002/met.1910>

Citations: [4](#)

Funding information Ferranti's time was funded by EPSRC Fellowship, Grant/Award Number: EP/R007365/1

Rail infrastructure is vulnerable to extreme weather events, resulting in damage and delays to networks. The impact of heat is a major concern for the London Underground (LU) by Transport for London (TfL) both now and in future, but existing studies are limited to passenger comfort on the deep tube and do not focus on infrastructure or the vast majority of the network, which is in fact above ground. For the first time, the present empirical study examines quantitatively the statistical relationship between LU delays (by synthesizing 2011–2016 industry data) with air temperature data (from Met Office archives). A range of testing shows strong statistical relationships between most delay variables and high temperatures, though not causality. Relationships were found between high temperatures and delays associated with different asset classes on different LU lines. Track-related delays, often the focus of high-temperature research (i.e. track buckling), show a relationship, although this is small relative to delays caused by other assets. Using UK Climate Projections 2009 (UKCP09) and assuming a similar future performance indicates that the share of annual delays owed to temperatures > 24°C may increase in frequency and length, depending on the emissions scenario. Recommendations include extending the analysis to the LU asset scale and considering the local environment to understand failure causality in order to mitigate future heat risk. A review of how TfL and other infrastructure operators capture delays for future analysis is necessary to facilitate climate resilience benchmarking between networks.

<https://heatisland.lbl.gov/sites/default/files/cuhi/docs/211420-mallick-doc.pdf>

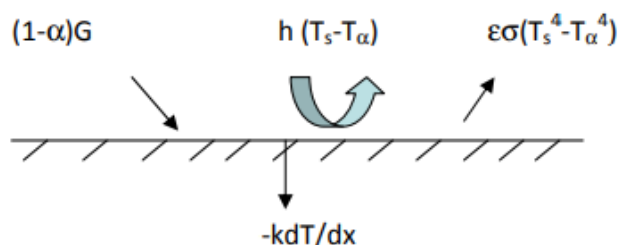
Reduction of Urban Heat Island Effect through Harvest of Heat Energy from Asphalt Pavements

Rajib B. Mallick*, Civil and Environmental Engineering, Worcester Polytechnic Institute (WPI), 100 Institute Road, Worcester, MA 01609, USA, rajib@wpi.edu Bao-Liang Chen, Civil and Environmental Engineering, Worcester Polytechnic Institute (WPI), 100 Institute Road, Worcester, MA 01609, USA, rickchentt@gmail.com Sankha Bhowmick, Mechanical Engineering, University of Massachusetts Dartmouth, 285 Old Westport Road, North Dartmouth, MA 02747, USA, sbhowmick@umass.edu * Corresponding author

ABSTRACT Asphalt pavement surfaces contribute significantly to the urban heat island effect. Their relatively high temperature, caused by absorption of solar energy, results in emission of heat to the surrounding air, leading to a rise in its temperature, deterioration of its quality, and an increase in energy consumption of the surrounding buildings. The proposed concept is that the heat from the pavement can be removed by flowing an appropriate fluid in a piping system combined with high conductivity layers, and this would lead to a reduction of temperature in the pavement, and lowering of heat emitted from the surface to the surrounding air. The concept, results of laboratory experiments and finite element modeling/simulation are presented. Comparison of results from the application of the proposed concept with those from changing the albedo of existing pavements is made. The conclusions are that a significant lowering of surface temperature and emitted radiation is possible, and the reduction in temperature is affected by the conductivity of the mix, the type of paint/layer on the surface, the heat-exchanger system, and the temperature of the fluid. The results could be used to engineer a system with optimum piping location and spacing, and properties of the fluid to achieve the desirable result.

Introduction Solar radiation absorbed by an asphalt pavement raises its temperature. There are four predominant mechanisms in the transfer of heat to a pavement (Bejan, 1993): (Figure 1) solar radiation in and emitted radiation out of the pavement, conductive transfer of heat through the pavement, and convective transfer of heat above the pavement through wind. Figure 1: Thermal Problem Associated with Pavement Heating (G = irradiation, h = heat transfer coefficient, k = thermal conductivity, T_a = air temperature, T_s = surface temperature, T_{sur} = surrounding temperature; α = reflected component, ϵ = emissivity of the surface) $(1-\alpha)G$ $h(T_s-T_a)$ $\epsilon\sigma(T_s^4-T_a^4)$ $-kdT/dx$

Figure 1: Thermal Problem Associated with Pavement Heating (G = irradiation, h = heat transfer coefficient, k = thermal conductivity, T_a = air temperature, T_s = surface temperature, T_{sur} = surrounding temperature; α = reflected component, ϵ = emissivity of the surface)



https://www.tac-atc.ca/sites/default/files/conf_papers/shafieem-climate_change_and_asphalt_binder_selectio.pdf

Climate Change and Asphalt Binder Selection: Resilient Roads of the Future

Authors: Mohammad Shafiee, Ph.D., P.Eng., Research Officer Omran Maadani, Ph.D., Research Officer Ethan Murphy, CO-OP Student

National Research Council Canada

Paper prepared for presentation at the 2020 TAC Conference & Exhibition,

1 Abstract

Adapting flexible pavements systems to the impact of climate change is a challenge in Canada. It is well-known that increasing temperatures and more frequent extreme heat events represent risks for the flexible pavements. These vulnerabilities may put additional pressure on Canadian transportation infrastructure and economy, as weather begins to deviate more and more from historic temperatures. Selecting suitable Performance Graded Asphalt Cements (PGAC) for pavement construction heavily depends on temperature conditions at the site. Hence, the goal of this research paper is to evaluate the impact of climate change on PGAC selection for several Canadian cities based on different Representative Concentration Pathway (RCP) scenarios. In this study, projected temperature from ANUSPLIN datasets were used to obtain the necessary climatic parameters defined in the most recent PGAC algorithms. Projections of future changes highlighted the need for climate change adaptation policies and action sets in Canada